AXIONS AND WAVE-LIKE DARK MATTER

HARMONIZING THE HALOSCOPES

DESY WORKSHOP

CHELSEA BARTRAM 2024

Wave-like dark matter

$$\lambda_{dB} \approx \frac{2\pi}{mv}$$

De Broglie wavelength

Dark matter that behaves more like a wave than a particle

Proton in a linear accelerator: $\lambda \sim 10^{-12}$ m

WIMP dark matter: $\lambda \sim 10^{-13}$ m → Recoil experiments

Axion Dark Matter ($m \sim 10^{-6}$ eV): $\lambda \sim 100$ m → Something completely different…

Detection: Axion Haloscope

Photon coupling: cleanest channel for discovery

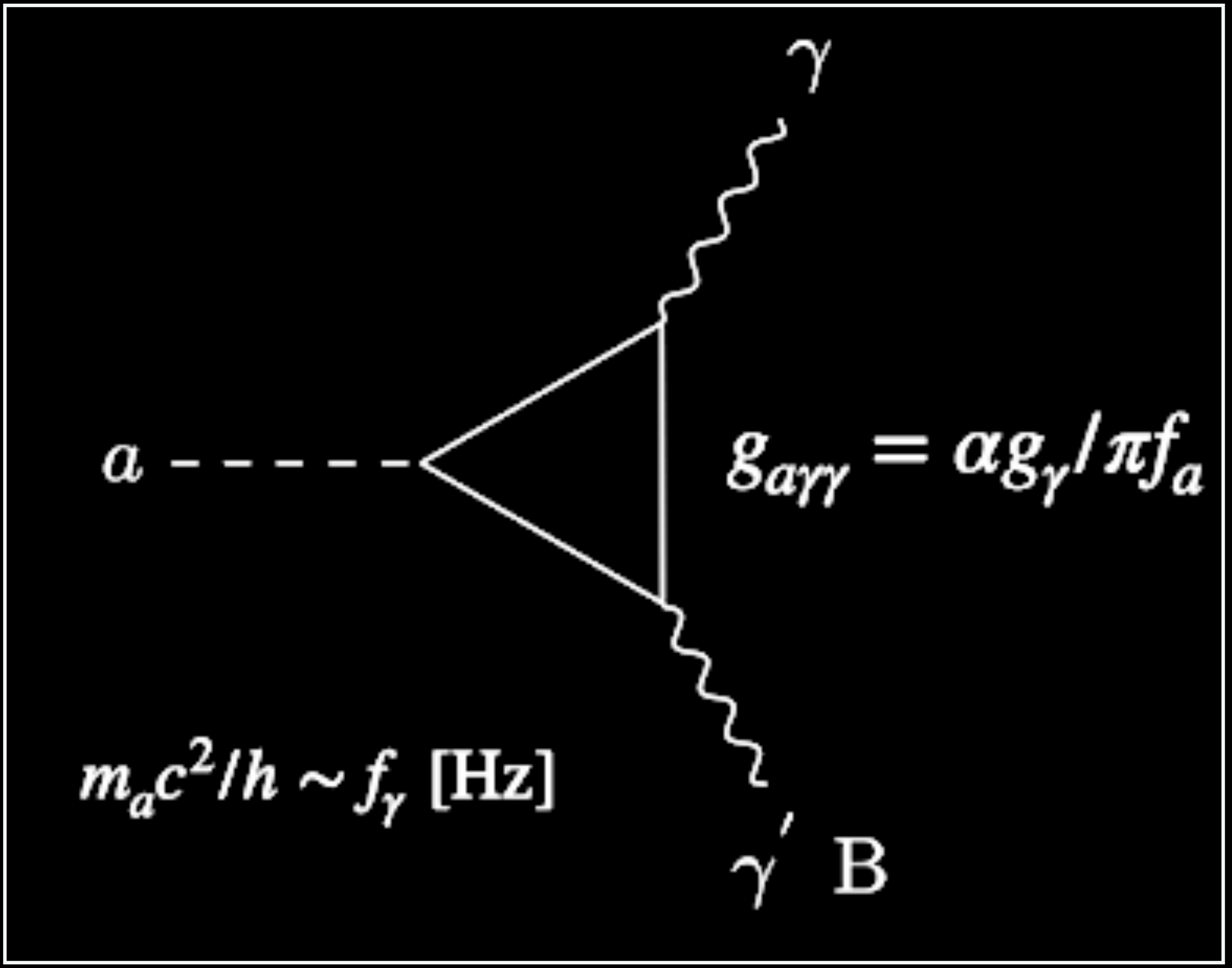

Inverse Primakoff Effect

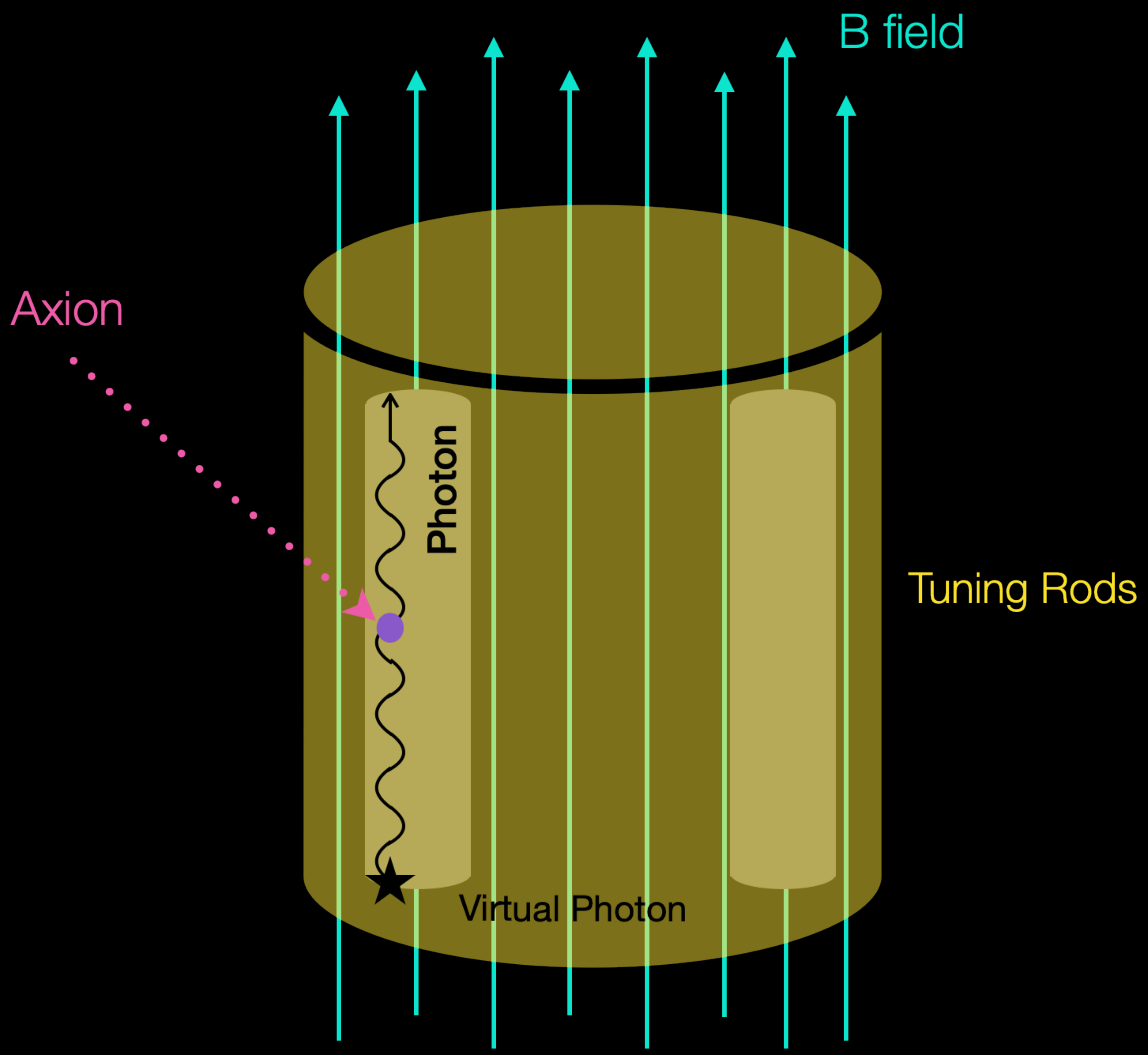

Resonant microwave cavity

Axion Mass Range

Lower bound set by size of dark matter halo size of dwarf galaxies

Upper bound set by SN1987A and white dwarf cooling time

Mass of axion (eV)

10^{-22} | 10^{-18} | 10^{-14} | 10^{-10} | 10^{-6} | 10^{-2}

10^{-8} | 10^{-4} | 1 | 10^{4} | 10^{8} | 10^{12}

Frequency of conversion photon (Hz)

Pre-inflation PQ phase transition

Post-inflation PQ phase transition

Adaptation of L. Winslow DPF Slide

Unexplored Parameter Space

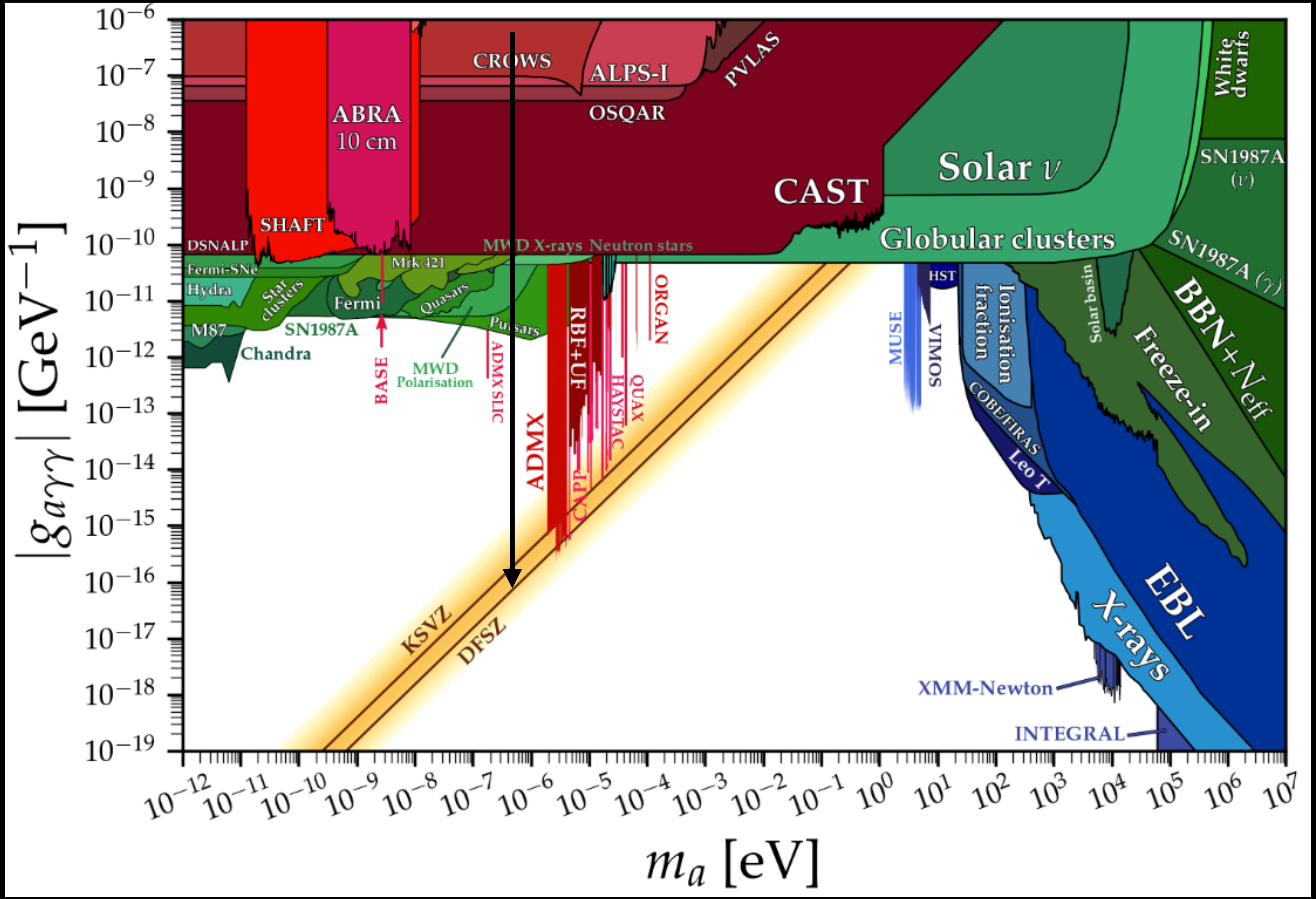

Plot courtesy of Ciaran O'Hare

Unexplored Parameter Space

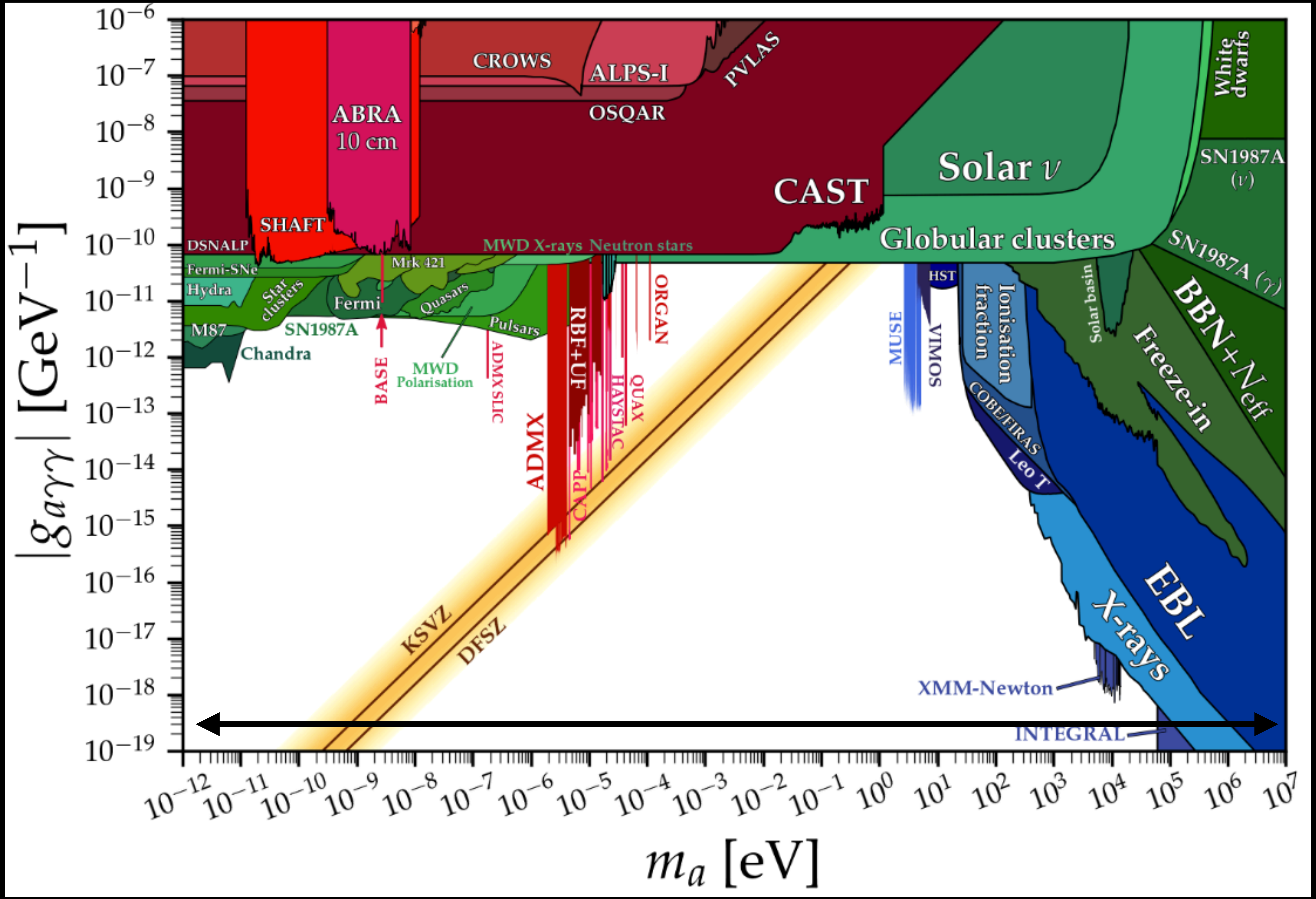

Plot courtesy of Ciaran O’Hare

Modified Electromagnetism

$$\nabla \times \mathbf{B_a} = \frac{\partial \mathbf{E_a}}{\partial t} - g_{a\gamma\gamma} \mathbf{B_0} \frac{\partial a}{\partial t}$$

Modified Ampère's Law

Quasistatic Regime:
$\lambda_{comp} >> R_{exp}$
e.g. ABRA, DM Radio

Cavity Regime:
$\lambda_{comp} \sim R_{exp}$
e.g. ADMX

Radiation Regime:
$\lambda_{comp} << R_{exp}$
e.g. MADMAX

AXIONS AND WAVE-LIKE DARK MATTER

LUMPED ELEMENT REGIME

DM RADIO

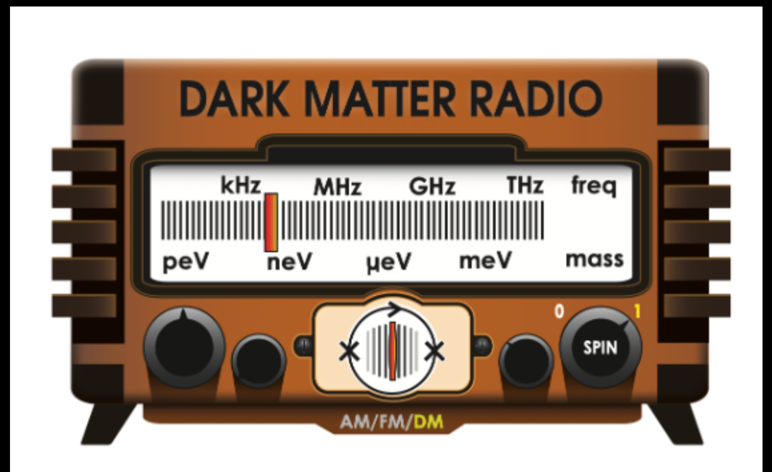

DM Radio Collaboration

H.M. Cho, W. Craddock, D. Li, W. J. Wisniewski
Stanford Linear Accelerator Center

C. Bartram, J. Corbin, C. S. Dawson, P. W. Graham, K. D. Irwin, F. Kadribasic, S. Kuenstner, N. M. Rapidis, M. Simanovskaia, J. Singh, E. C. van Assendelft, K. Wells
Department of Physics
Stanford University

A. Droster, A. Keller, A. F. Leder, K. van Bibber
Department of Nuclear Engineering
University of California Berkeley

S. Chaudhuri, R. Kolevatov
Department of Physics
Princeton University

L. Brouwer
Accelerator Technology and Applied Physics Division
Lawrence Berkeley National Lab

B. A. Young
Department of Physics
Santa Clara University

J. W. Foster, J. T. Fry, J. L. Ouellet, K. M. W. Pappas, C. P. Salemi, L. Winslow
Laboratory of Nuclear Science
Massachusetts Institute of Technology

R. Henning
Department of Physics
University of North Carolina Chapel Hill / Triangle Universities Nuclear Laboratory

Y. Kahn
Department of Physics
University of Illinois at Urbana-Champaign

A. Phipps
California State University, East Bay

B. R. Safdi
Department of Physics
University of California Berkeley

Lumped Element Haloscope

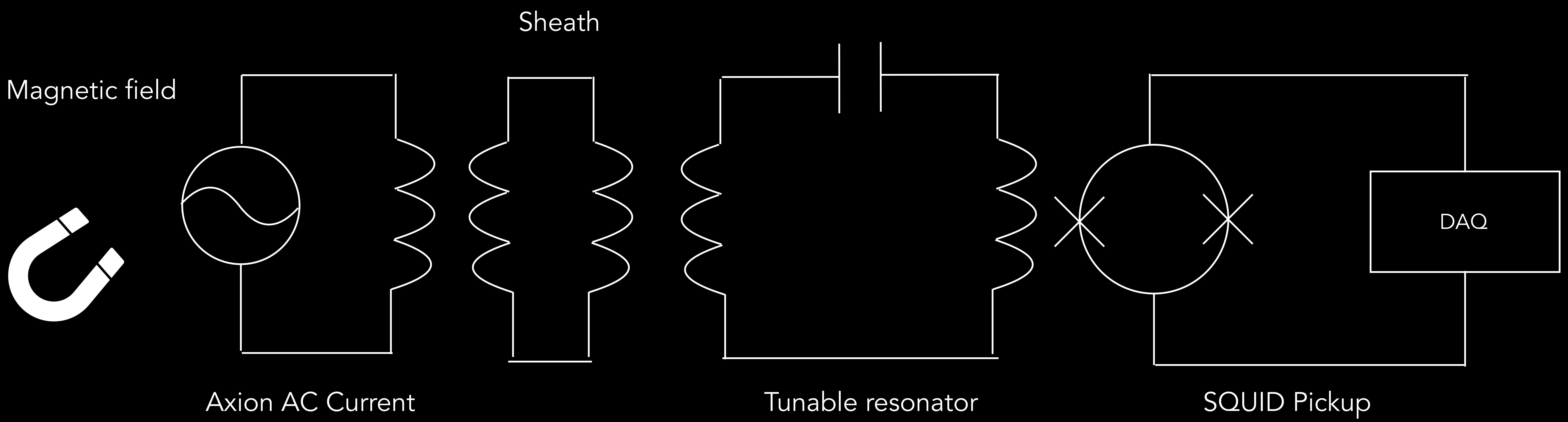

Figure inspired by Chiara Salemi

Lumped Element Haloscope

Case Study: Static Toroidal magnet

- Magnetic field B_0

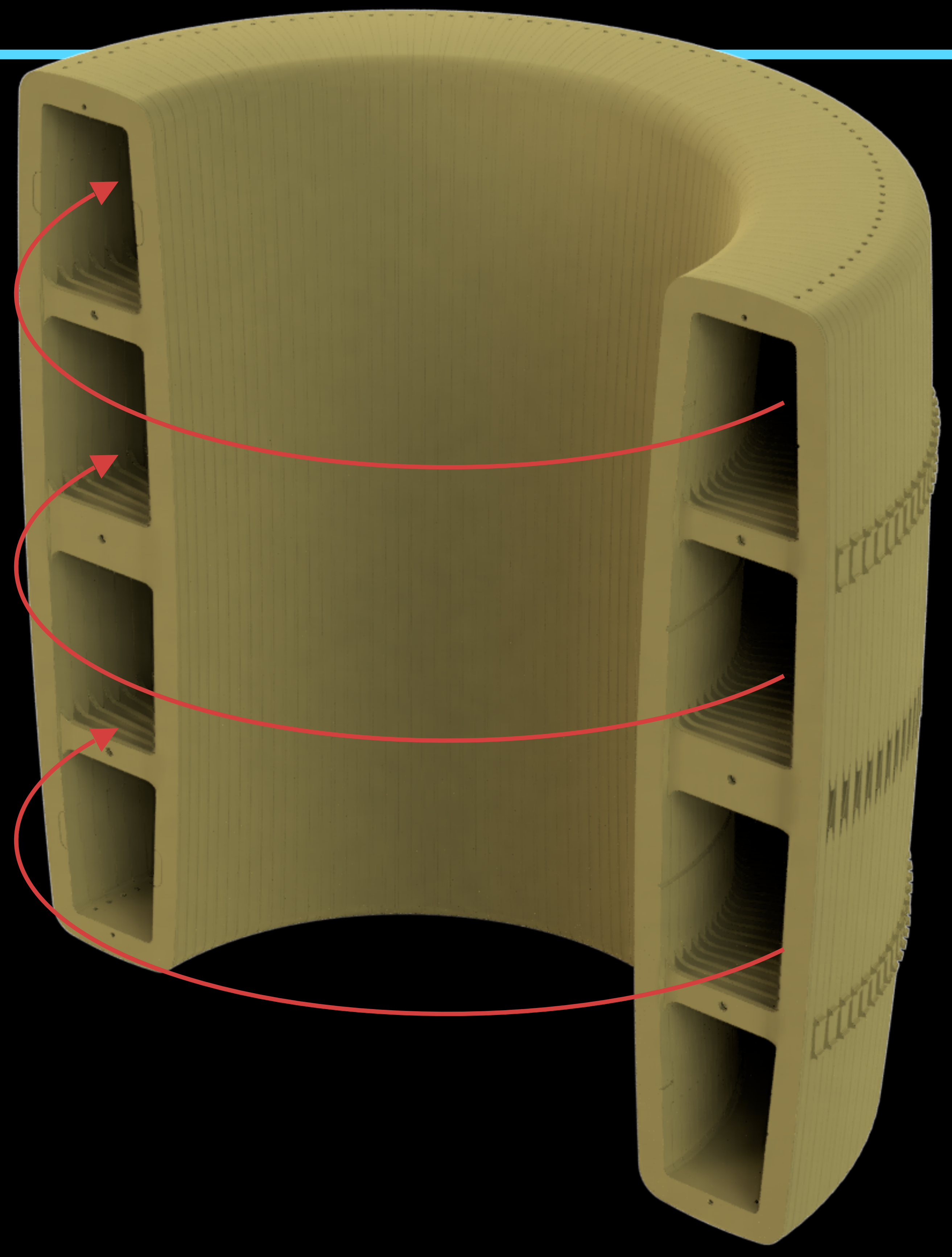

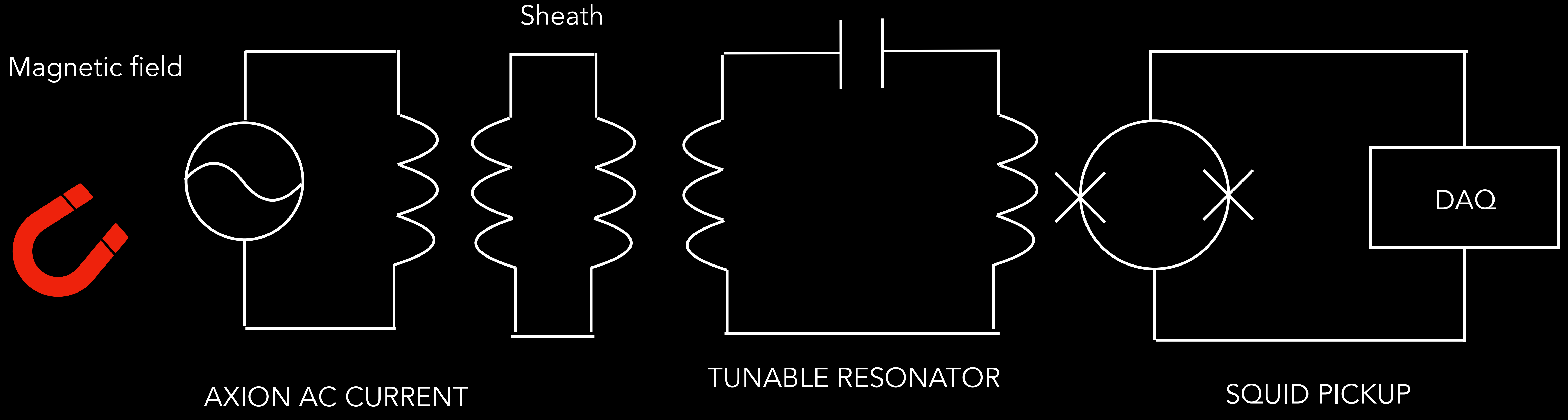

Figure courtesy of Chiara Salemi

Lumped Element Haloscope

Case Study: Static Toroidal magnet

- Magnetic field $\mathbf{B_0}$
- AC axion current $\mathbf{J_a}$

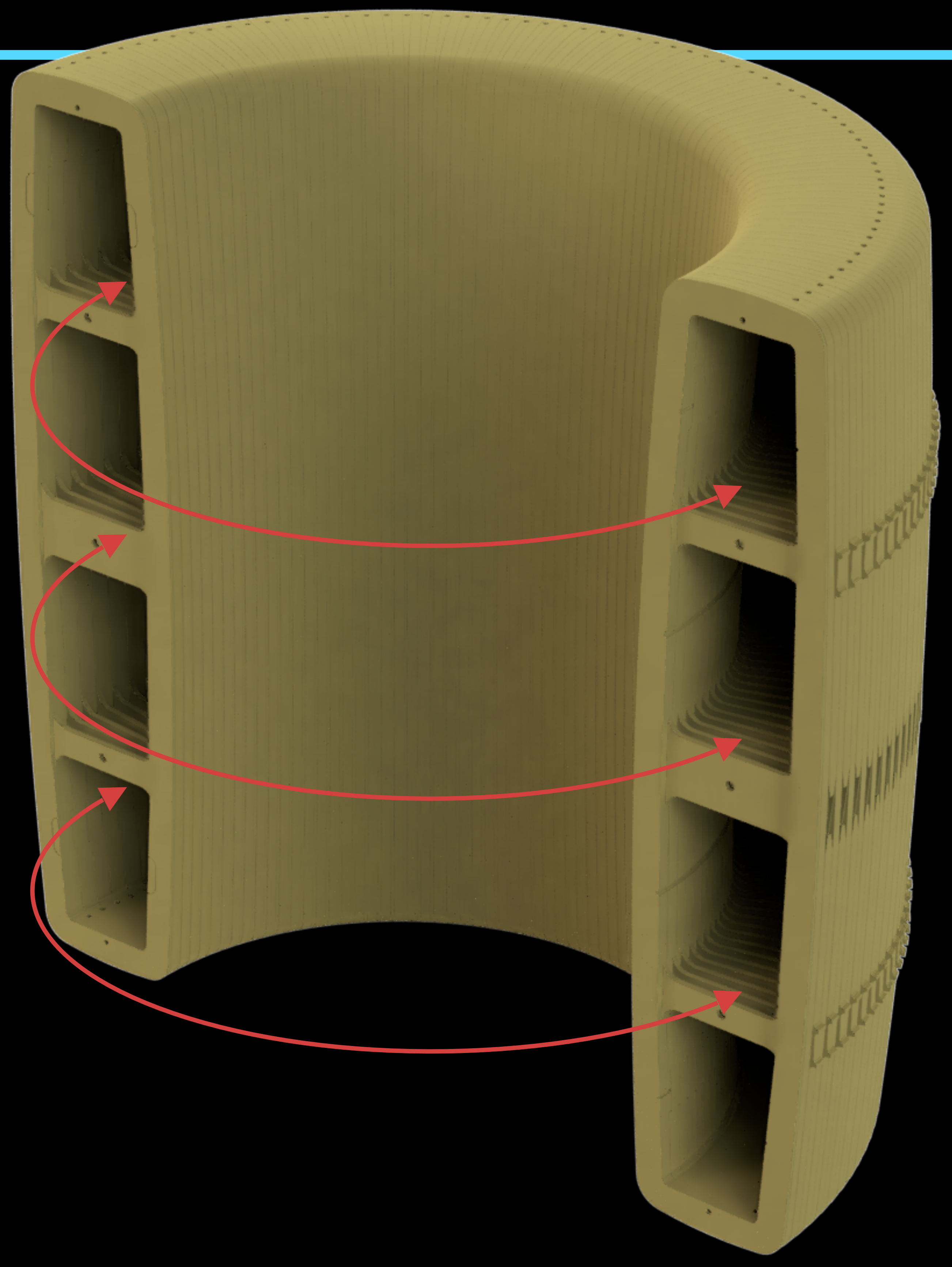

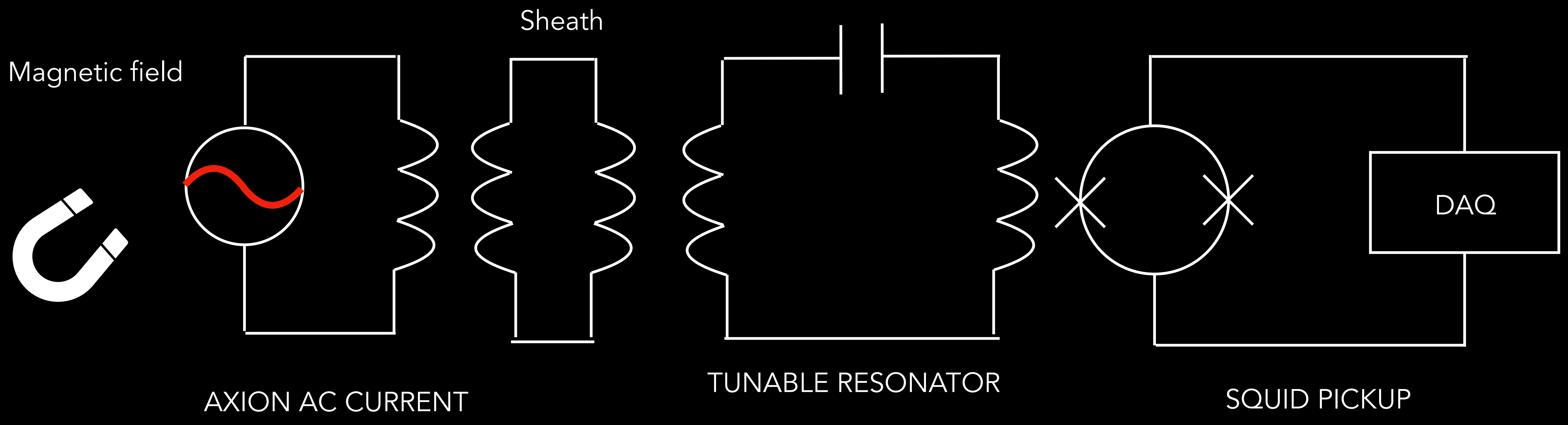

Figure courtesy of Chiara Salemi

Lumped Element Haloscope

Case Study: Static Toroidal magnet

- Magnetic field B_0
- AC axion current J_a
- Oscillating magnetic field

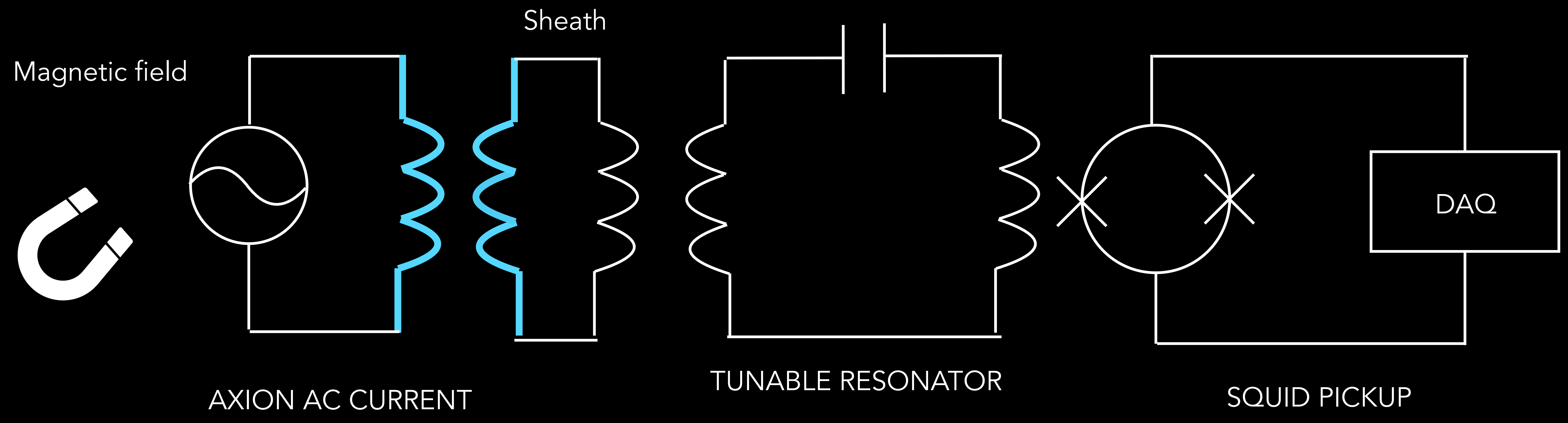

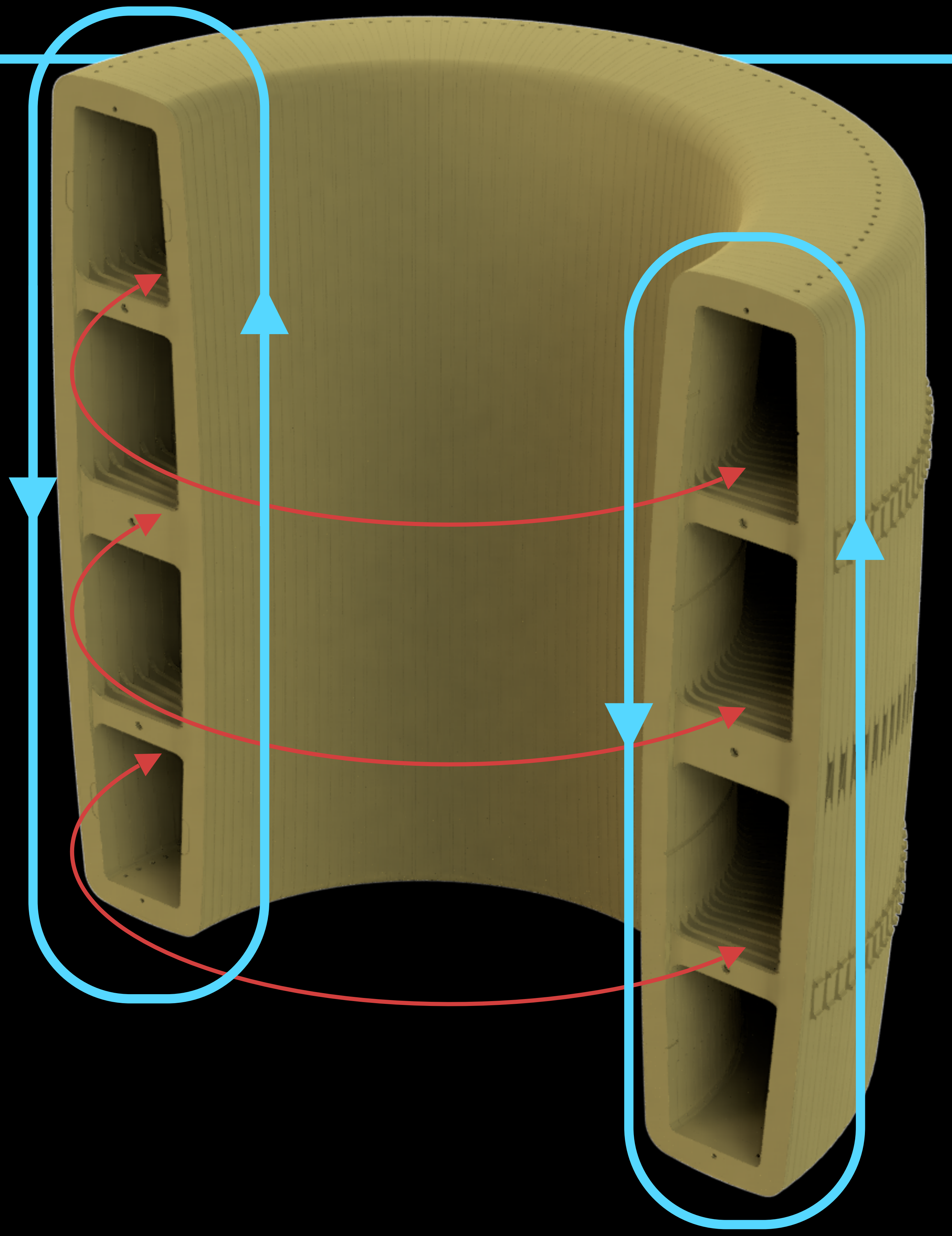

Figure courtesy of Chiara Salemi

Lumped Element Haloscope

Case Study: Static Toroidal magnet

- Magnetic field $\mathbf{B_0}$
- AC axion current $\mathbf{J_a}$
- Oscillating magnetic field
- Induces currents on the sheath

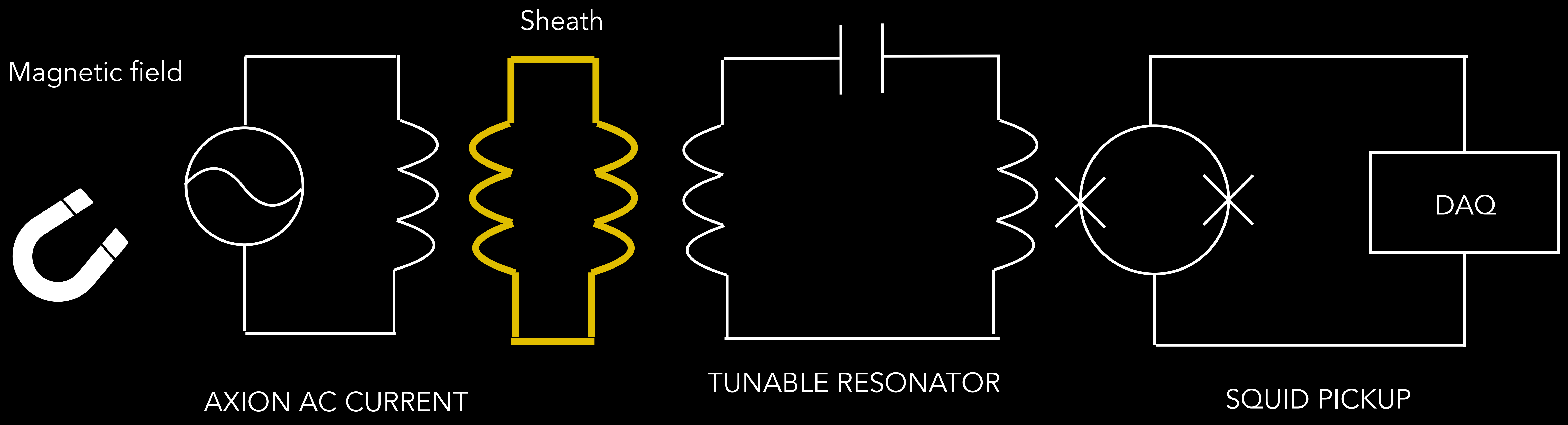

Figure courtesy of Chiara Salemi

Lumped Element Haloscope

Case Study: Static Toroidal magnet

- Magnetic field B_0
- AC axion current J_a
- Oscillating magnetic field
- Induces currents on the sheath
- Oscillating magnetic field

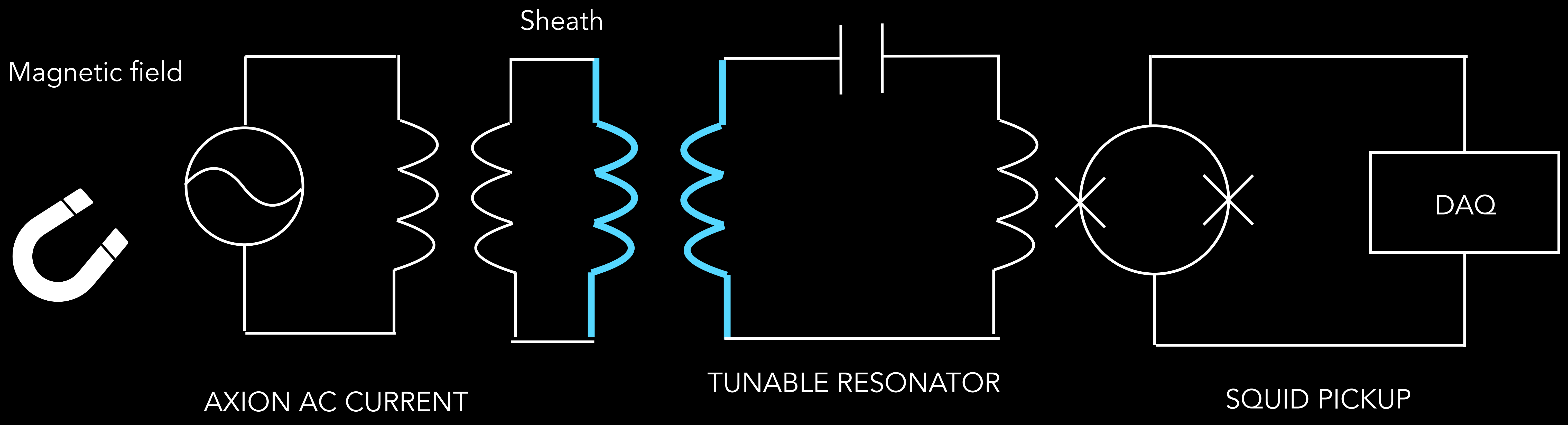

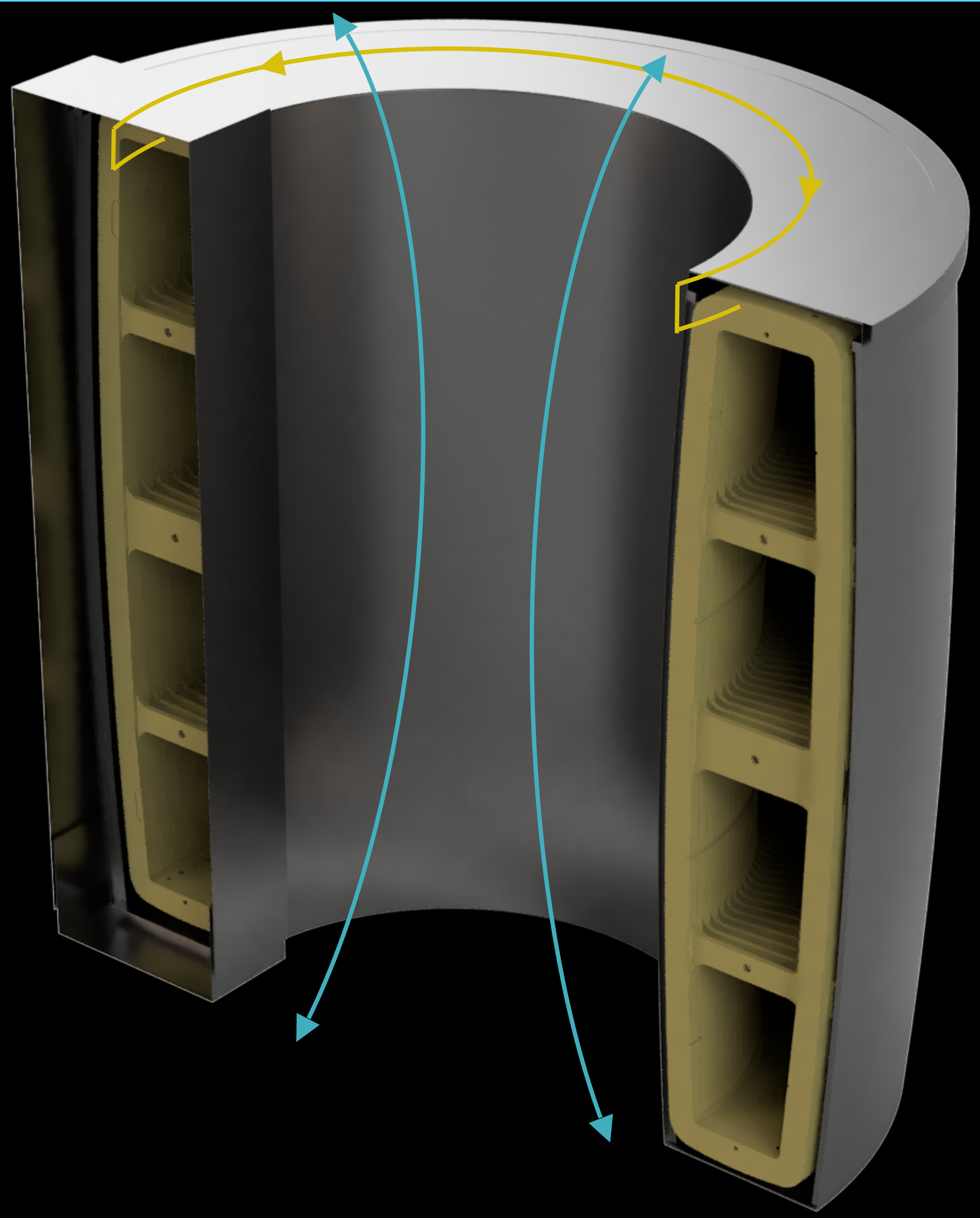

Figure courtesy of Chiara Salemi

Lumped Element Haloscope

Case Study: Static Toroidal magnet

- Magnetic field B_0
- AC axion current J_a
- Oscillating magnetic field
- Induces currents on the sheath
- Oscillating magnetic field
- Ringing up a resonator

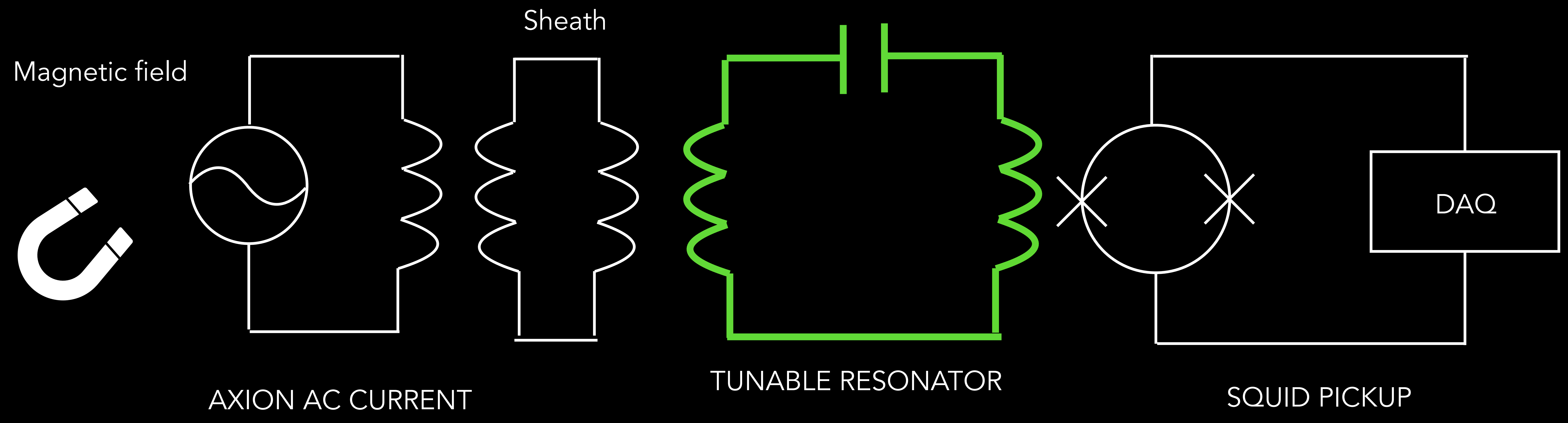

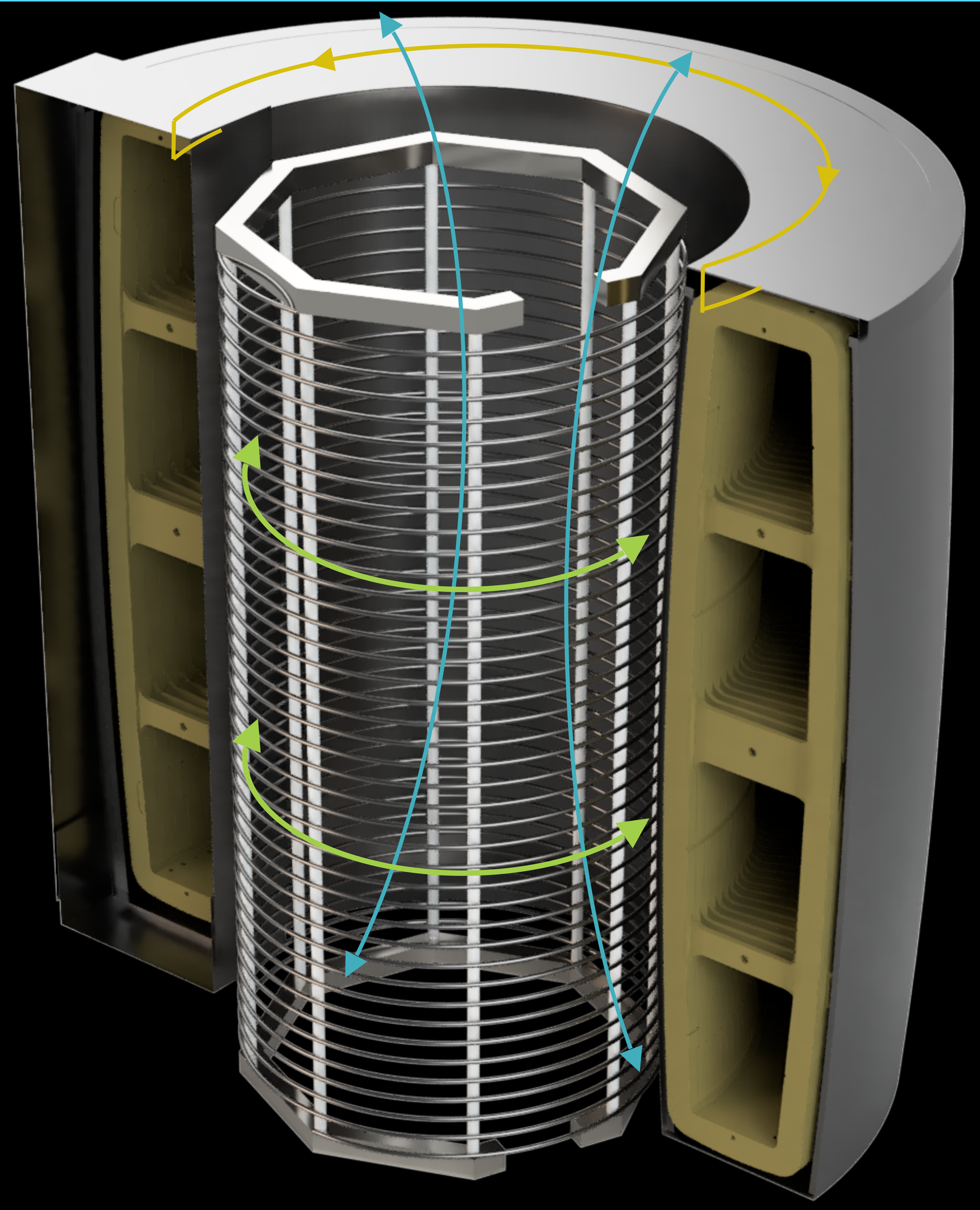

Figure courtesy of Chiara Salemi

Lumped Element Haloscope

Case Study: Static Toroidal magnet

- Magnetic field $\mathbf{B_0}$
- AC axion current $\mathbf{J_a}$
- Oscillating magnetic field
- Induces currents on the sheath
- Oscillating magnetic field
- Ringing up a resonator

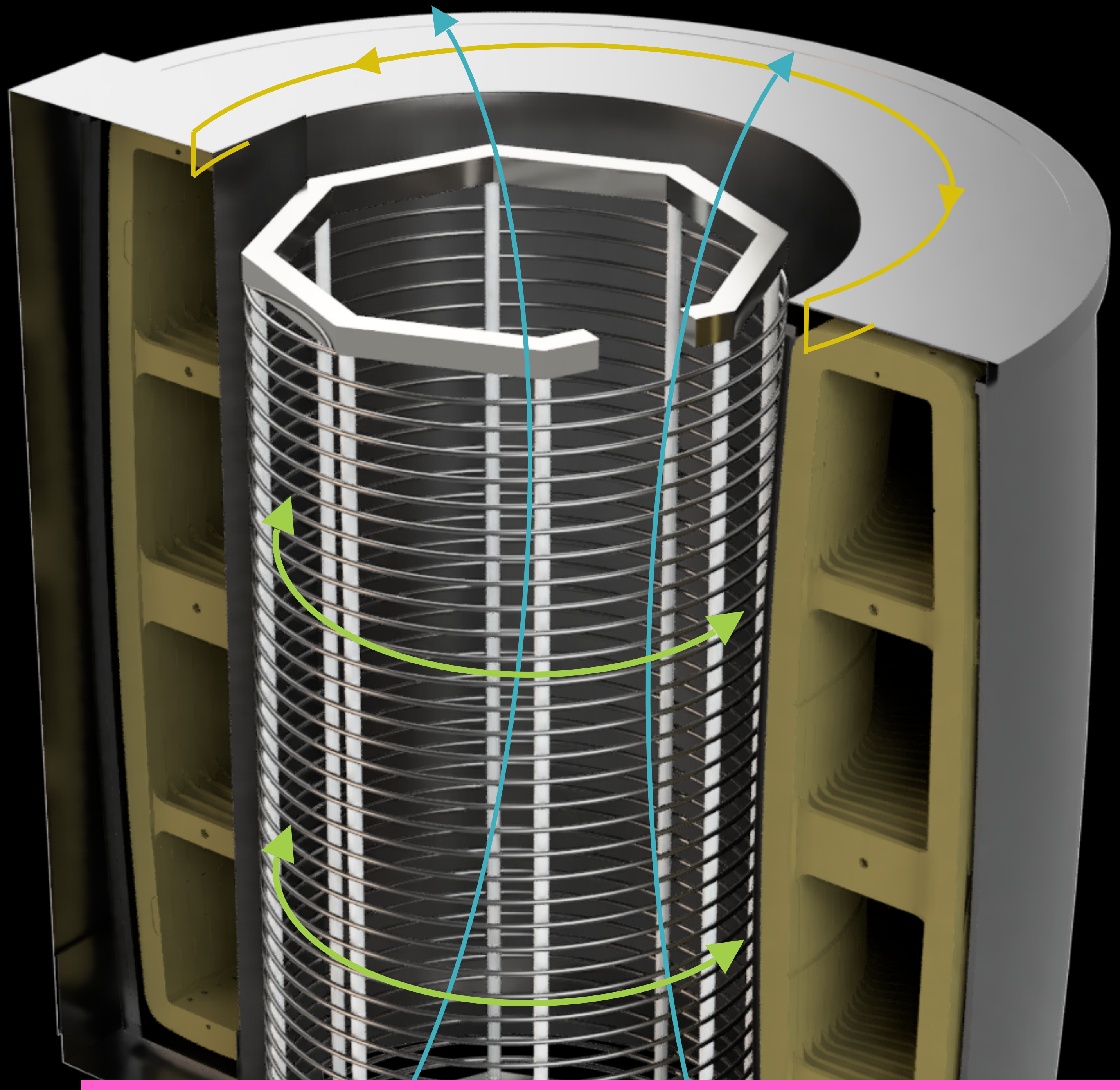

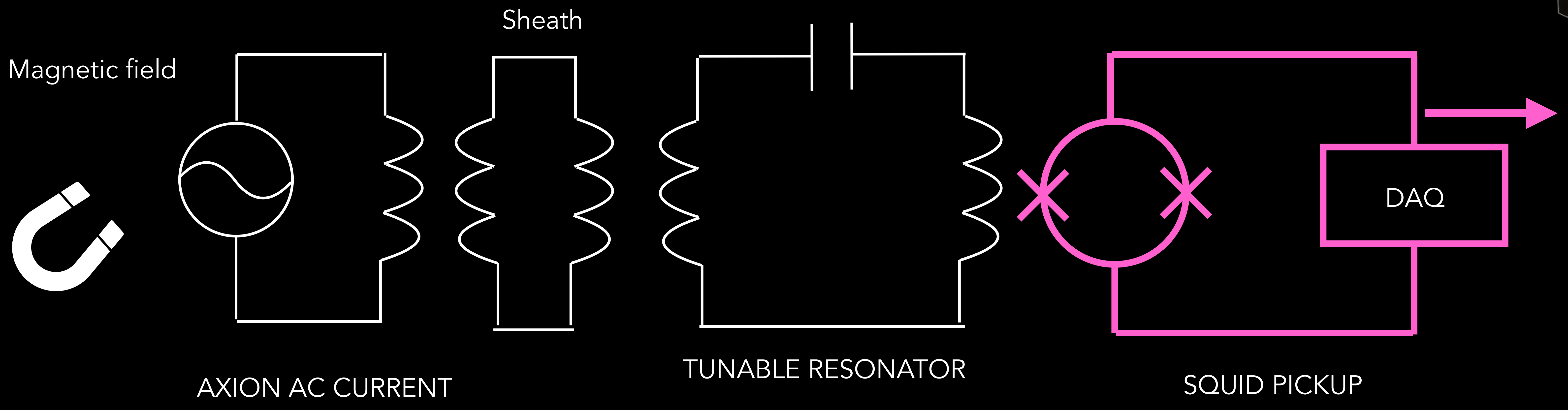

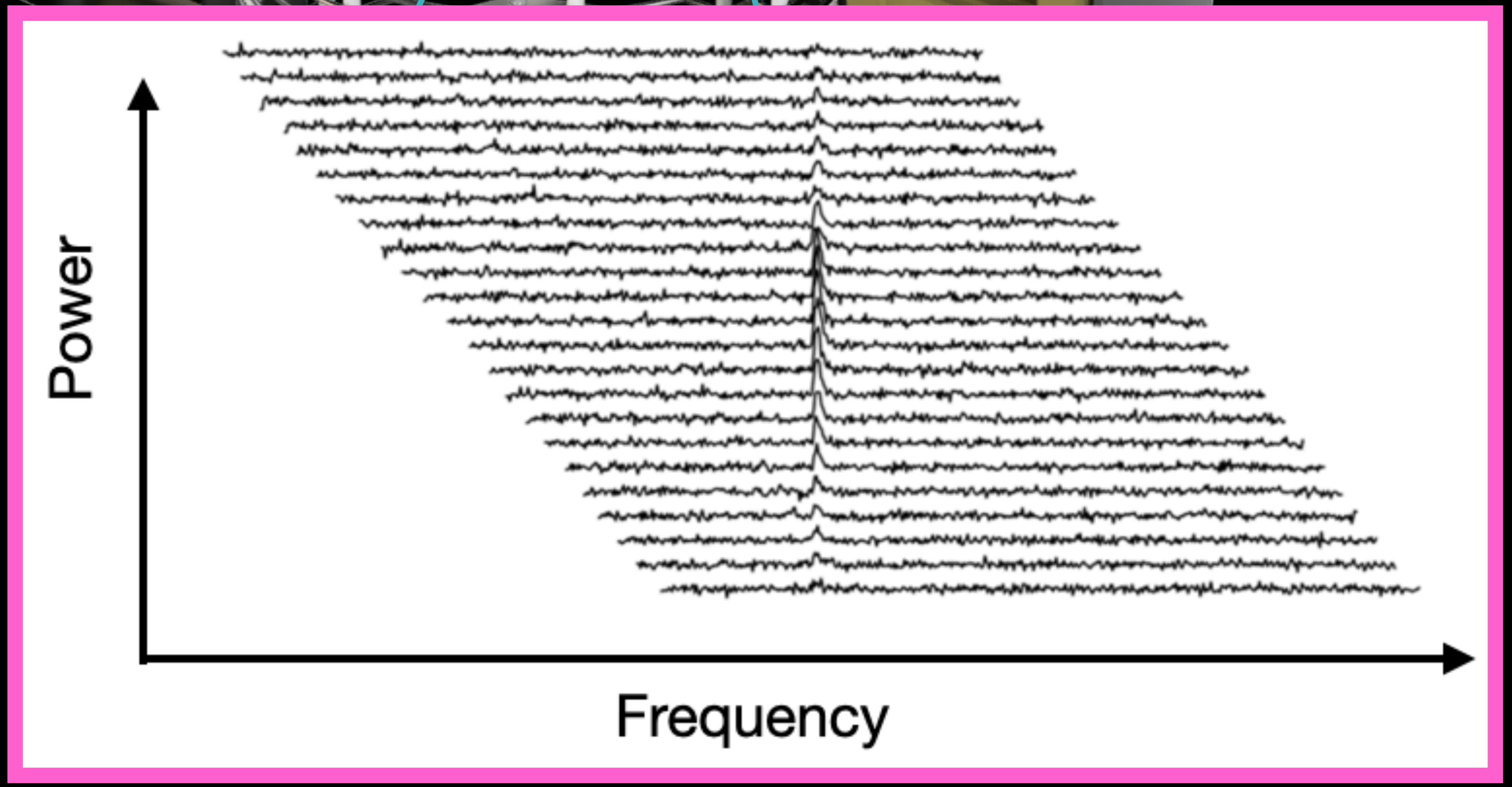

Figure courtesy of Chiara Salemi

DMRadio-50L Target

- 5 kHz — 5 MHz (20 peV — 20 neV)
- Will serve as a prototyping platform: Testbed for quantum readout technologies
- Toroidal magnet with field strength of 1 T (~113 A)
- 20 mK base temperature
- Sensitivity goal of $g_{a\gamma\gamma}=5\times10^{-15}$ GeV^{-1}

Sheath Design
Nicholas Rapidis

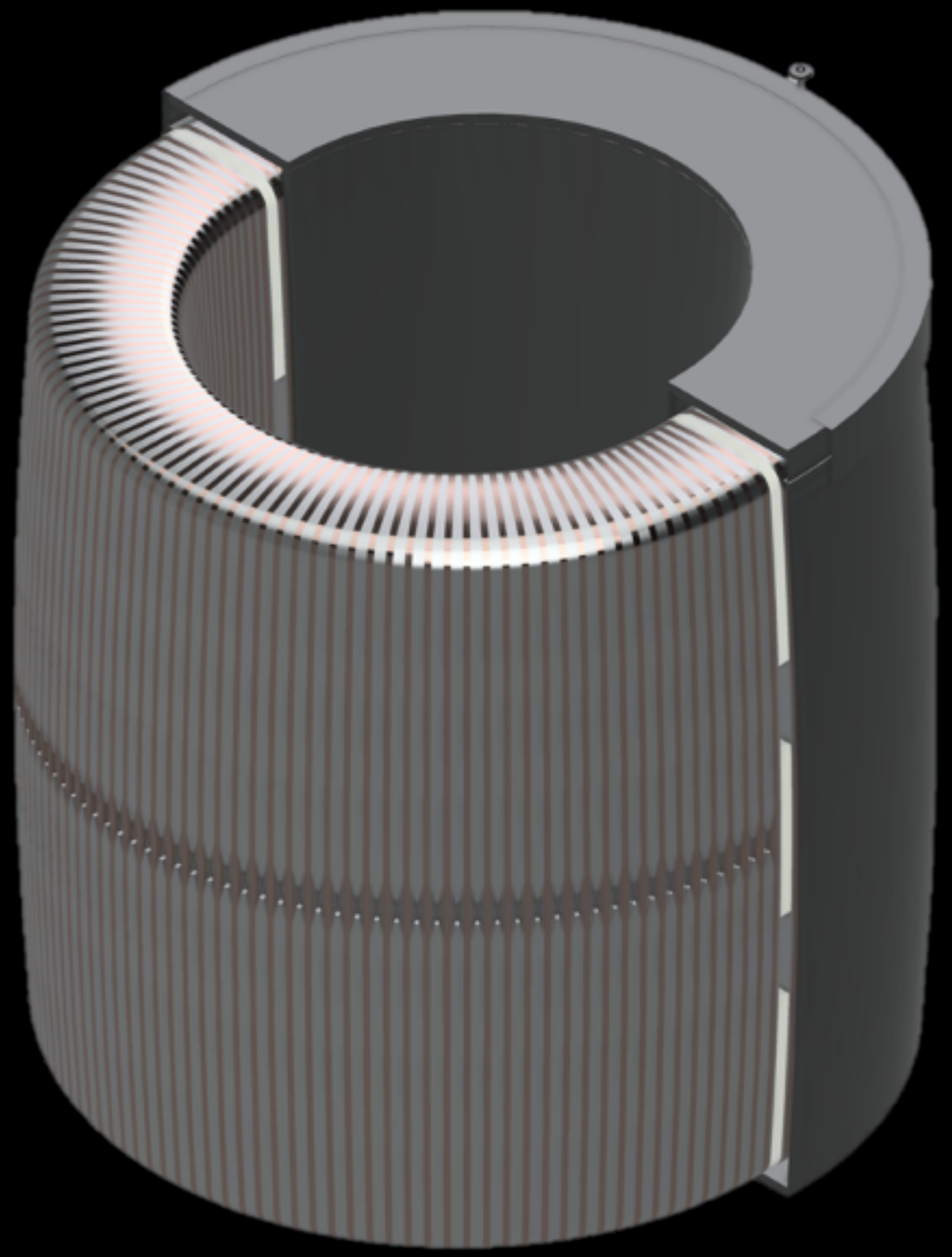

Aluminum mandrel with superconducting sheath

DMRadio-50L Resonator

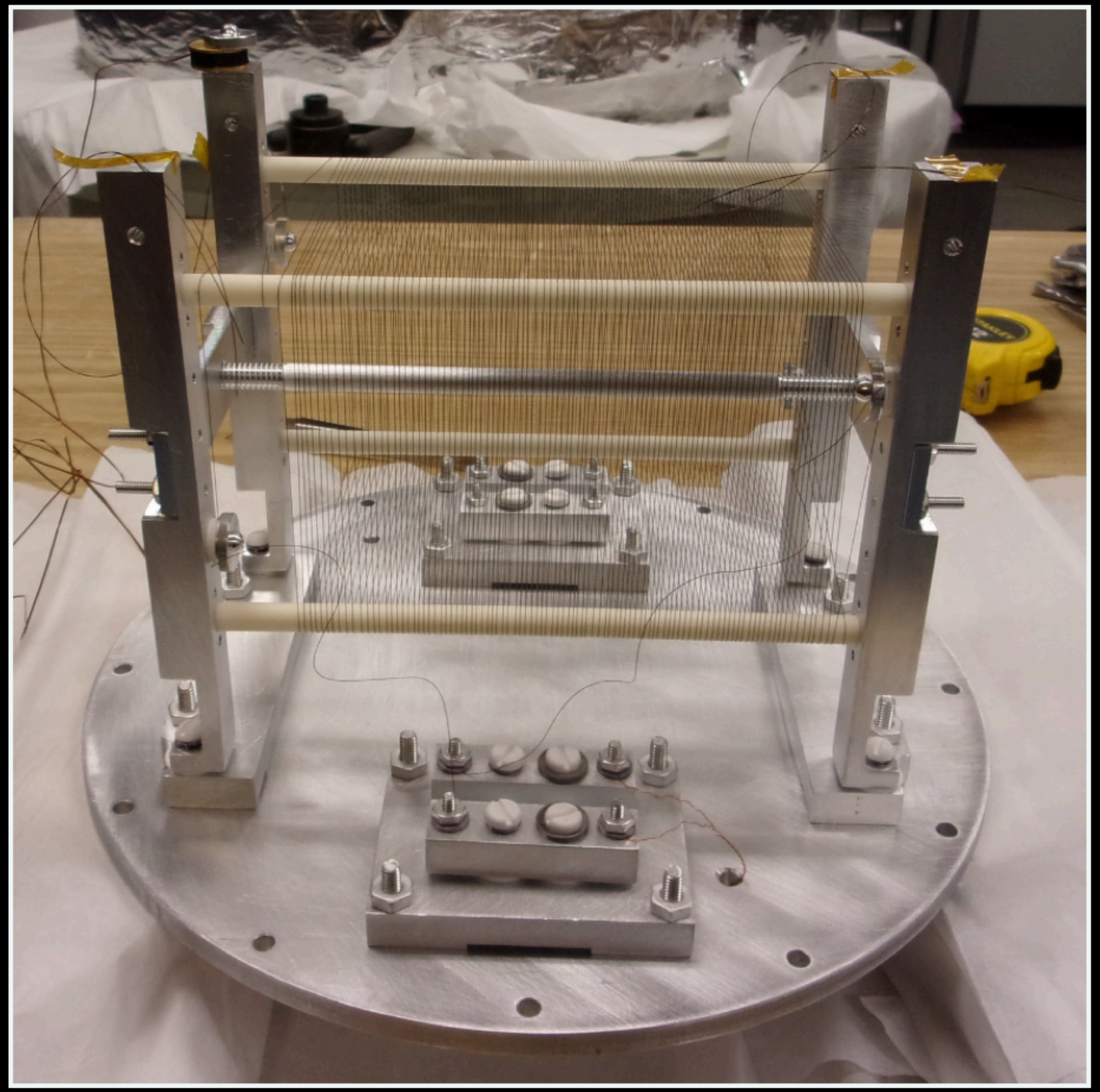

Inductor winding
Saptarshi Chaudhuri
and Roman Kolevatov

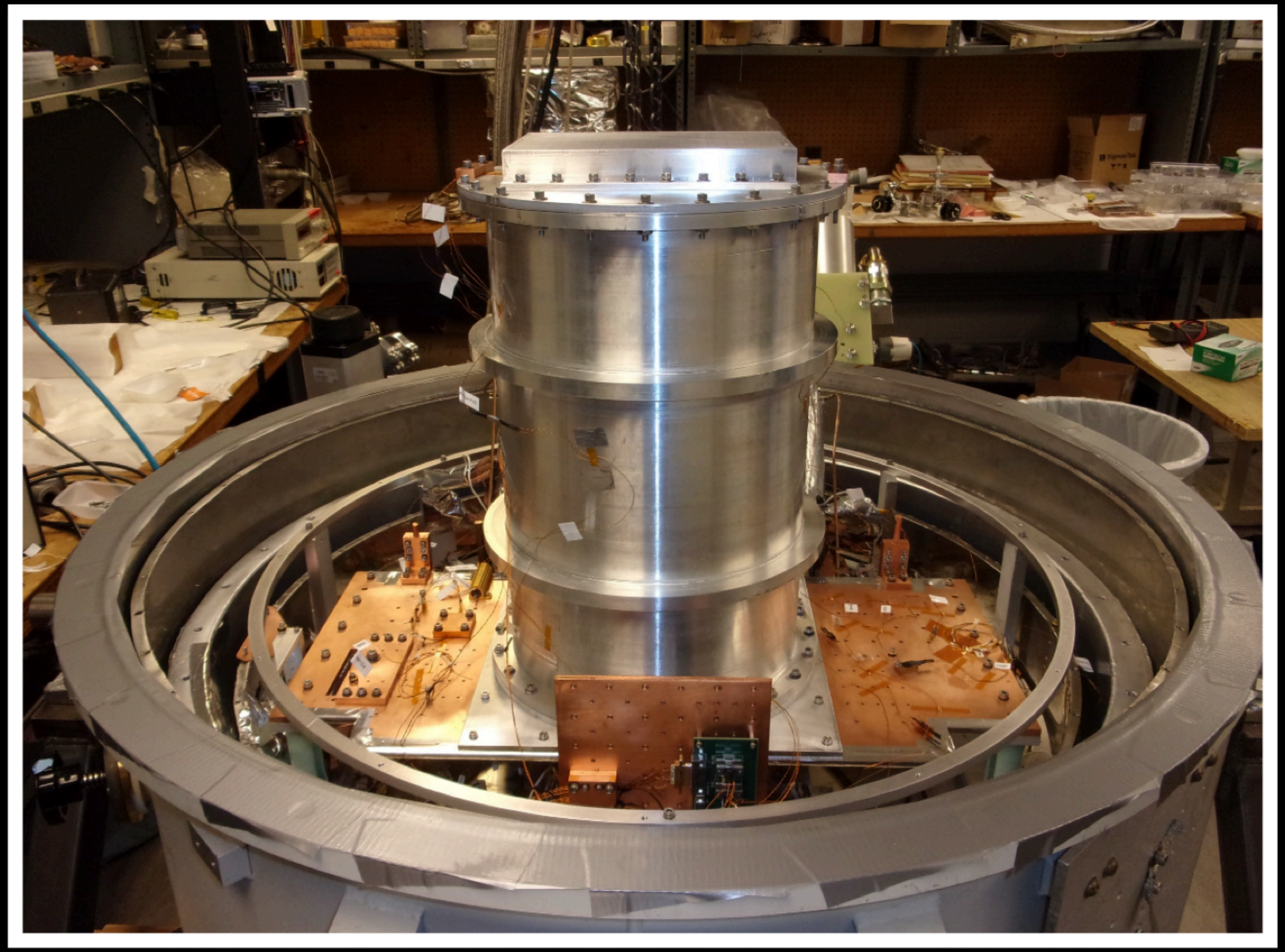

Resonator Q testing
Prototype Q = 374,000 at 300 kHz

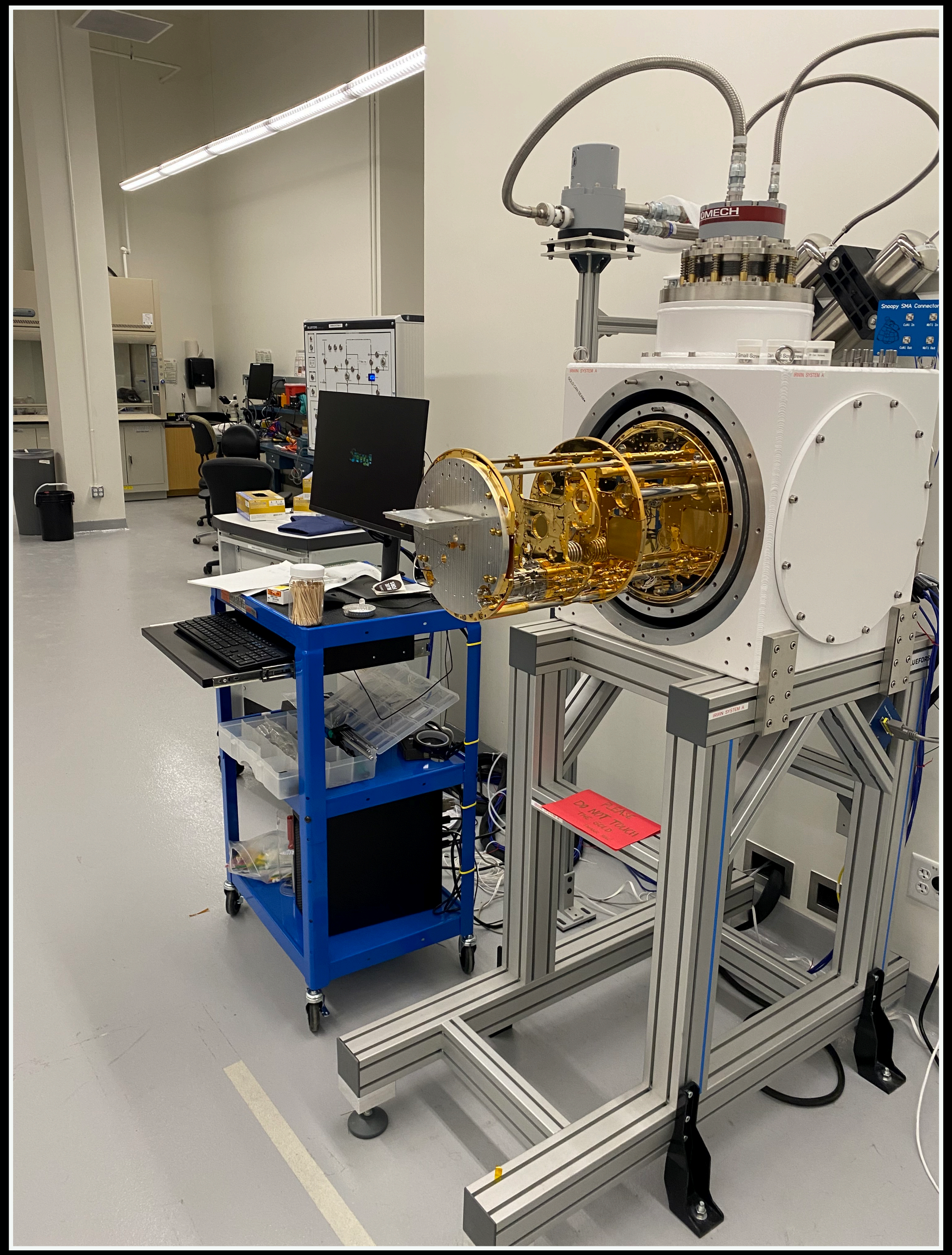

Tunable Capacitor
Joe Singh

DMRadio-50L Magnet

Structural and Thermal Connections
Alex Droster, Johny Echevers, Jessica Fry

Mandrel construction and winding

Superconducting Systems Inc

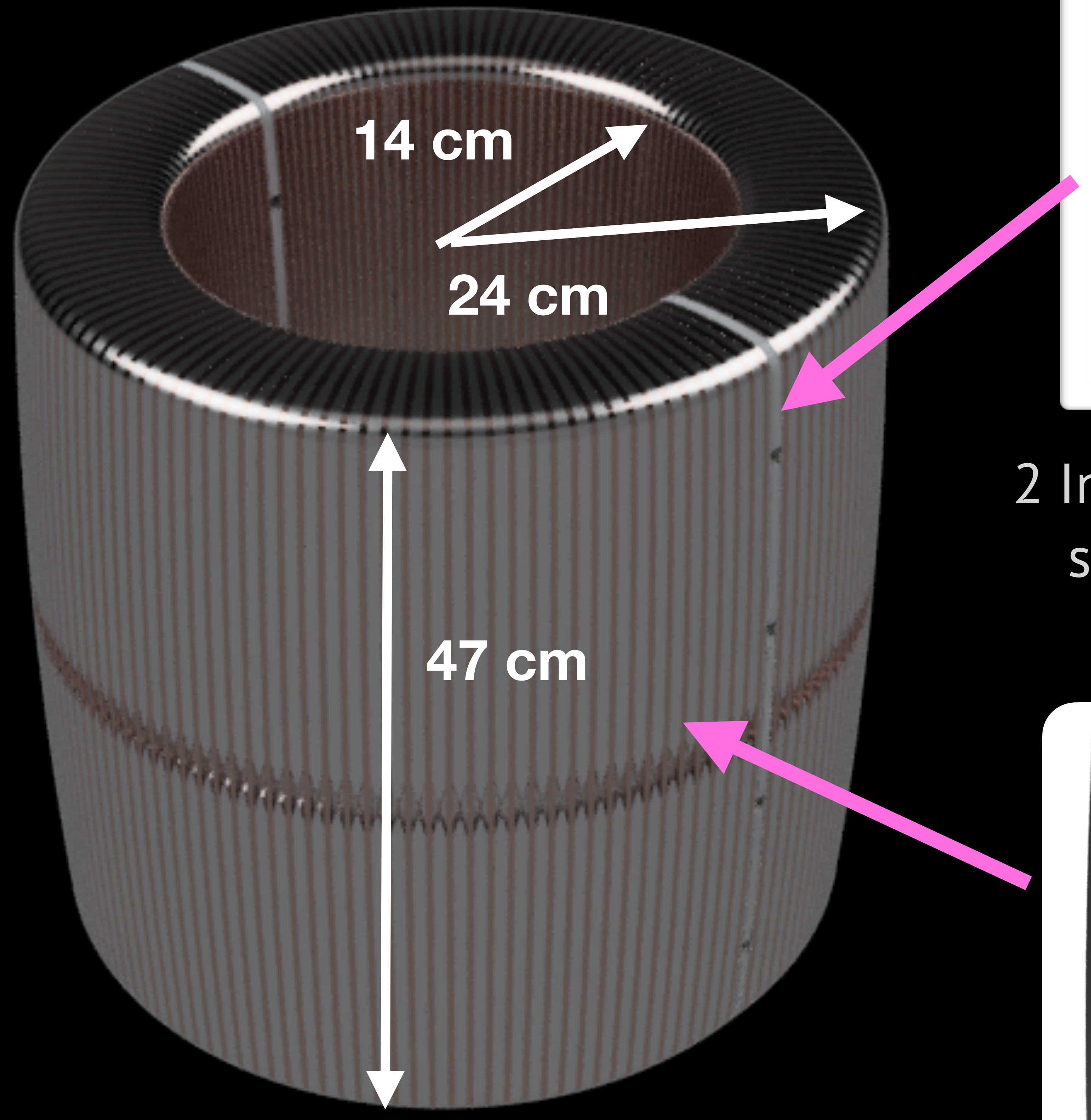

Aluminum mandrel

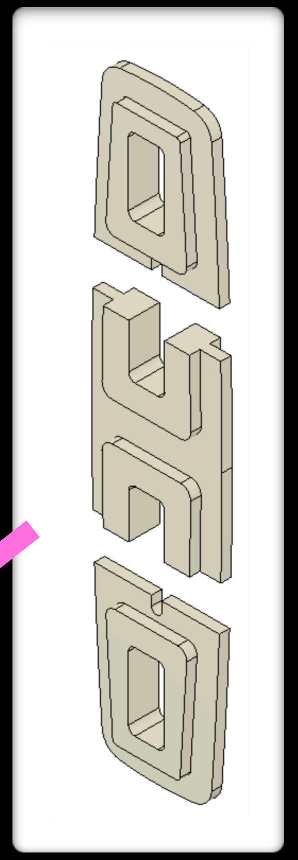

2 Insulating spacers

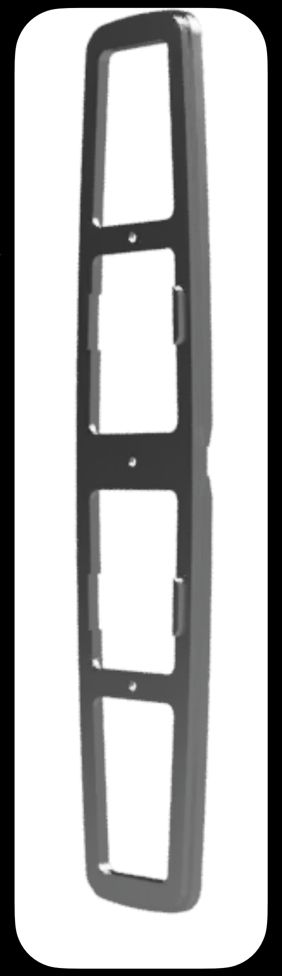

69x2 Mandrel wedges

DMRadio-50L Cryostat

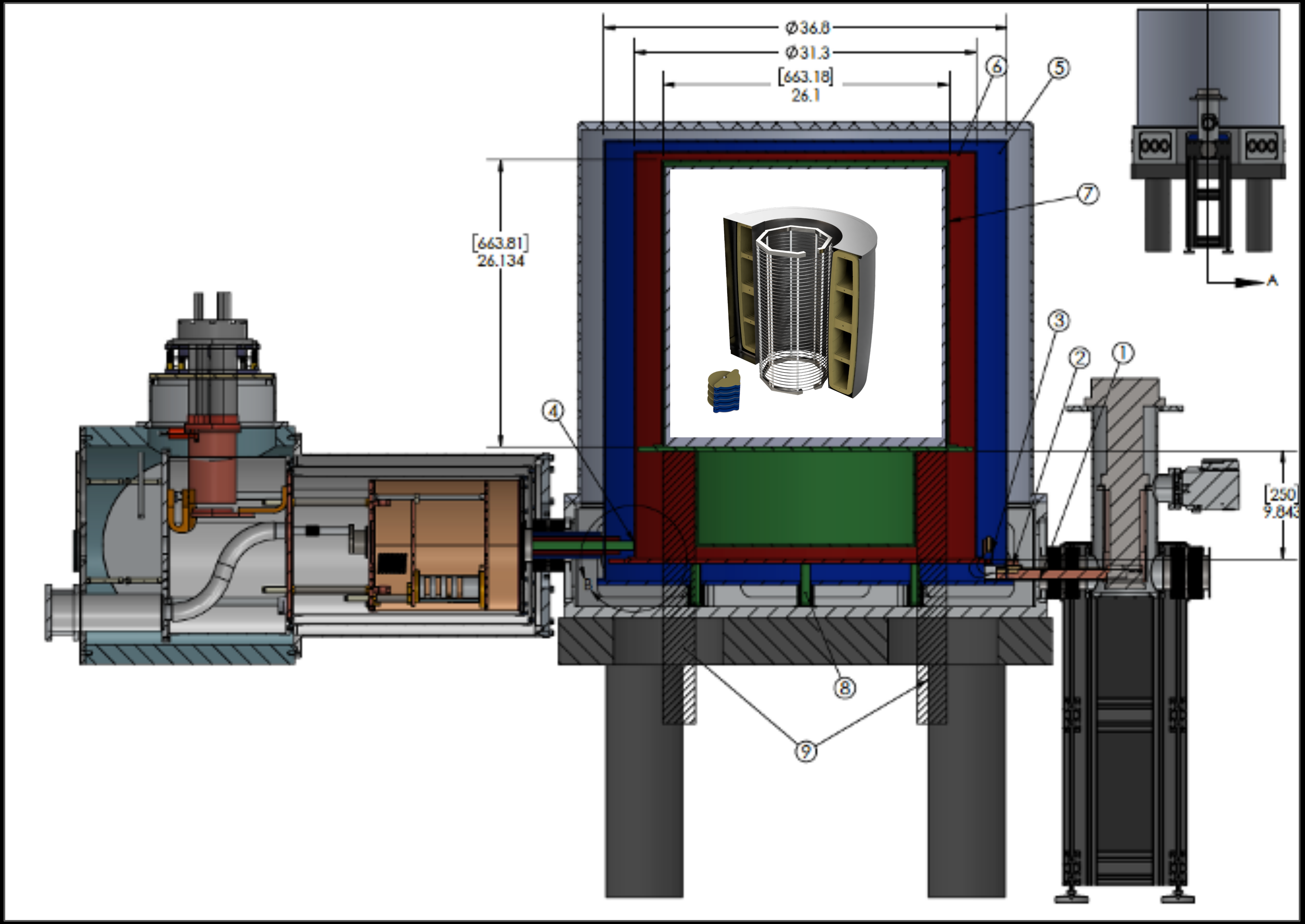

- Cryostat: Fournine Design
- BlueFors LH Dilution Refrigerator
- Cold snout to cool resonator

Maria Simanovskaia,
Aya Keller

Quantum sensing techniques + R&D

- Increasing the bandwidth via SQUID coupling to the resonator

- Radiofrequency Quantum Upconverters (RQUs)

- Bode-Fano Evasion

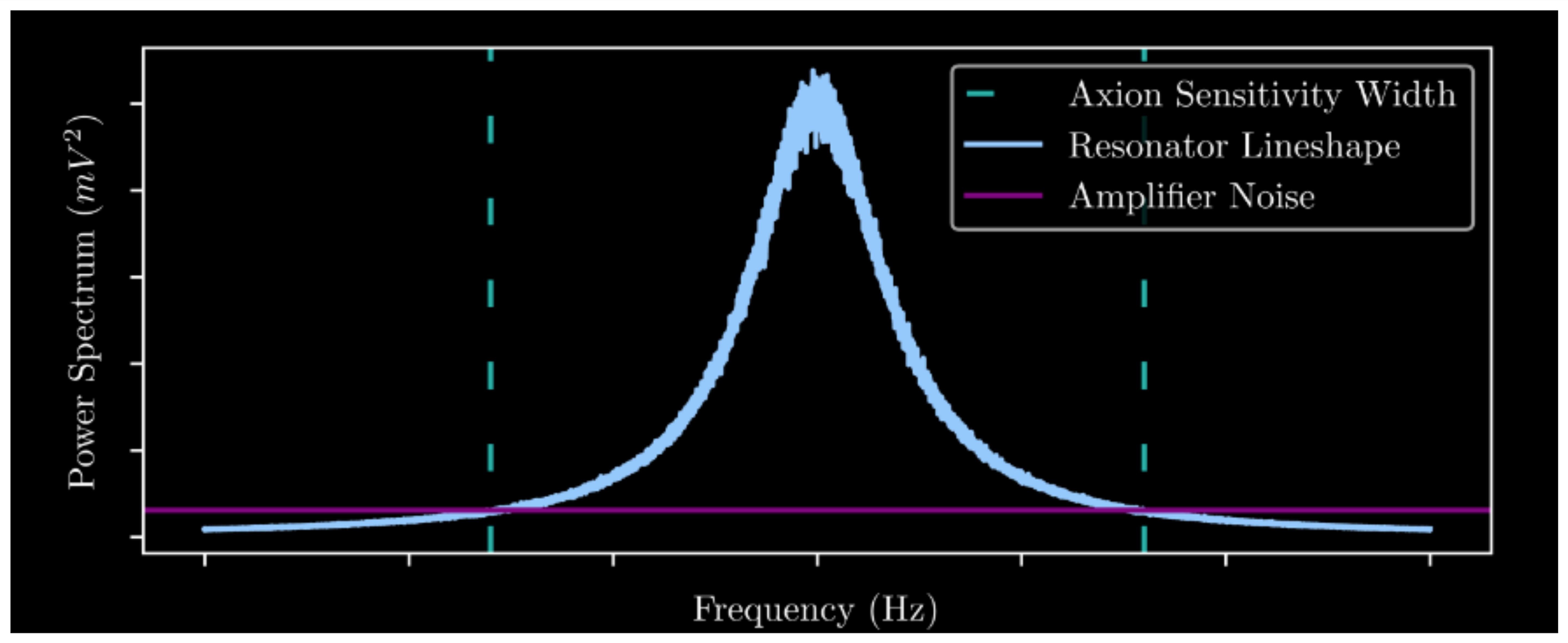

…happy to field more questions later!

DMRadio-m^3 Target

- 10 — 200 MHz (40 neV — 1.2 μeV)
  - 30 — 200 MHz at DFSZ sensitivity
- Solenoidal magnet
- Coaxial copper pickup structure
- 20 mK base temperature
- 4.7 T magnetic field

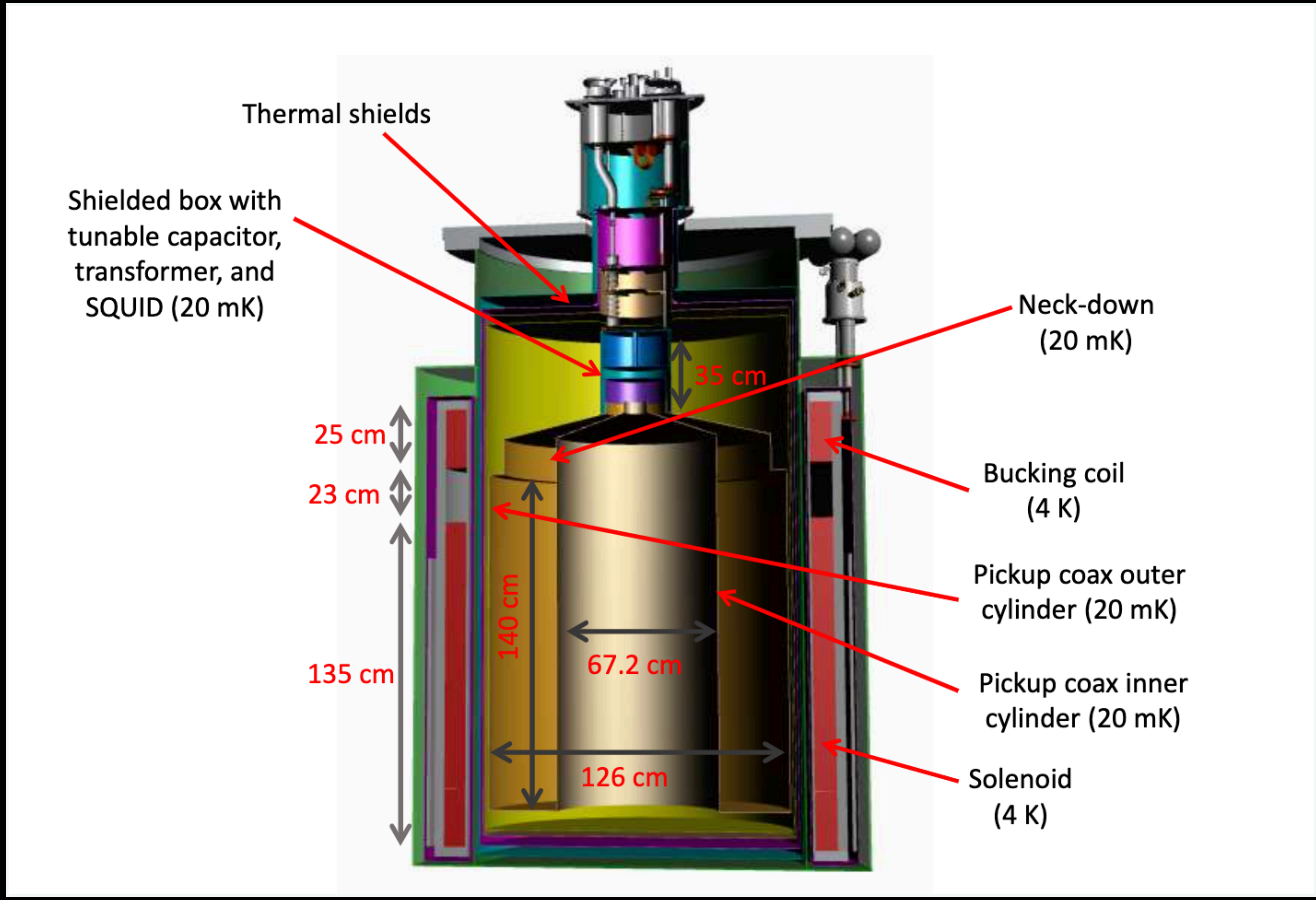

DMRadio-m^3 at SLAC

- DMRadio-m^3 has received DOE DMNI funding
- Will be constructed at SLAC National Lab
- Electromagnetic modeling and end-to-end sensitivity calculations are on the arXiv: *arXiv:2302.1408*
- Experience with design and operation of DMRadio-50L will inform design of DMRadio-m^3

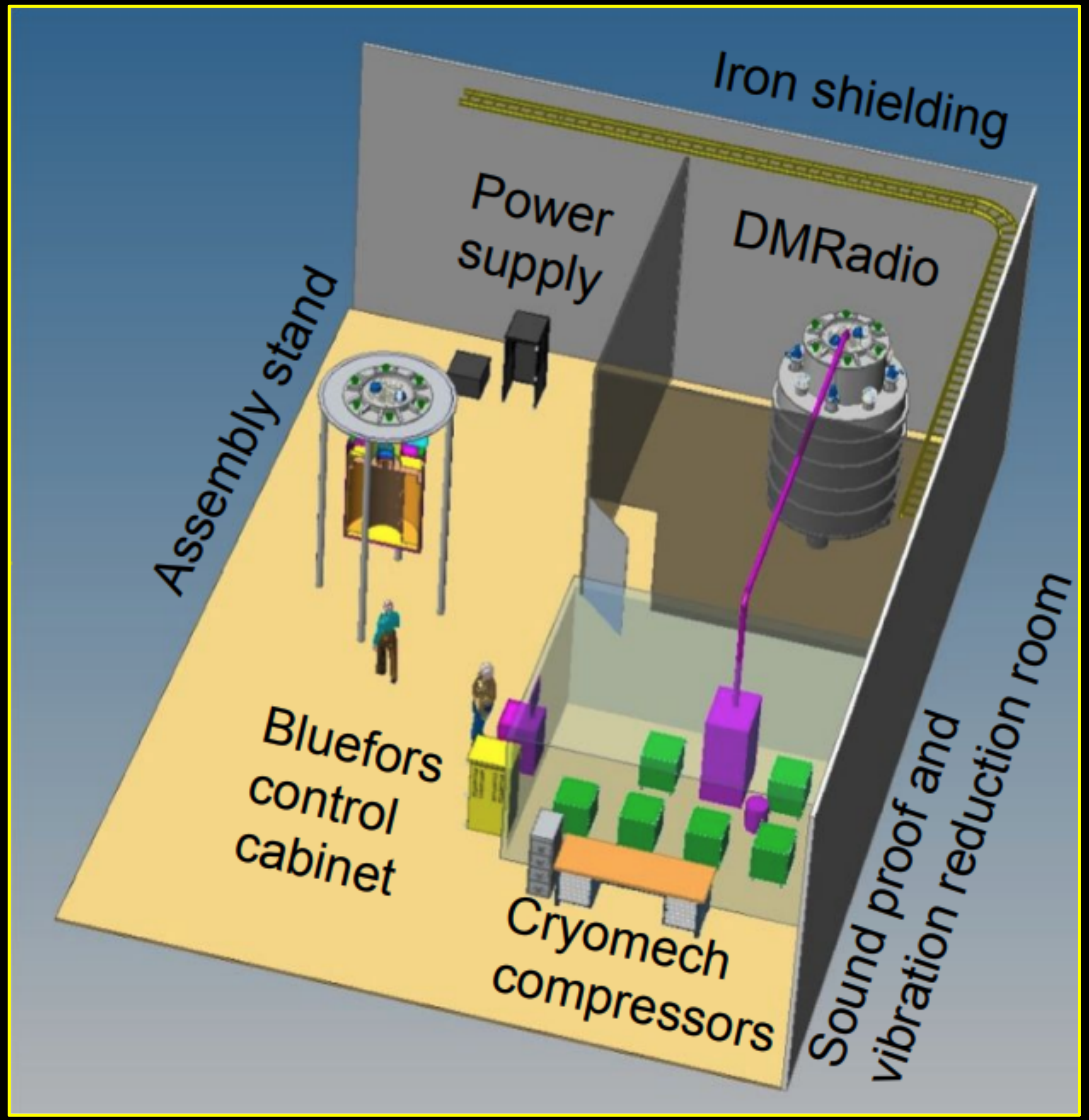

DMRadio Program

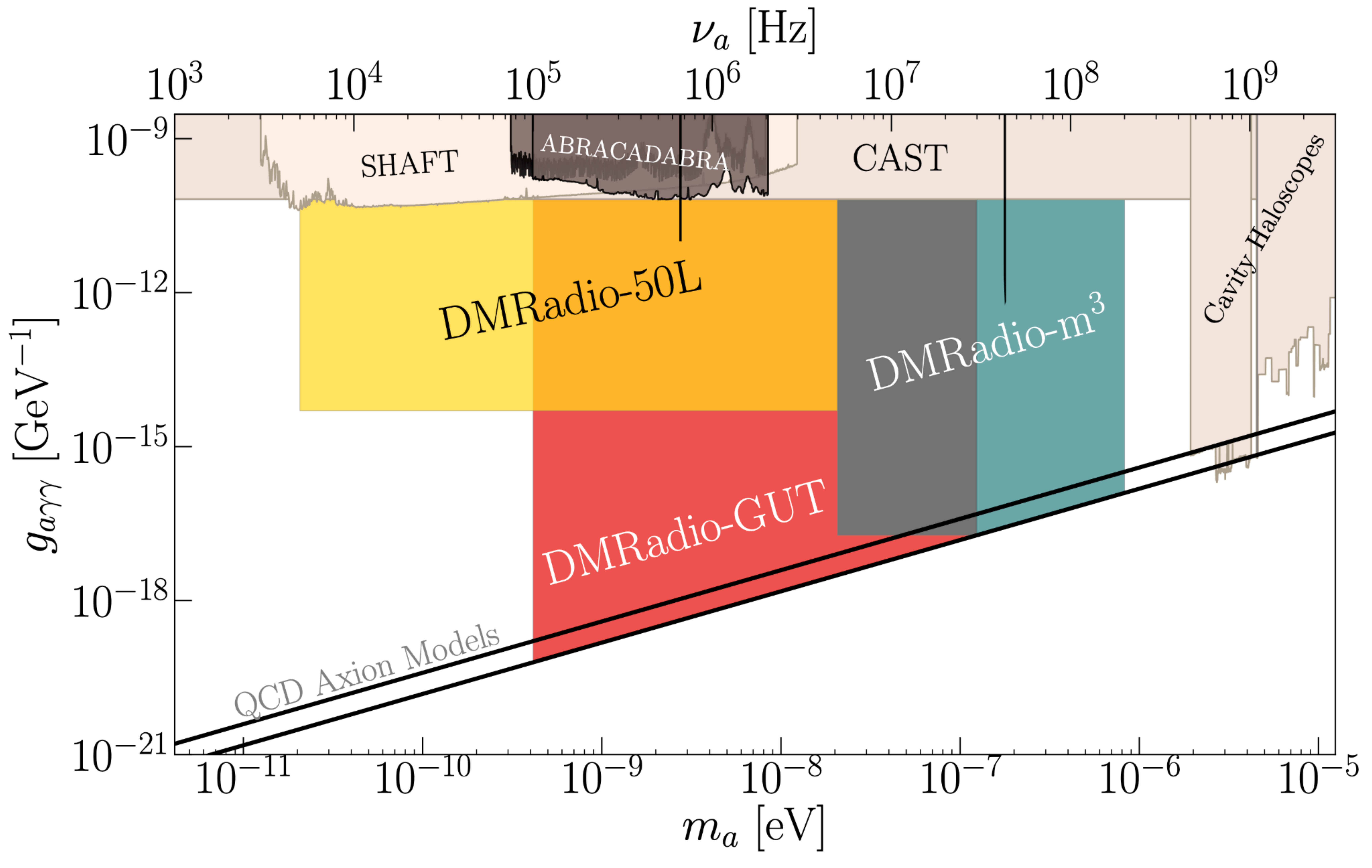

AXIONS AND WAVE-LIKE DARK MATTER

CAVITY REGIME

ADMX, CAPP, HAYSTAC, ORGAN…

ADMX
AXION DARK MATTER EXPERIMENT

ADMX Collaboration

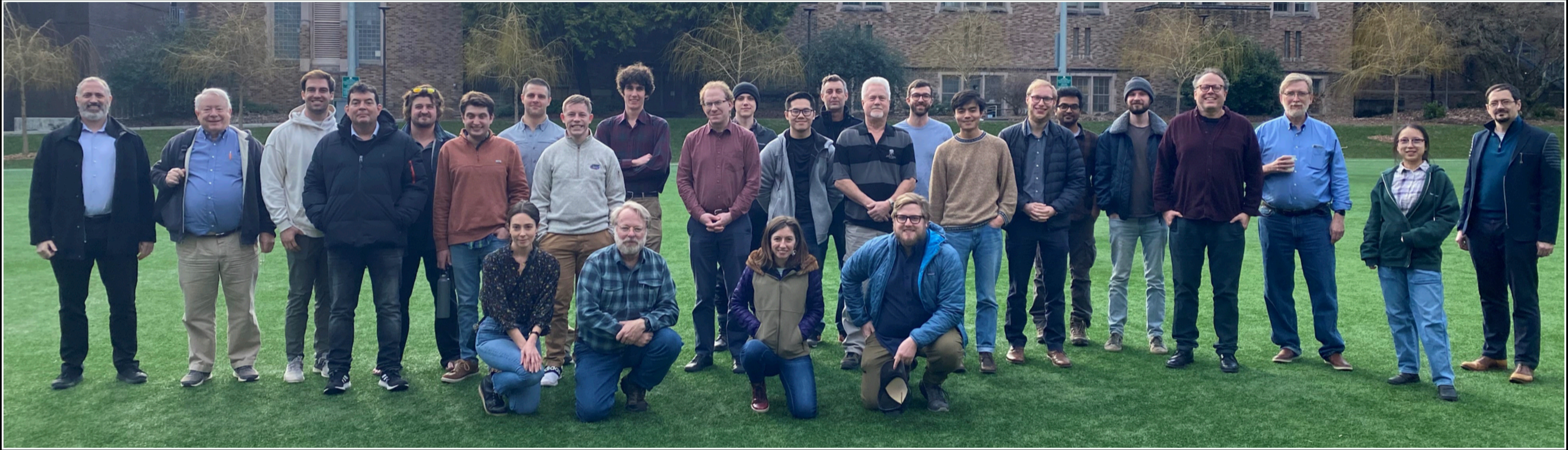

University of Washington 1861
Lawrence Livermore National Laboratory
Berkeley UNIVERSITY OF CALIFORNIA
The University of Chicago 1890
Fermilab
Pacific Northwest NATIONAL LABORATORY
Washington University in St. Louis 1853
UF UNIVERSITY of FLORIDA
The University Of Sheffield.
THE UNIVERSITY OF WESTERN AUSTRALIA
ILLINOIS INSTITUTE OF TECHNOLOGY
Los Alamos NATIONAL LABORATORY EST. 1943

Cavity Haloscope

Form factor describes coupling of the axion to the mode

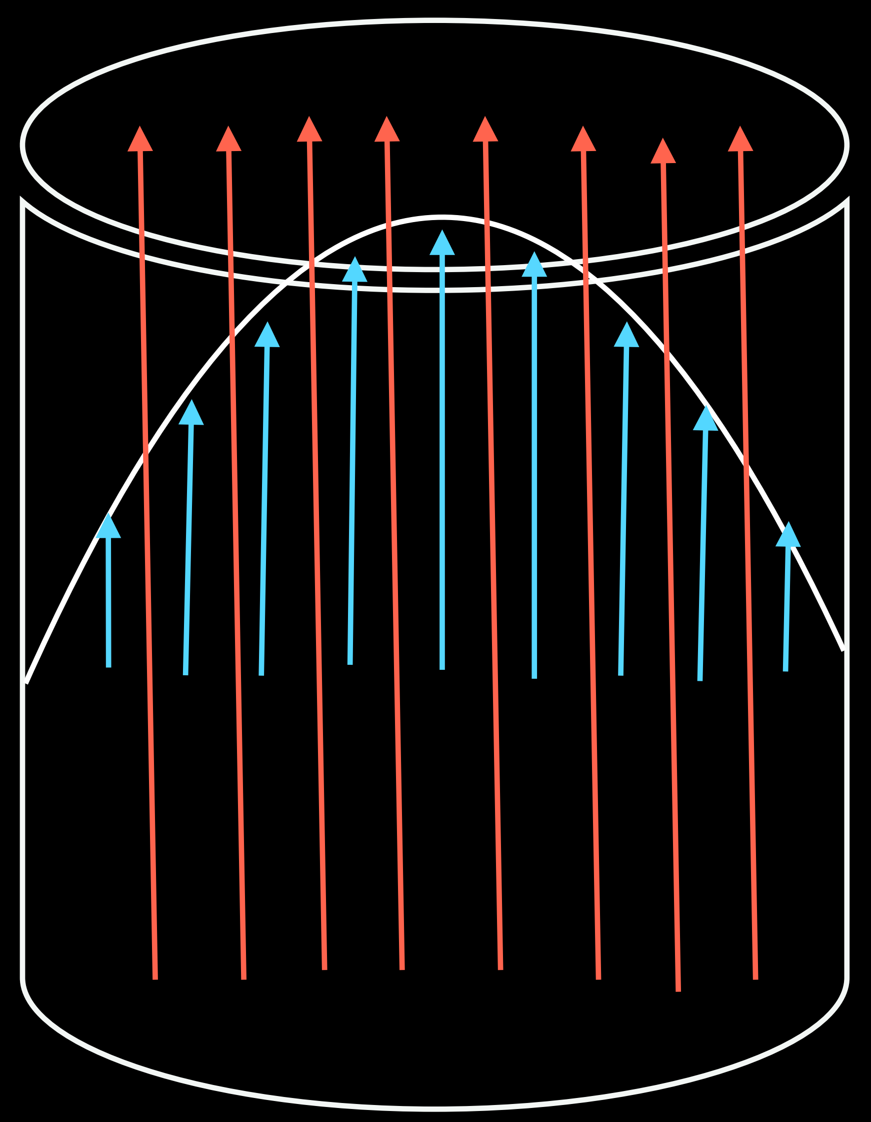

Non-zero form factor

Red is static magnetic field
Blue is axion electric field

$$C_{010} = \frac{\left|\int dV\, \vec{B}_{\rm ext} \cdot \vec{E}_{\rm a}\right|^2}{B_{\rm ext}^2 \int dV\, \epsilon_{\rm r} |\vec{E}_{\rm a}|^2}$$

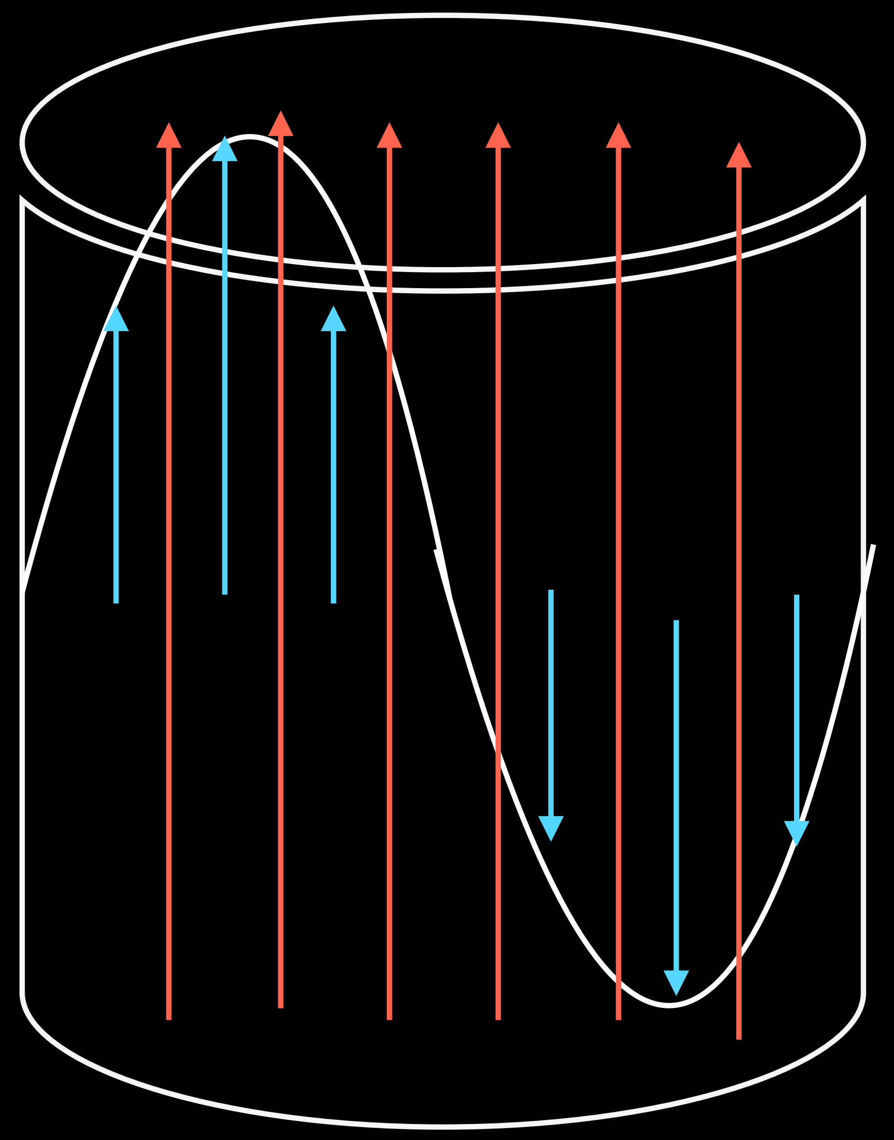

Zero form factor

ADMX: Axion couples most strongly to TM010 mode

Cavity Haloscope

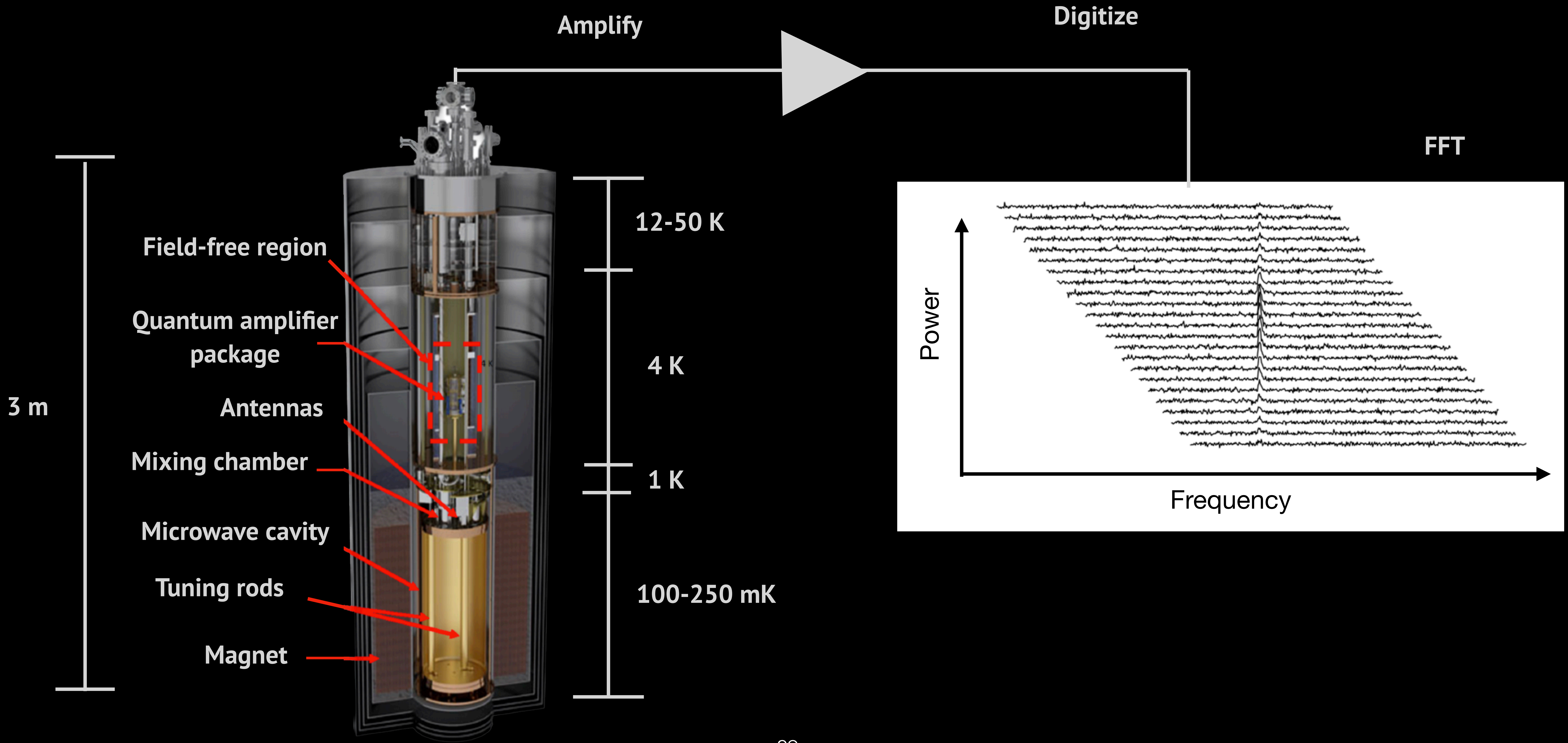

Cavity Haloscope

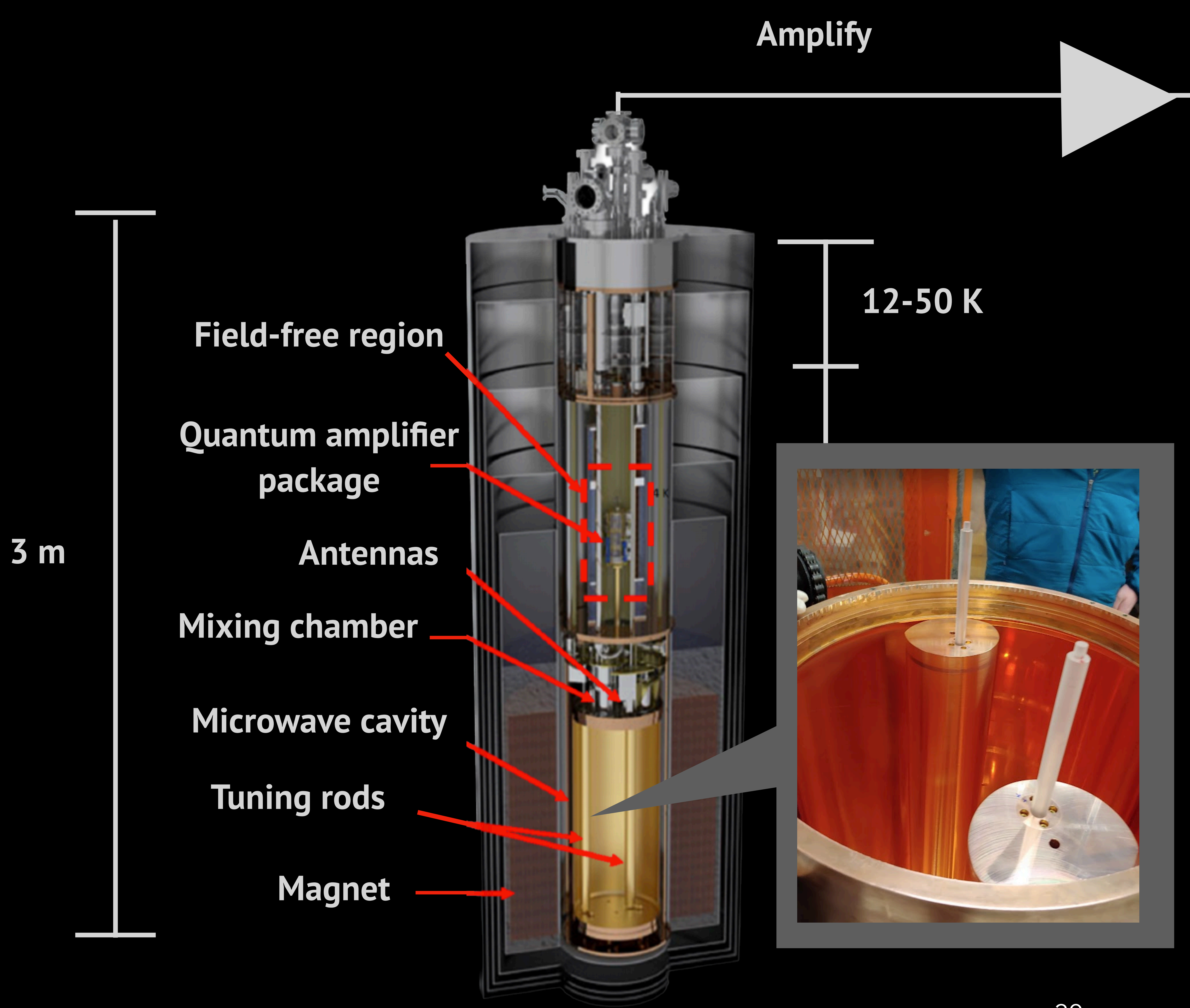

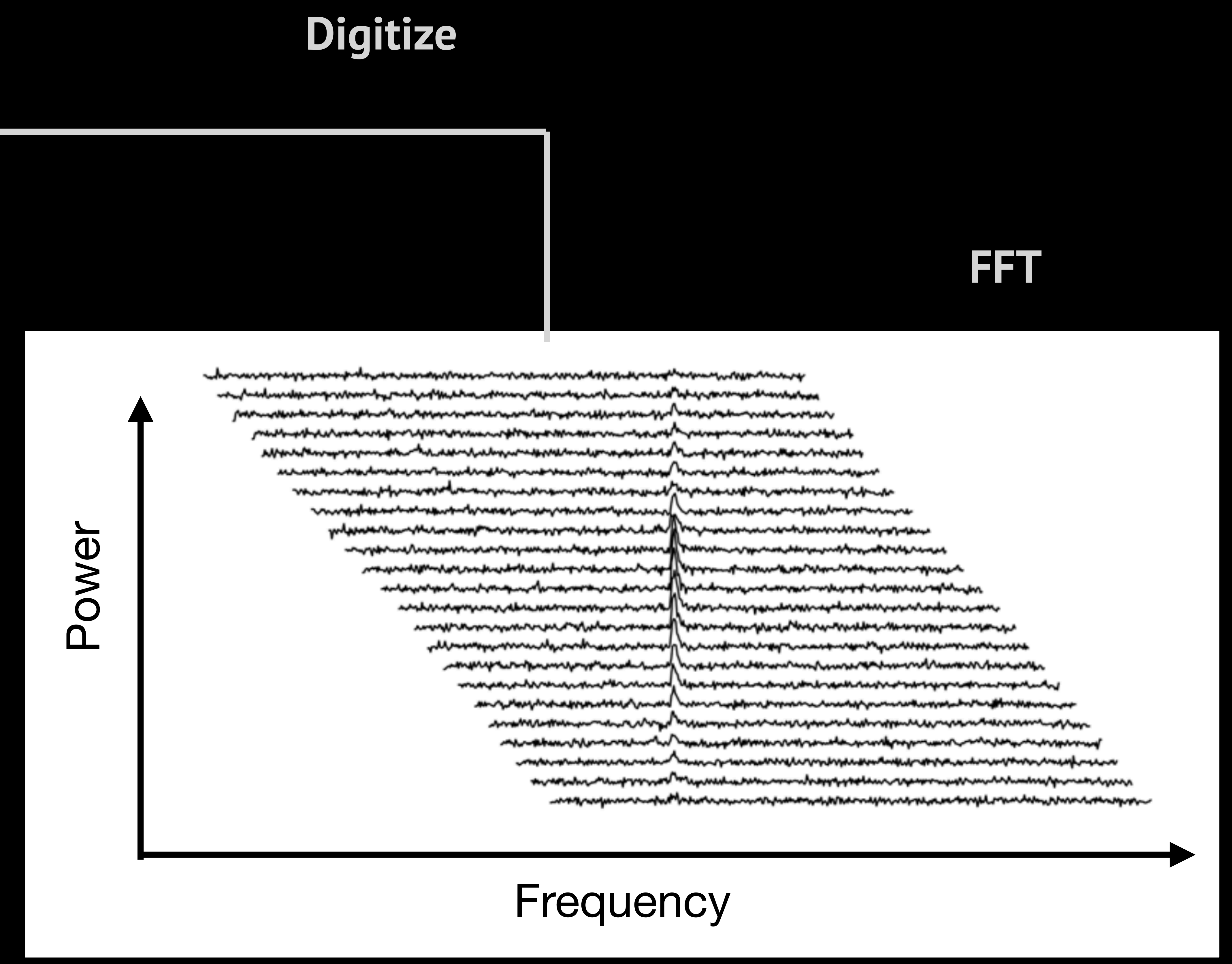

Axion mass unknown: tuning rods required

Cavity Haloscope

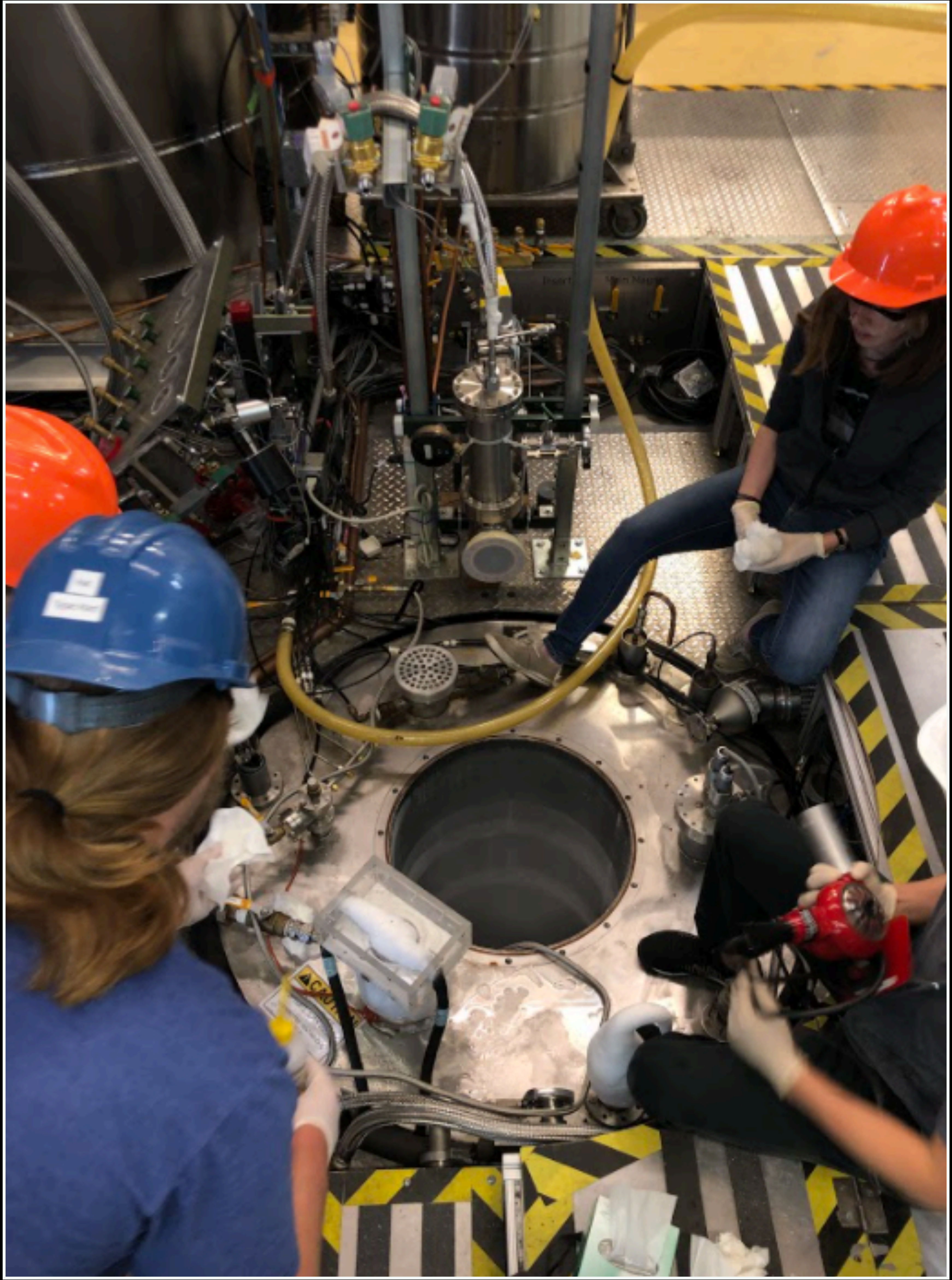

Ultra low noise receiver

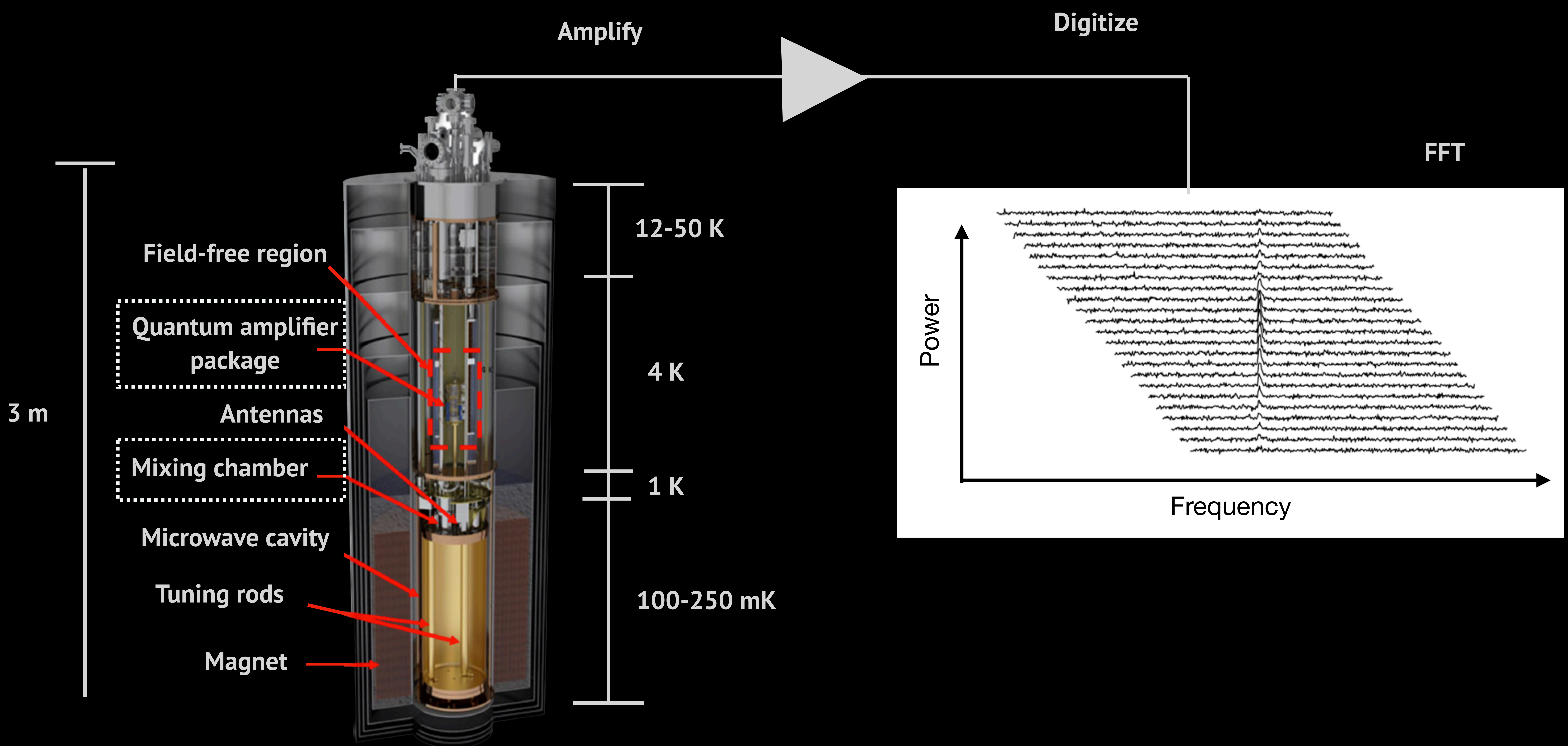

Quantum Amplification

- Microstrip SQUID Amplifier (2017)
- Josephson Parametric Amplifier (2018—today)
    - Anharmonicity leads to energy transfer from pump to signal
    - Josephson Junction is non-linear element

JPA courtesy of
Irfan Siddiqi

Figures courtesy of Shahid Jawas

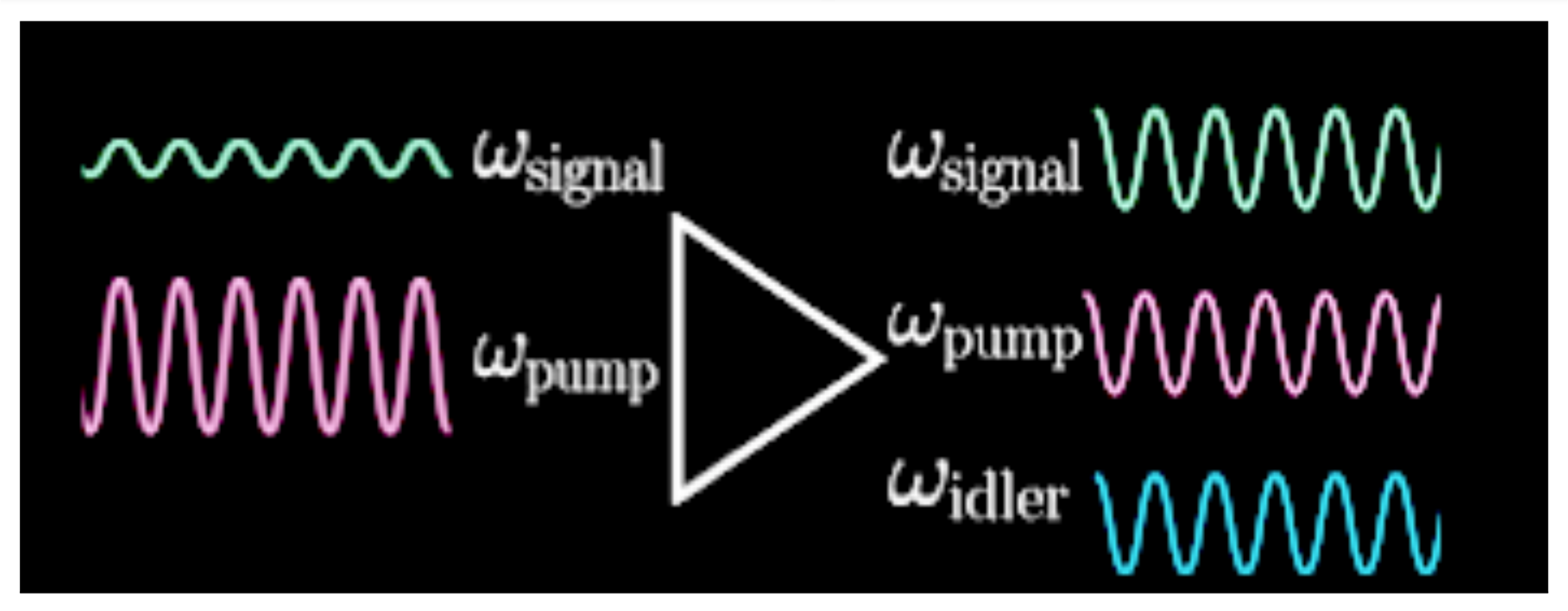

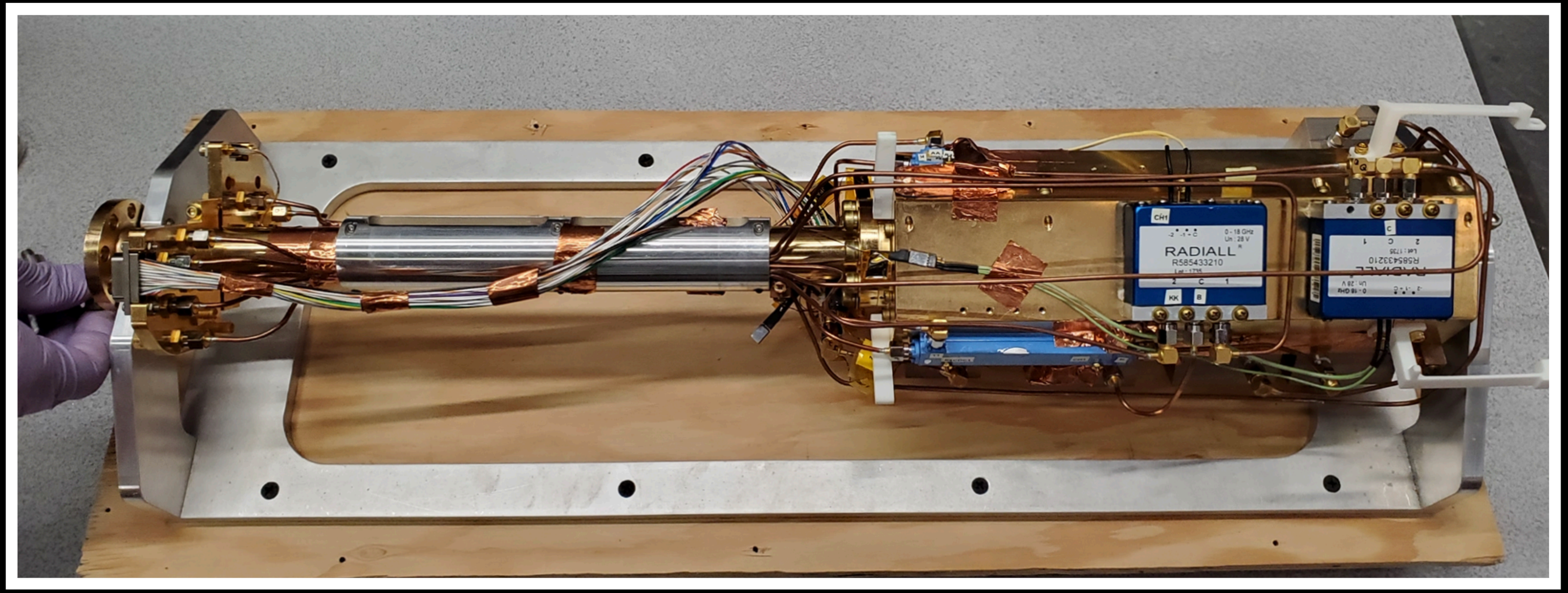

~2 ft

Field cancellation coil + Mu-metal shielding required for optimal performance

ADMX Exclusion Limits (Published)

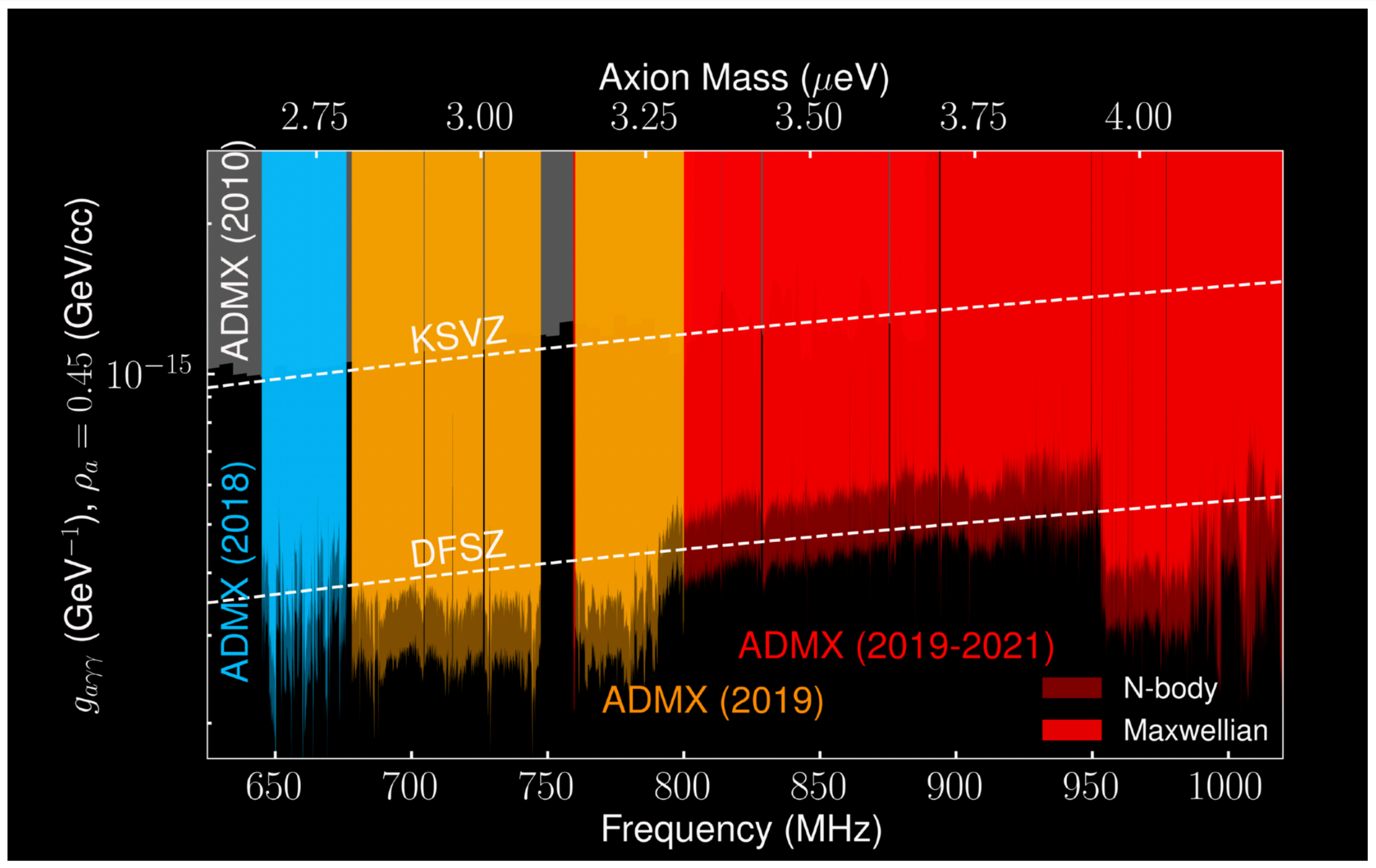

ADMX Preliminary Sensitivity

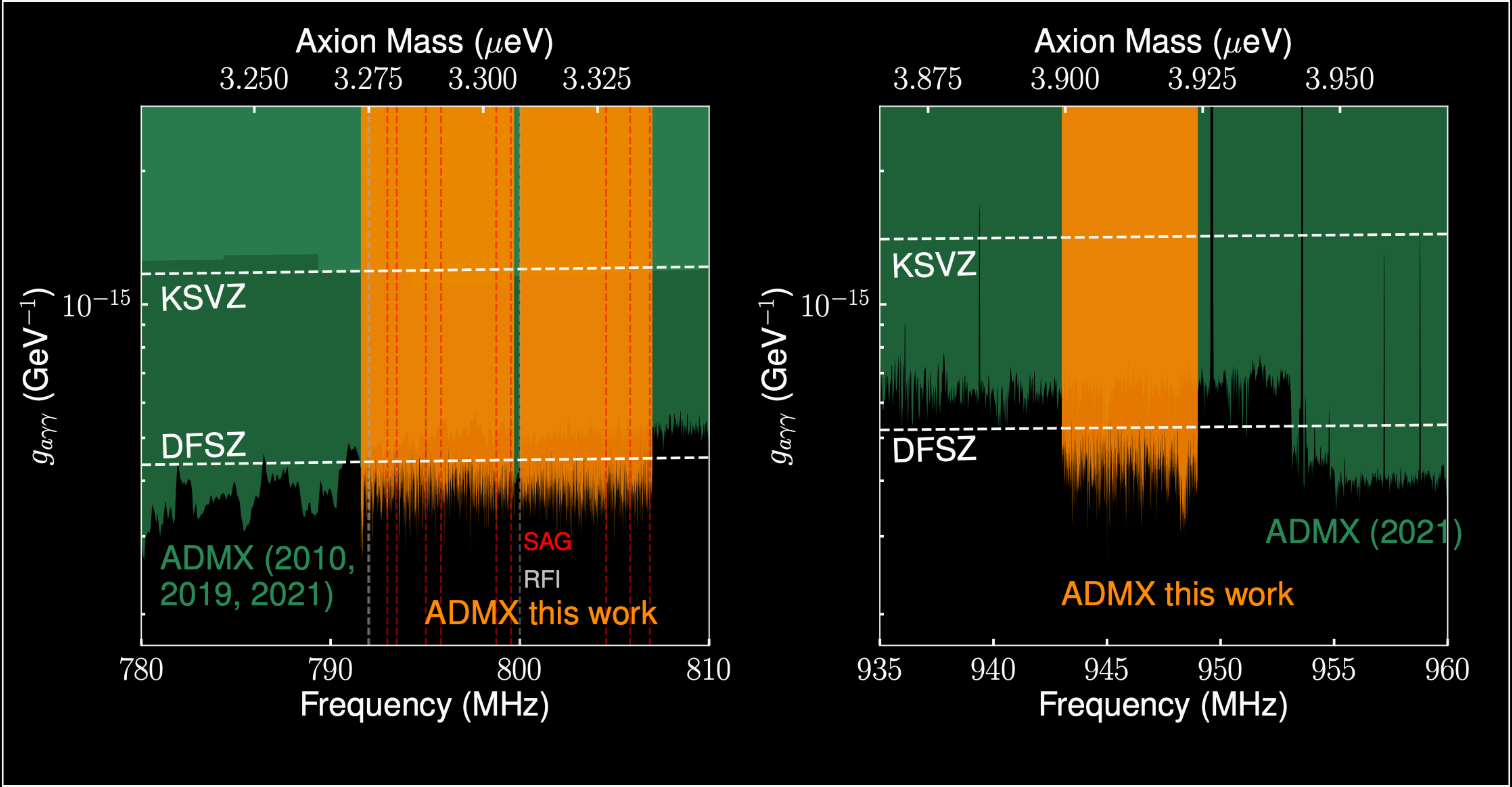

ADMX high frequency prototype

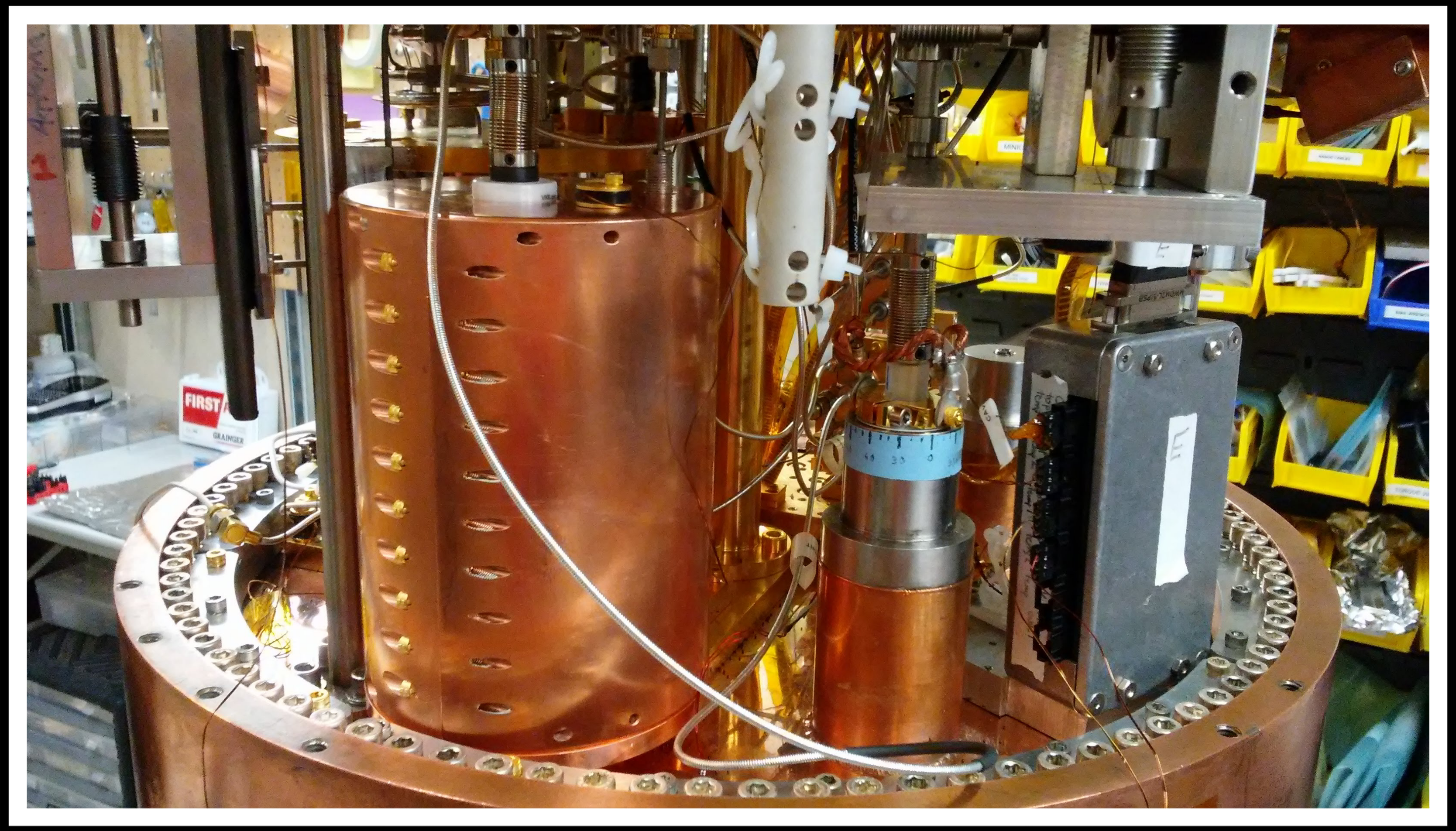

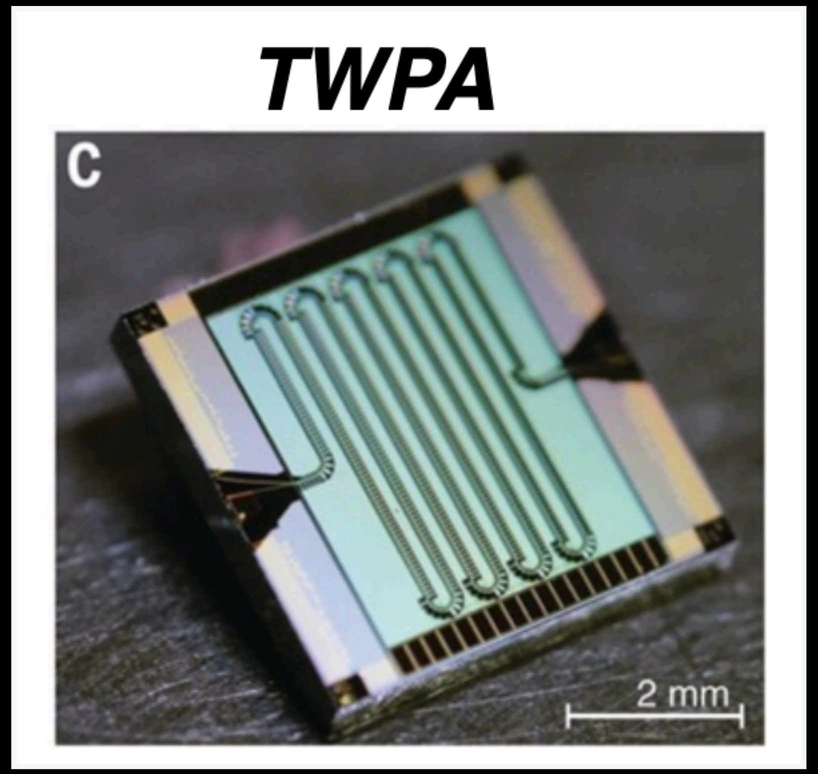

Sidecar is a small prototyping cavity that sits on top of the main cavity.

- Testing:
  - Traveling Wave Parametric Amplifier (TWPA)
  - Clamshell cavity design
  - Piezo motors for antenna and tuning rod

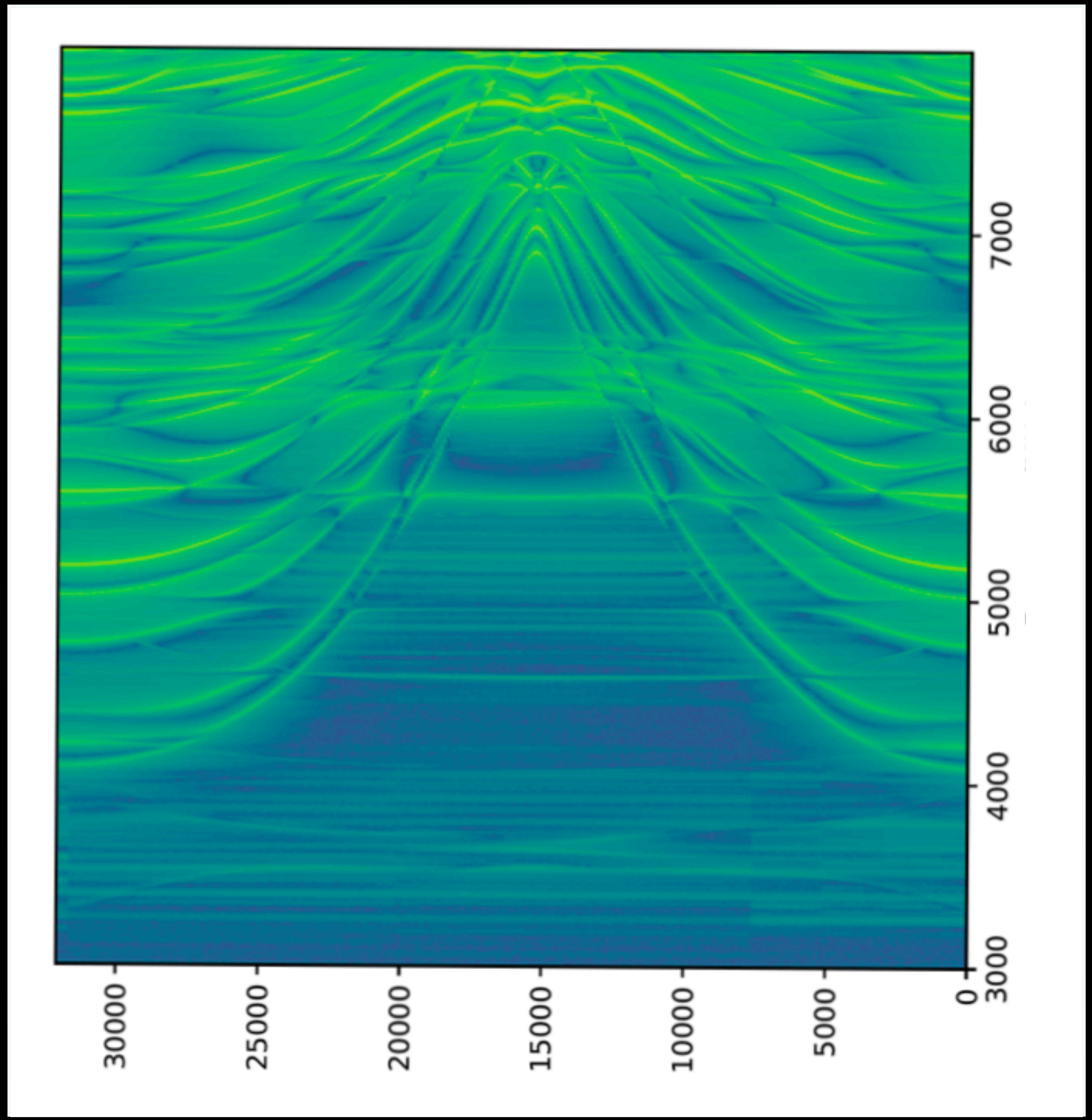

Sidecar mode map

First axion search with a JTWPA

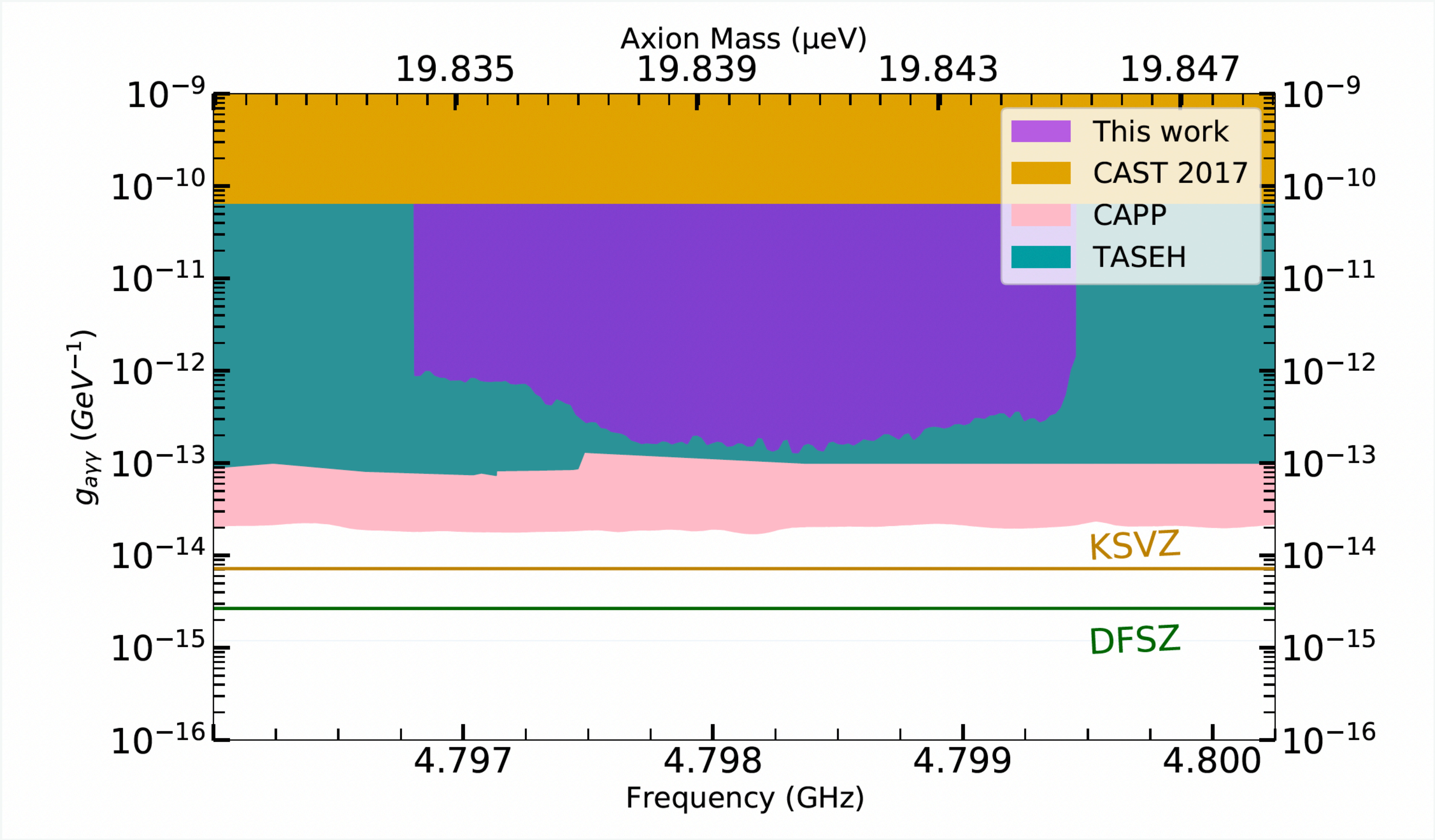

Bartram, C., et al. "Dark matter axion search using a Josephson traveling wave parametric amplifier". Review of Scientific Instruments 94.4 (2023): 044703

Sidecar now taking data at 5.2-5.6 GHz at 10x KSVZ with a Nb3Tn superconducting tuning rod!

ADMX-G2

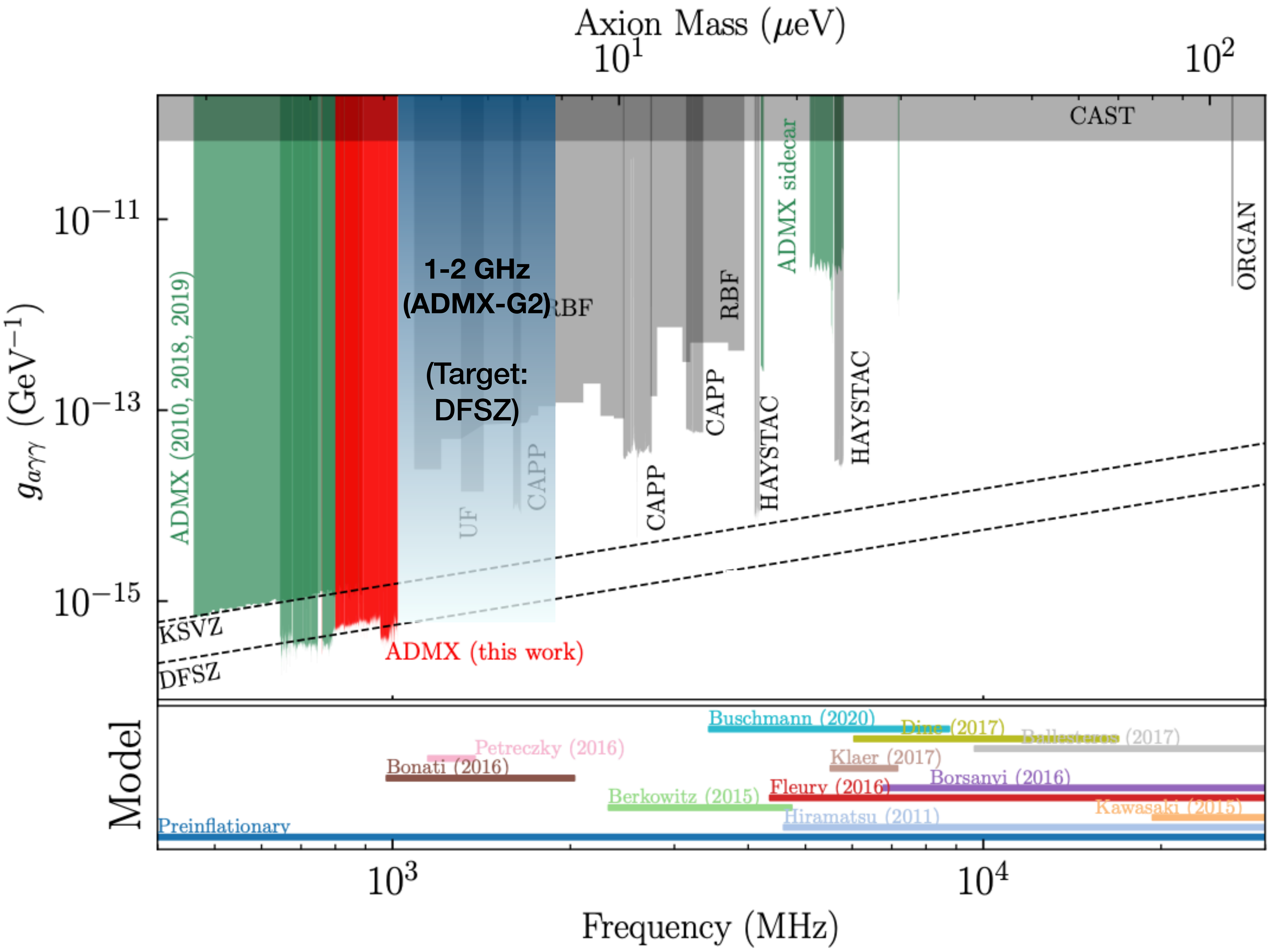

Axion Mass (μeV)
10^1
10^2
CAST
ORGAN
$g_{a\gamma\gamma}$ (GeV^{-1})
10^{-11}
10^{-13}
10^{-15}
ADMX (2010, 2018, 2019)
1-2 GHz
(ADMX-G2)
(Target:
DFSZ)
RBF
RBF
UF
CAPP
CAPP
CAPP
HAYSTAC
HAYSTAC
ADMX sidecar
KSVZ
DFSZ
ADMX (this work)
Model
Buschmann (2020)
Dine (2017)
Ballesteros (2017)
Petreczky (2016)
Klaer (2017)
Bonati (2016)
Borsanyi (2016)
Fleury (2016)
Berkowitz (2015)
Kawasaki (2015)
Hiramatsu (2011)
Preinflationary
10^3
10^4
Frequency (MHz)

ADMX-G2

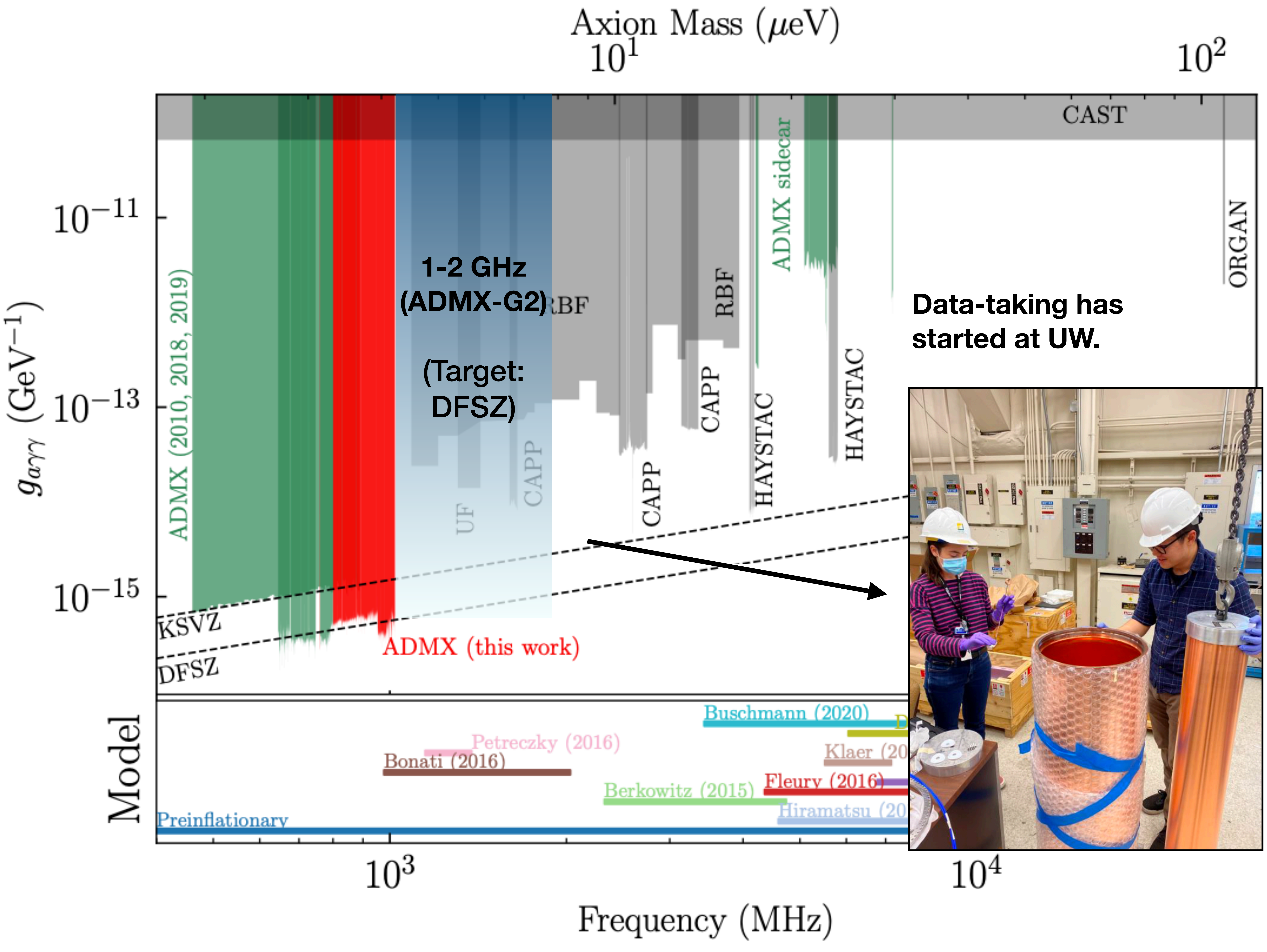

1-2 GHz (ADMX-G2)

(Target: DFSZ)

Data-taking has started at UW.

ADMX-EFR

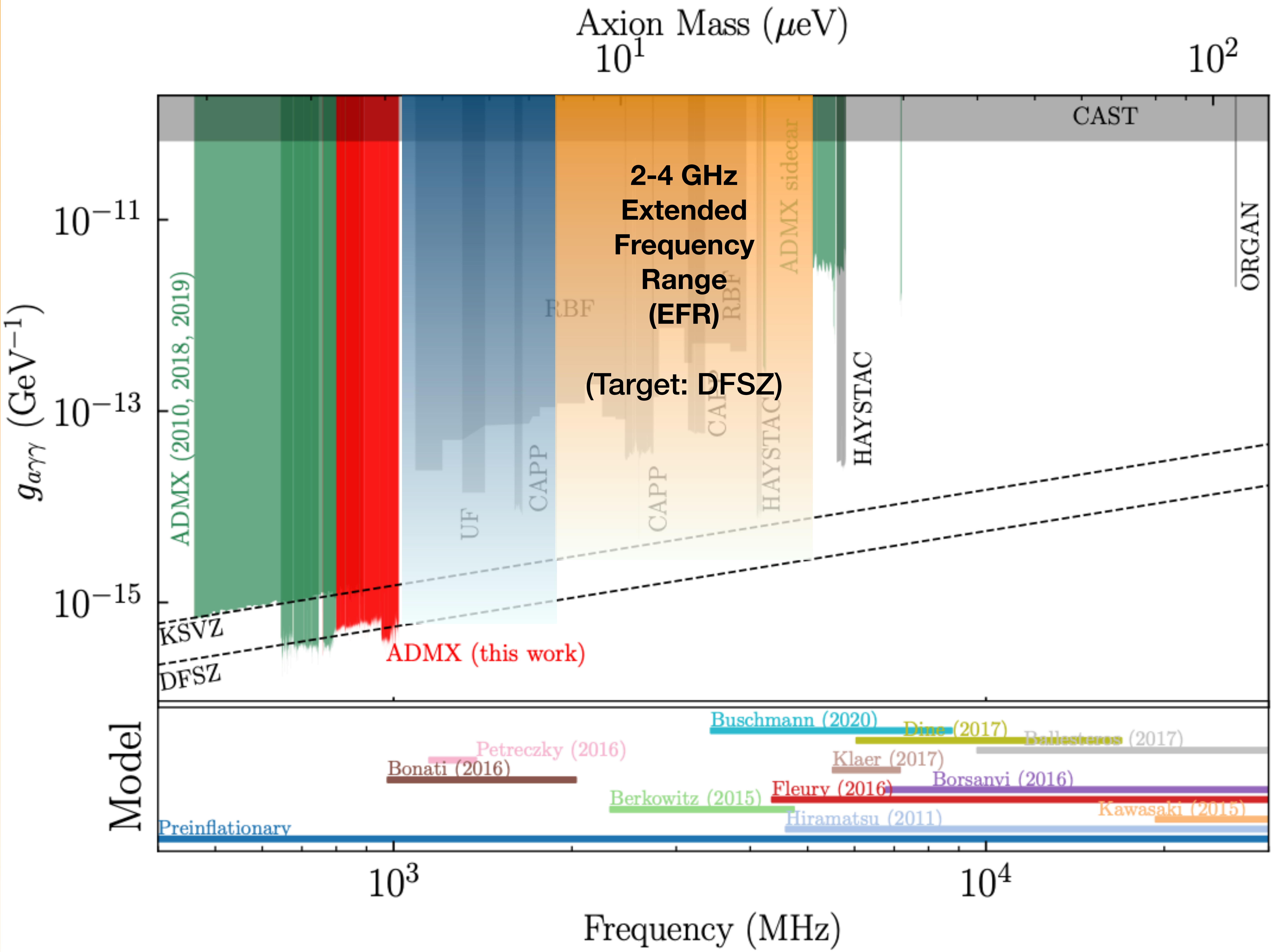

Axion Mass (μeV)
10^1
10^2
CAST
2-4 GHz
Extended
Frequency
Range
(EFR)
(Target: DFSZ)
ADMX sidecar
ORGAN
RBF
HAYSTAC
CAPP
UF
10^{-11}
10^{-13}
10^{-15}
$g_{a\gamma\gamma}$ (GeV^{-1})
ADMX (2010, 2018, 2019)
KSVZ
DFSZ
ADMX (this work)
Model
Buschmann (2020)
Dine (2017)
Ballesteros (2017)
Petreczky (2016)
Klaer (2017)
Bonati (2016)
Borsanyi (2016)
Fleury (2016)
Berkowitz (2015)
Kawasaki (2015)
Hiramatsu (2011)
Preinflationary
10^3
10^4
Frequency (MHz)

Scan speed for cavity haloscope

$$\frac{df}{dt} \approx 323 \frac{\mathrm{MHz}}{\mathrm{yr}} \left(\frac{g_\gamma}{0.36}\right)^2 \left(\frac{\rho}{0.45\,\mathrm{GeV/cm^3}}\right)^2 \left(\frac{f}{1\,\mathrm{GHz}}\right)^2 \left(\frac{3.5}{\mathrm{SNR}}\right)^2 \left(\frac{B_0}{7.6\ \mathrm{T}}\right)^4 \left(\frac{V}{136\ \ell}\right)^2 \left(\frac{Q_L}{30,000}\right) \left(\frac{C_{lmn}}{0.4}\right)^2 \left(\frac{0.35\ \mathrm{K}}{\mathrm{T_{sys}}}\right)^2$$

Maximize	Can't Control	Minimize

• B Field
• Volume
• Quality Factor
• Form Factor
	• Frequency
	• Coupling
	• Dark Matter Density
		• System noise:
		  • Amplifier Noise
		  • Physical Noise

***Similar equation for quasistatic haloscope**

ADMX EFR (2-4 GHz)

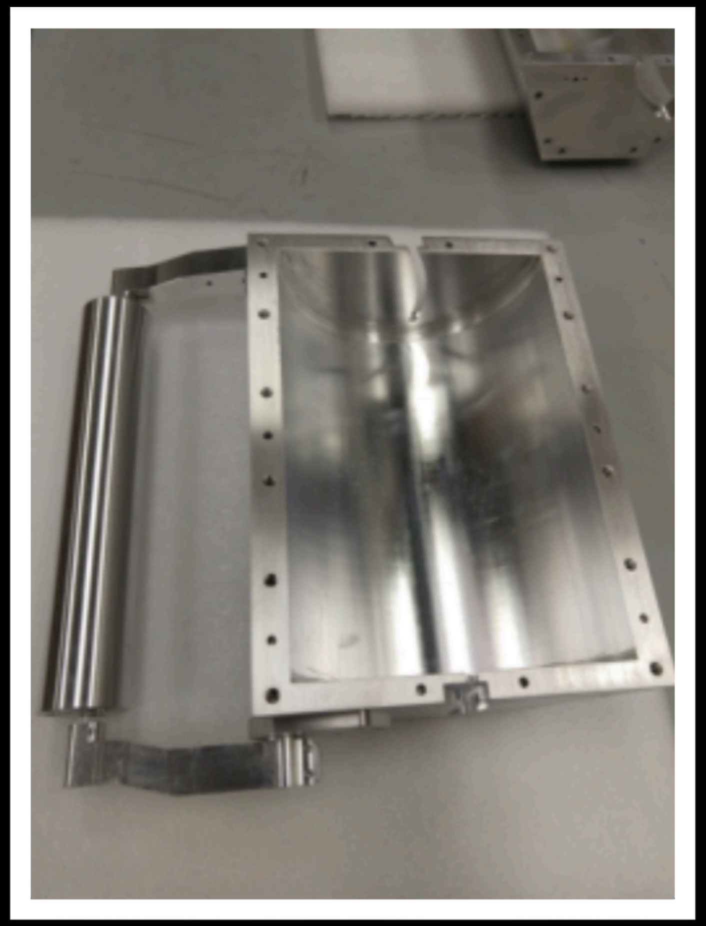

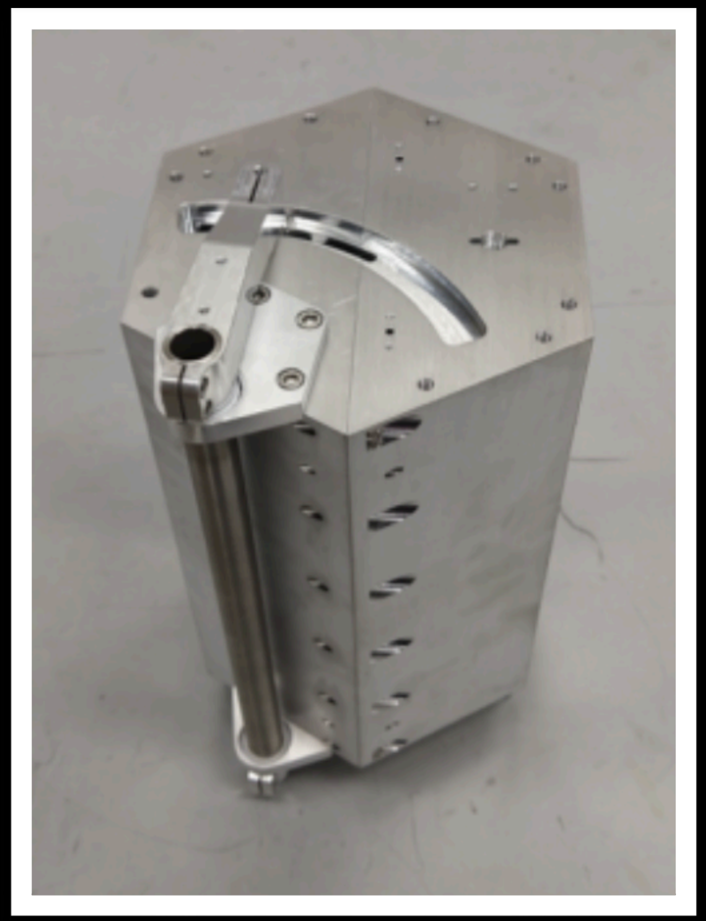

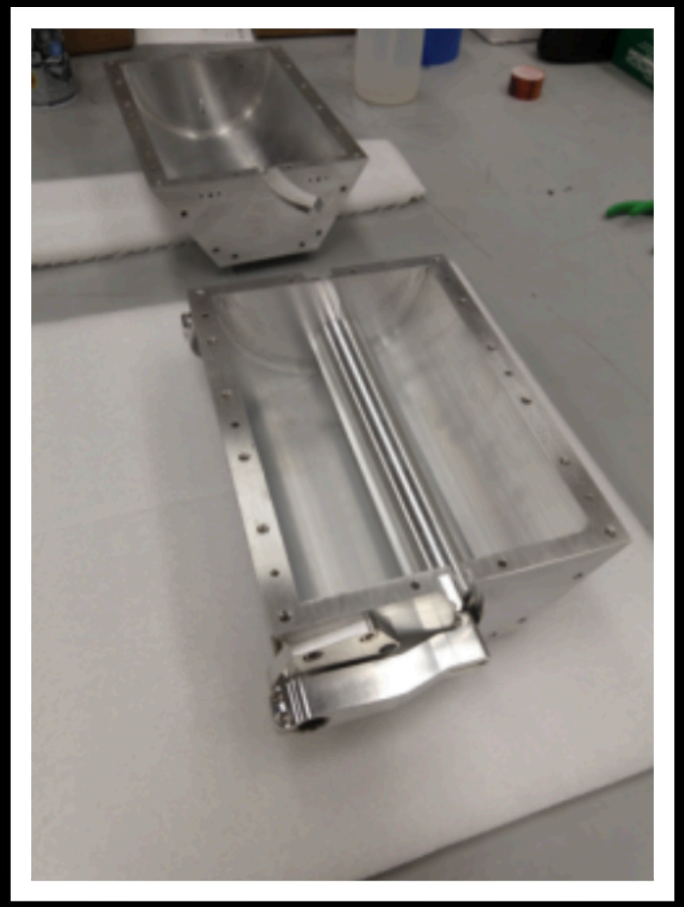

Prototype cavity testing

18-JPA receiver

9.4 T Magnet

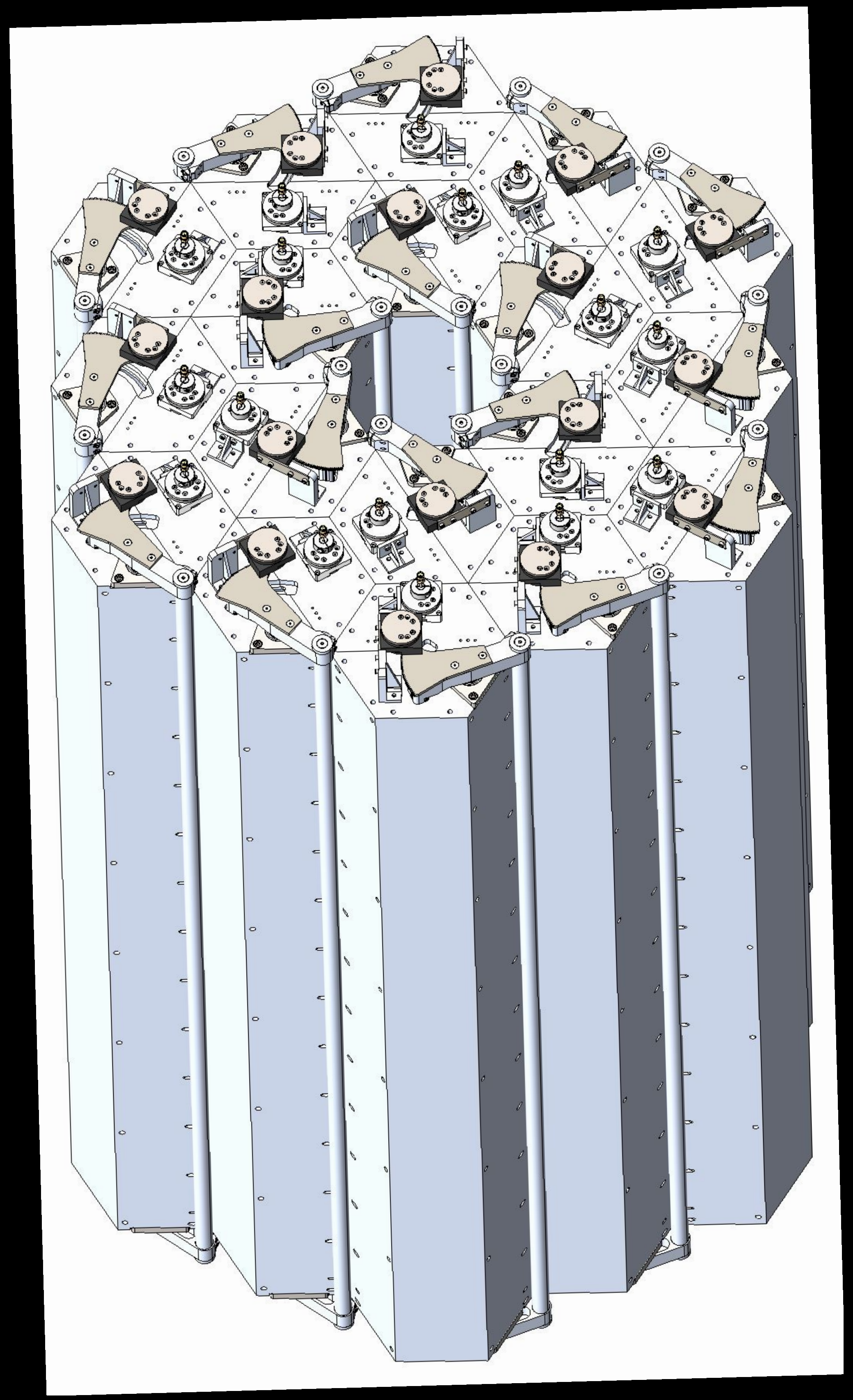

18-cavity array simulations

ADMX EFR (2-4 GHz)

- Horizontal magnet bore
- Extra modularity: cavity electronics are separate from magnet bore
- Large magnet volume: 258 liters
- Other: Squeezing? Superconducting cavities?

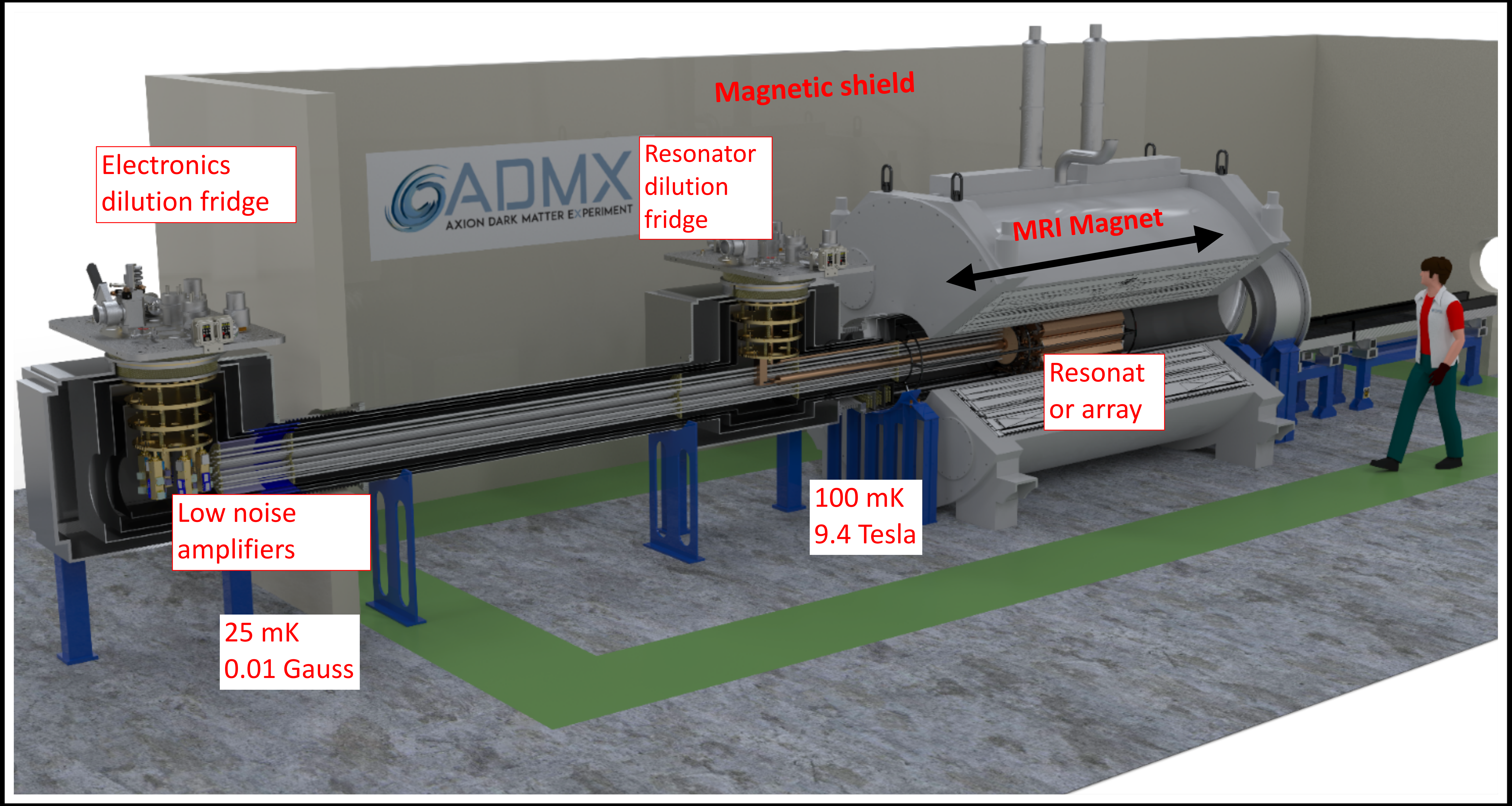

(ADMX EFR Design)

ADMX-VERA (7-? GHz)

Width sets frequency of fundamental (TM_{010}) compatible with **solenoid B field**

Decouple frequency and volume.

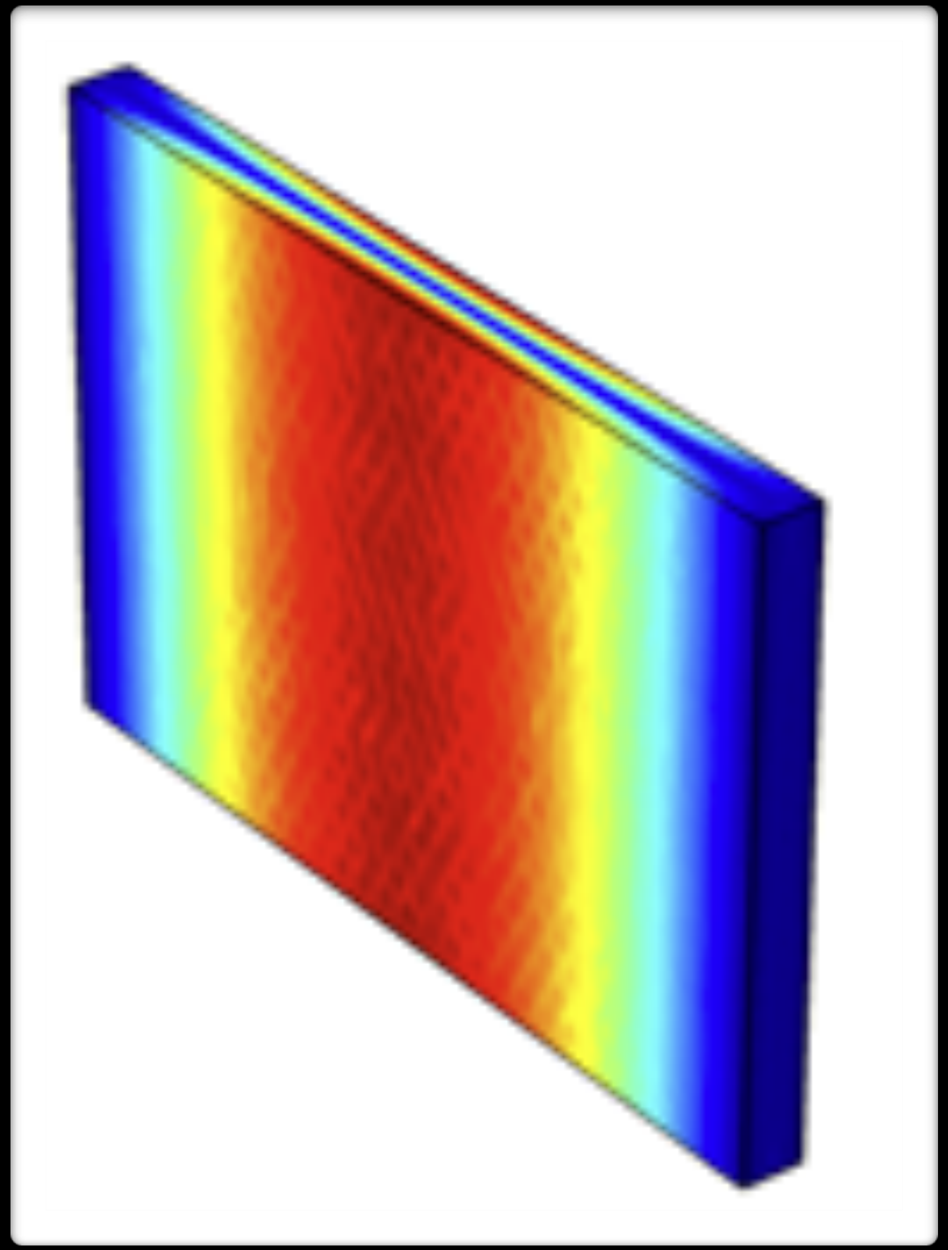

Volume can be scaled arbitrarily in other dimensions

ADMX-VERA (7-? GHz)

Width sets frequency of fundamental (TM_{010}) compatible with **solenoid B field**

Decouple frequency and volume.

TM010 mode still supported.

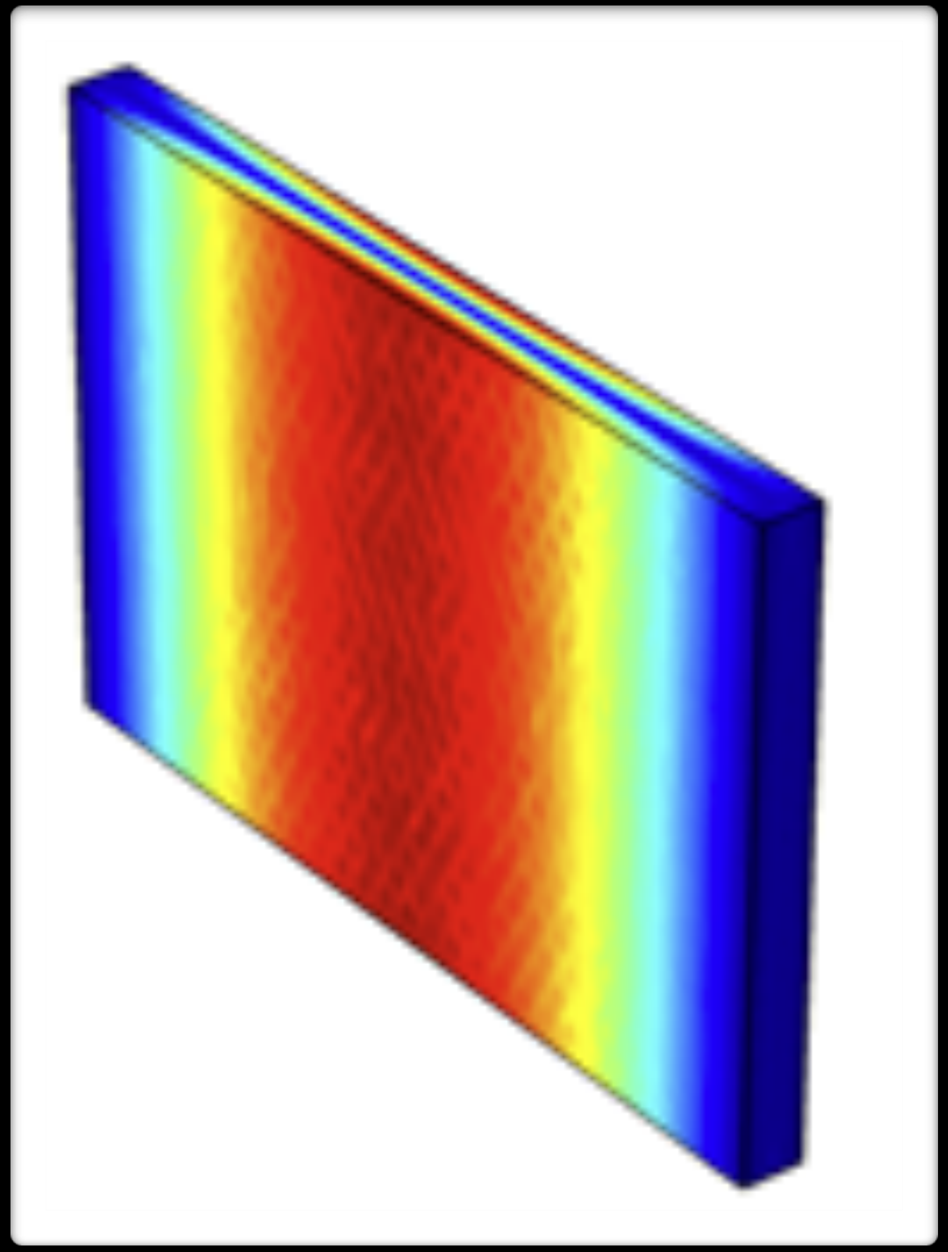

Wrap

Volume can be scaled arbitrarily in other dimensions

ADMX-VERA (7-? GHz)

Decouple frequency and volume.

Width sets frequency of fundamental (TM_{010}) compatible with **solenoid B field**

Volume can be scaled arbitrarily in other dimensions

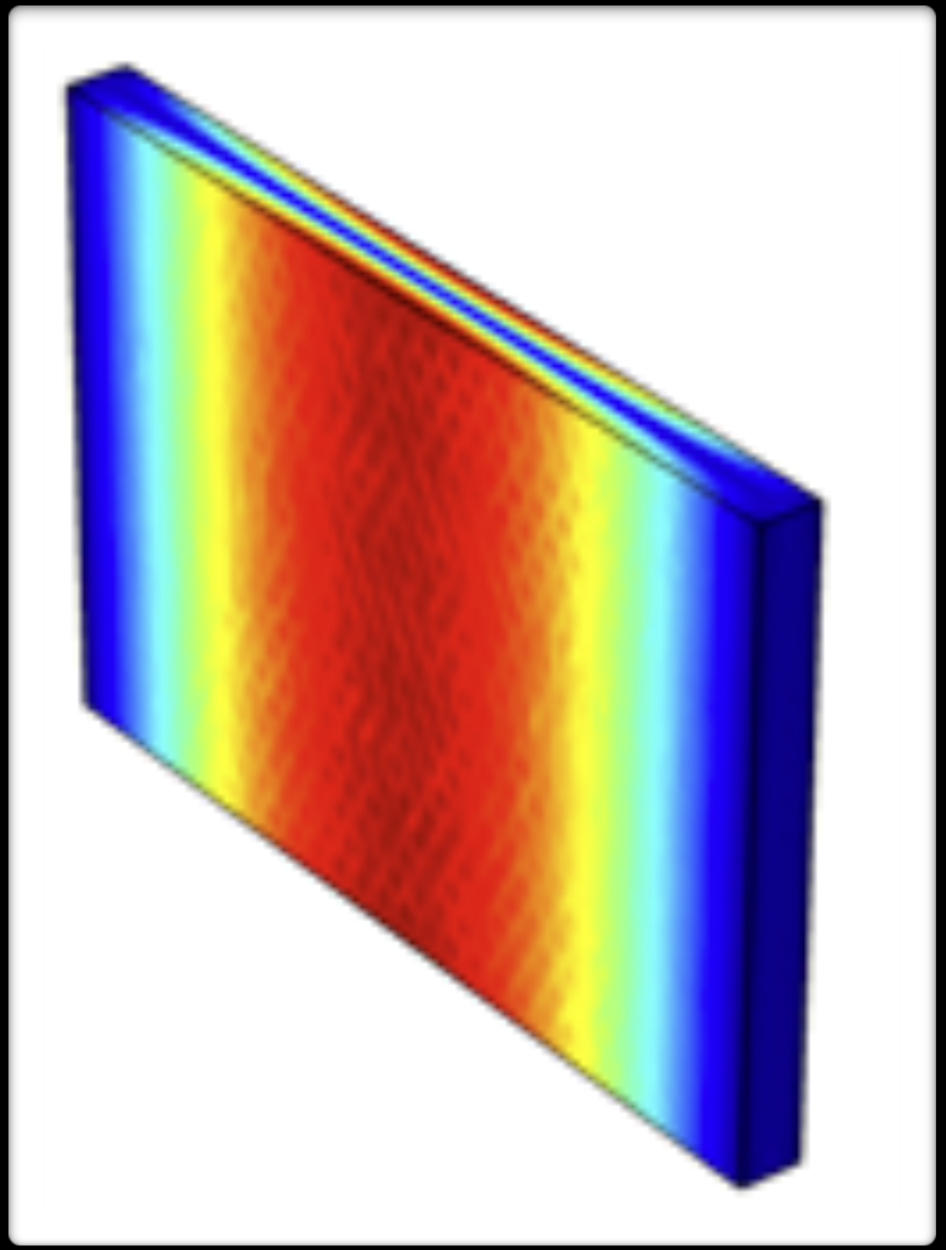

Wrap

TM010 mode still supported.

Convolute

JCAP 02 (2021) 018
JCAP 06 (2020) 010

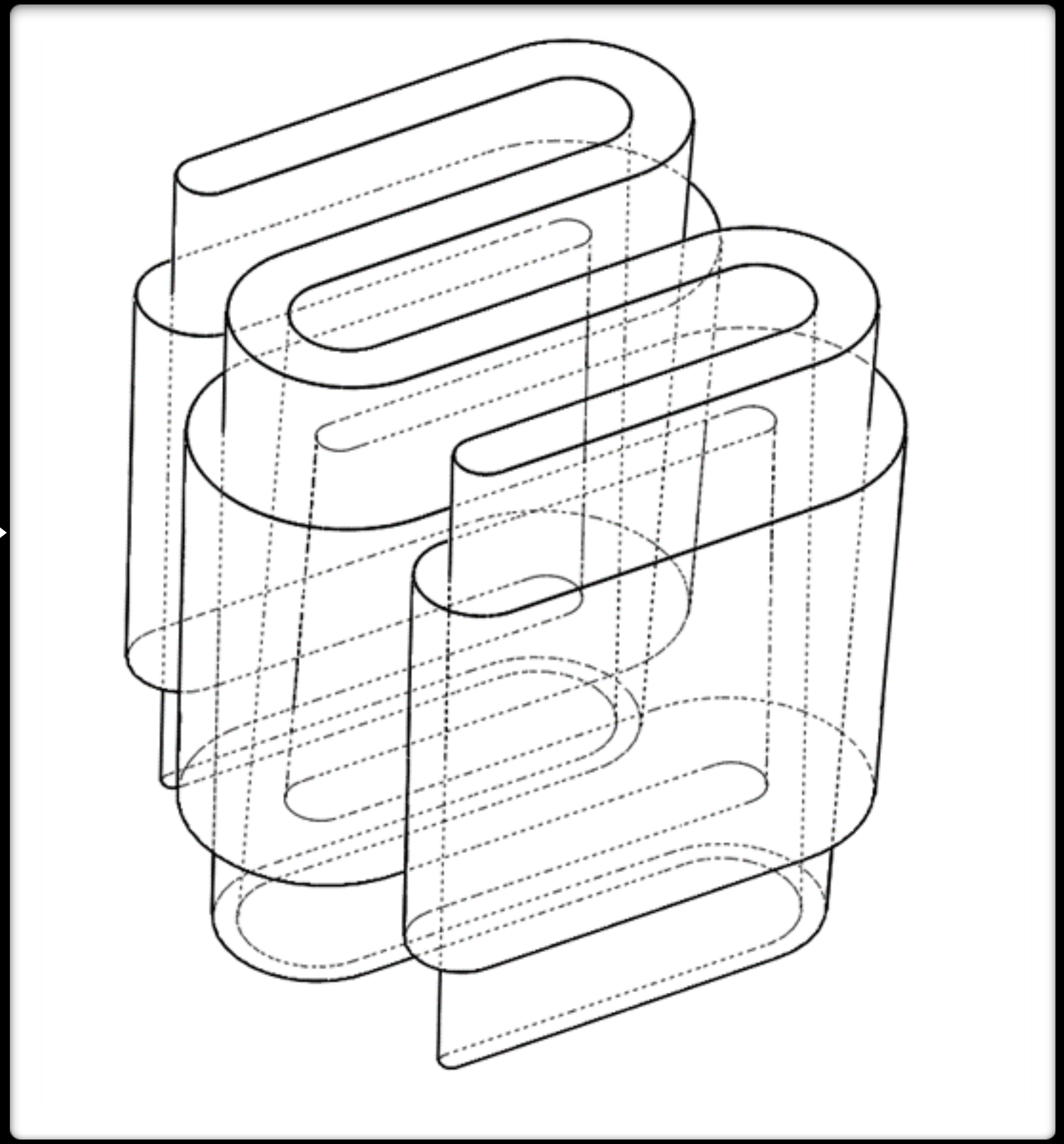

CAPP

CAPP-12TB

- Second cavity search at DFSZ
- ~10 T superconducting magnet
- 25 mK base temperature
- 36.85 L cavity

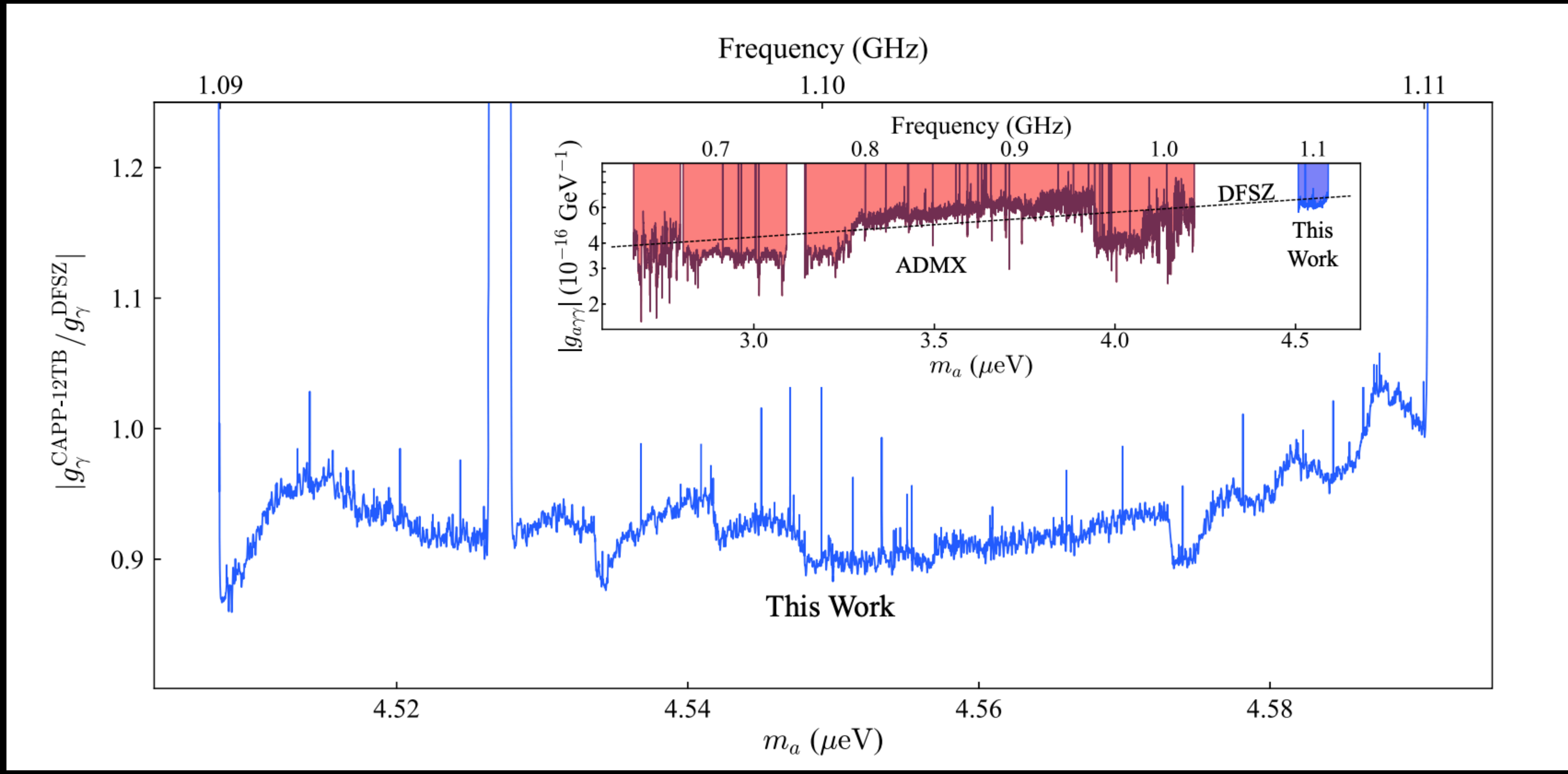

Andrew, K. Yi, et al. "Axion Dark Matter Search around 4.55 μ eV with Dine-Fischler-Srednicki-Zhitnitskii Sensitivity." *Physical Review Letters* 130.7 (2023): 071002.

HAYSTAC

- Exploring higher frequency axions
- Using squeezed state receiver:
- Phys. Rev. X 9, 021023 (2019)
- Exploring Bayesian techniques:
- Phys. Rev. D 101, 123011 (2020)
- Phase 1 results complete
- Phase 2 underway

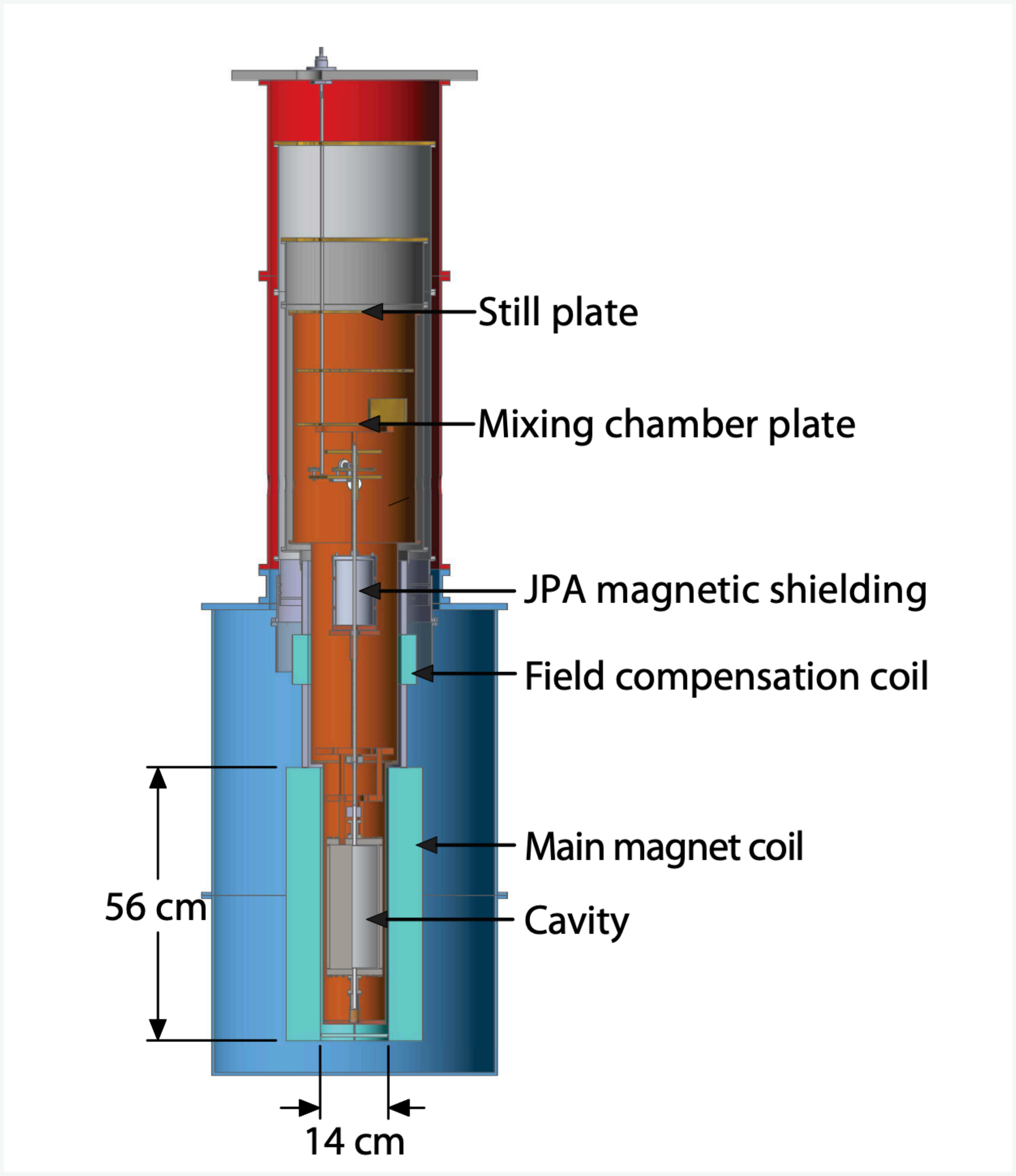

ORGAN

Higher frequencies 26.6 ~GHz (110 ueV)

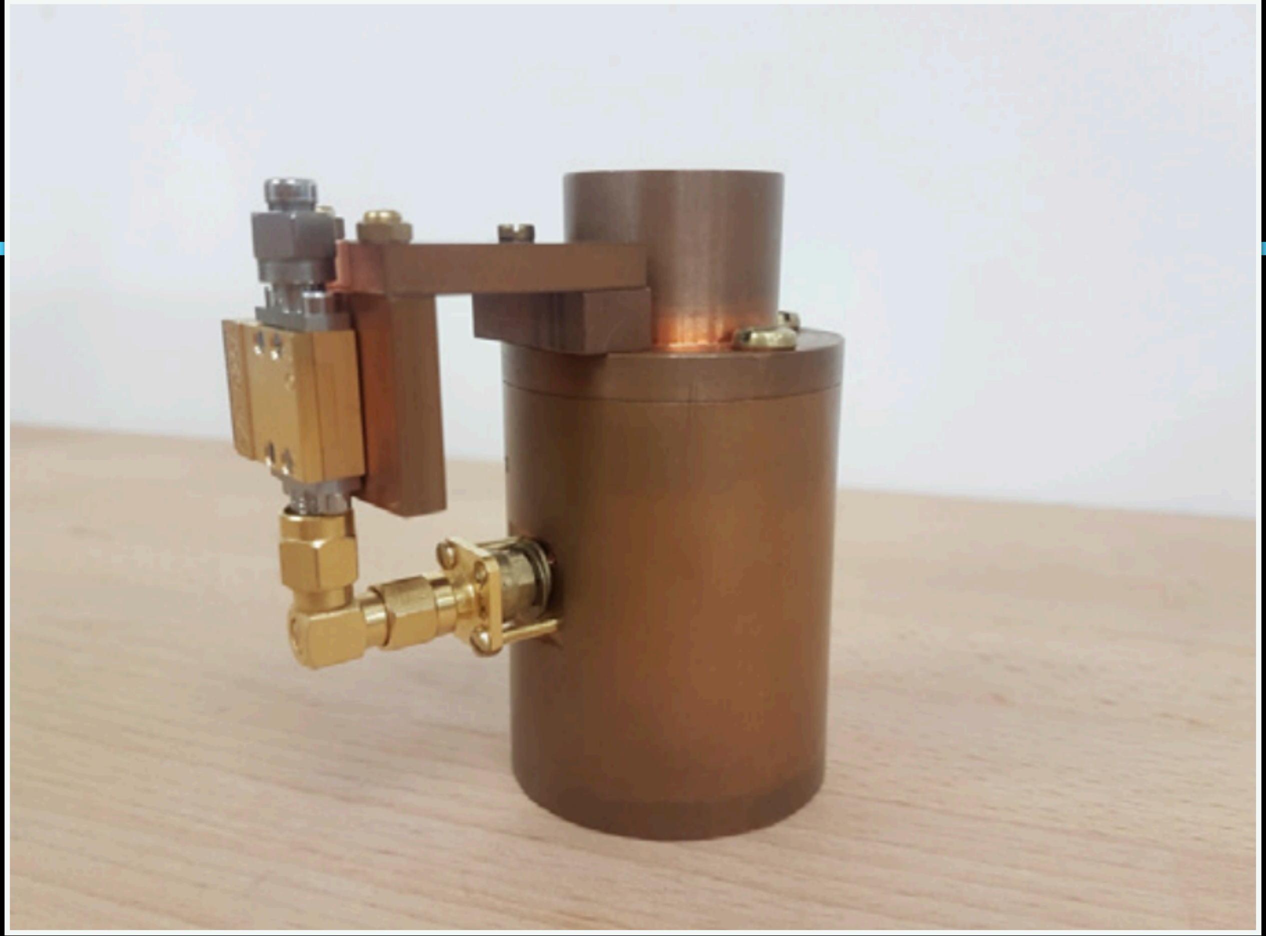

AXIONS AND WAVE-LIKE DARK MATTER

RADIATION REGIME

MADMAX, BREAD AND MORE...

MADMAX: Dielectric Haloscope

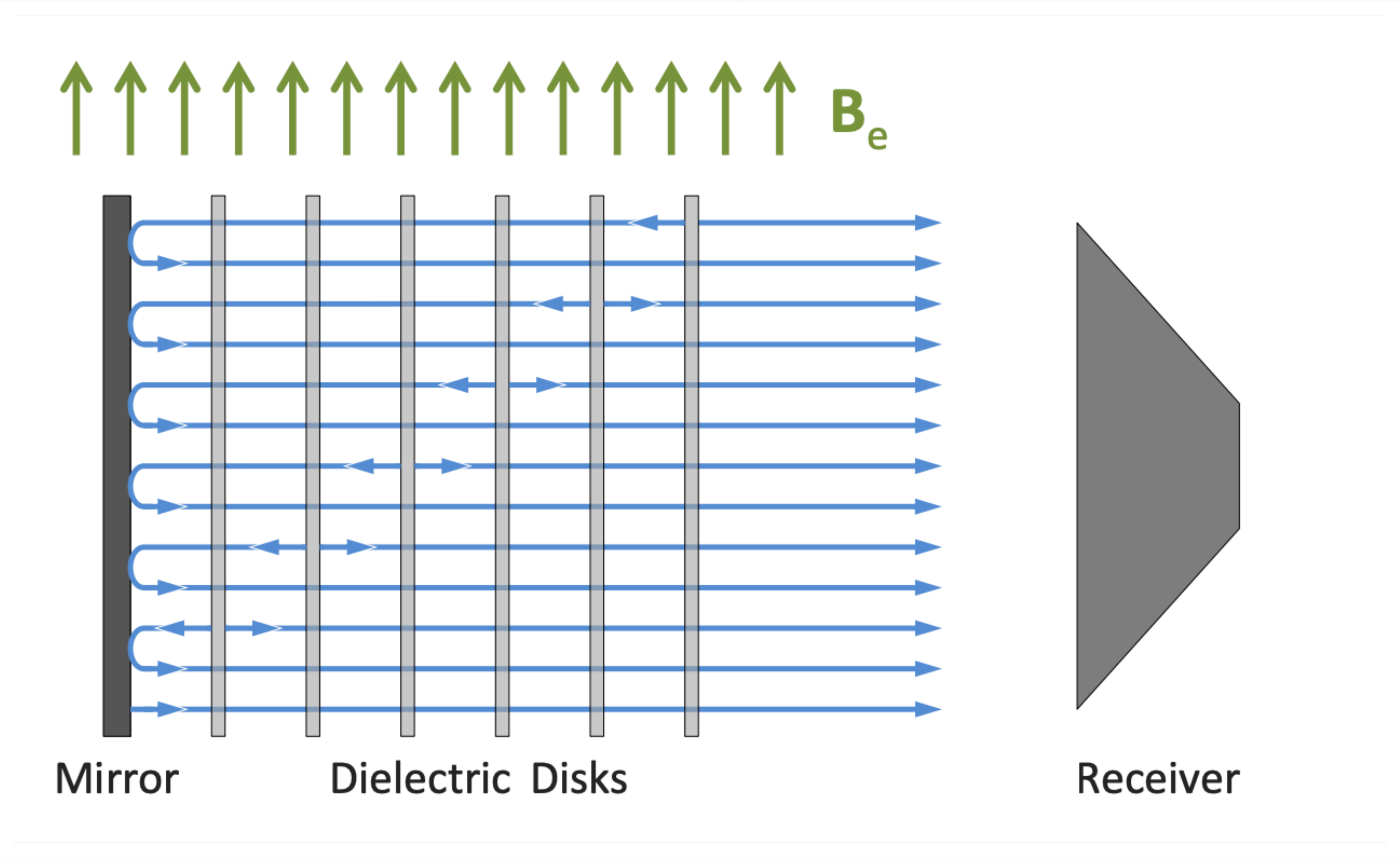

- Will probe 40-400 μeV range (10-100 GHz)
- 10 T field
- ~80 disks
- Prototype phase using dipole magnet at CERN

B. Majorovits and MADMAX interest groupt 2020 J. Phys.: Conf. Ser. 1342 012098

Stefan Knirck and MADMAX interest group 2020 J. Phys.: Conf. Ser. 1342 012097

BREAD: Inverted Dish Antenna

Conical structure focuses the light to a single photon detector.

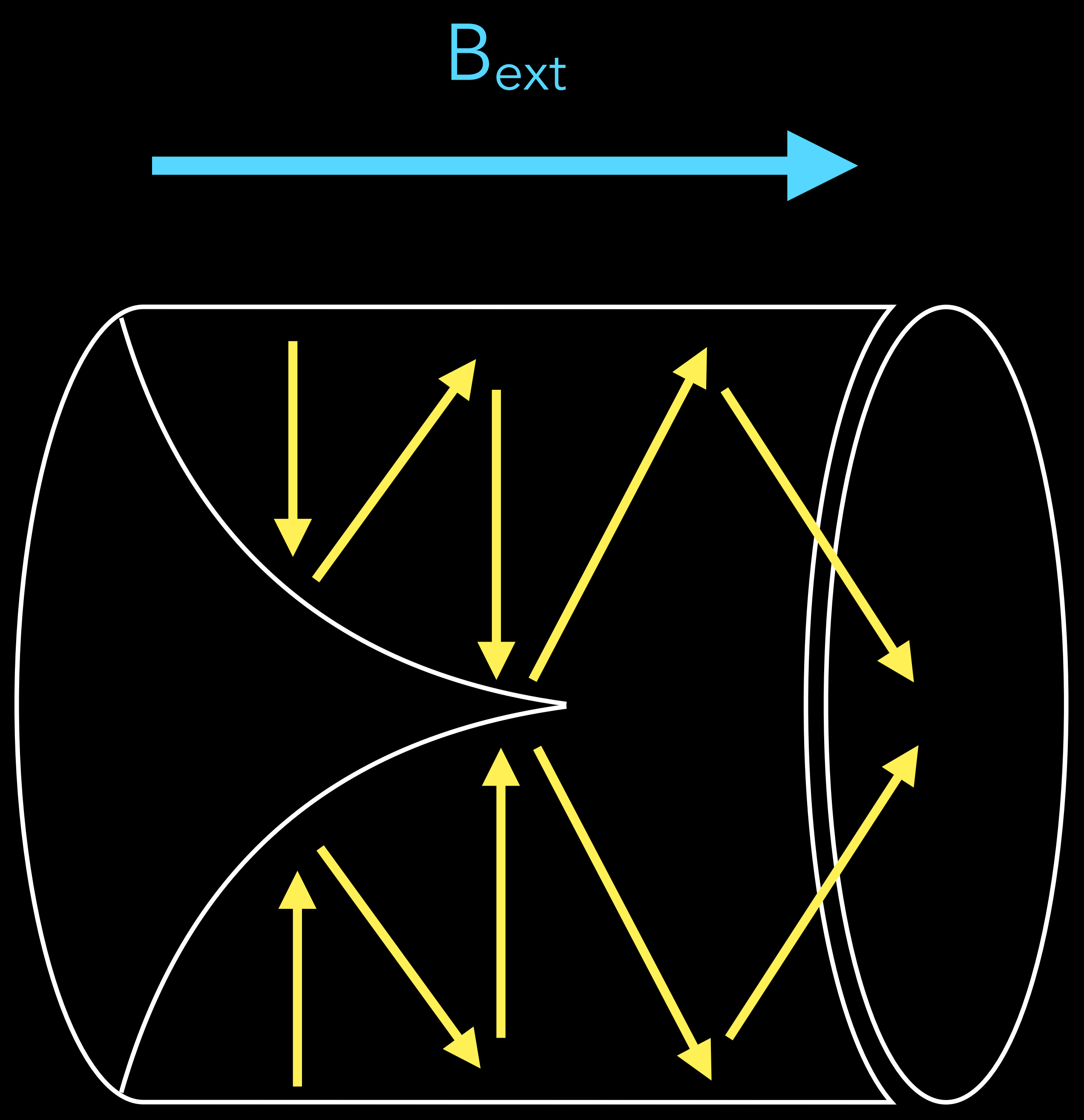

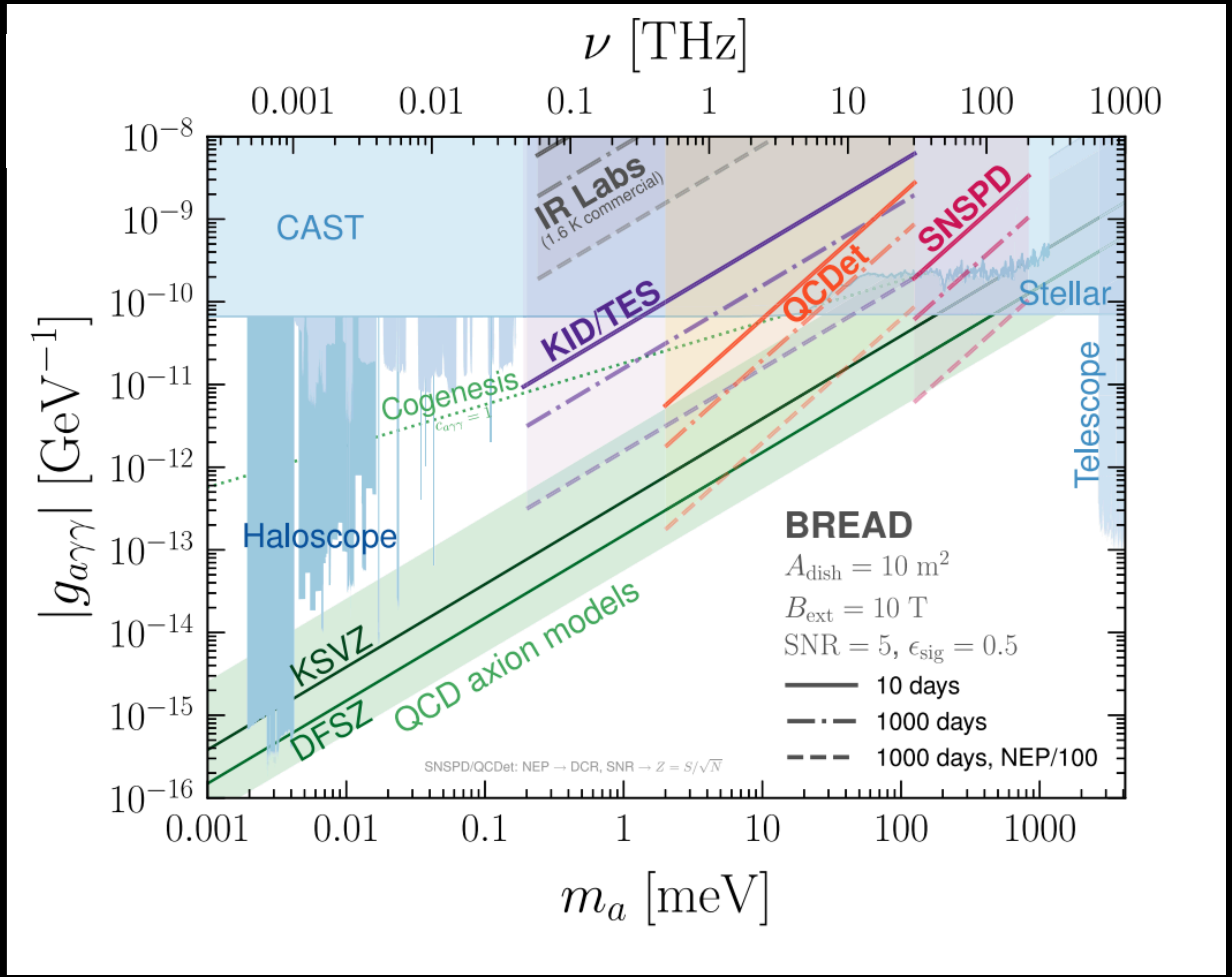

Liu, Jesse, et al. "Broadband solenoidal haloscope for terahertz axion detection." *Physical Review Letters* 128.13 (2022): 131801.

Conclusions

- Variety of haloscopes to search for axions.
  - Lumped element detectors
  - Cavity resonators
  - Dielectric haloscopes and more
- Field is growing rapidly
- New techniques from fields of quantum information and quantum measurement.

Backup Slides

AXIONS AND WAVE-LIKE DARK MATTER

LIGHT-SHINING-THROUGH-WALLS

ALPS-II

Quantum sensing techniques + R&D

- Increasing the bandwidth via SQUID coupling to the resonator
- Radiofrequency Quantum Upconverters (RQUs)
- Bode-Fano Evasion

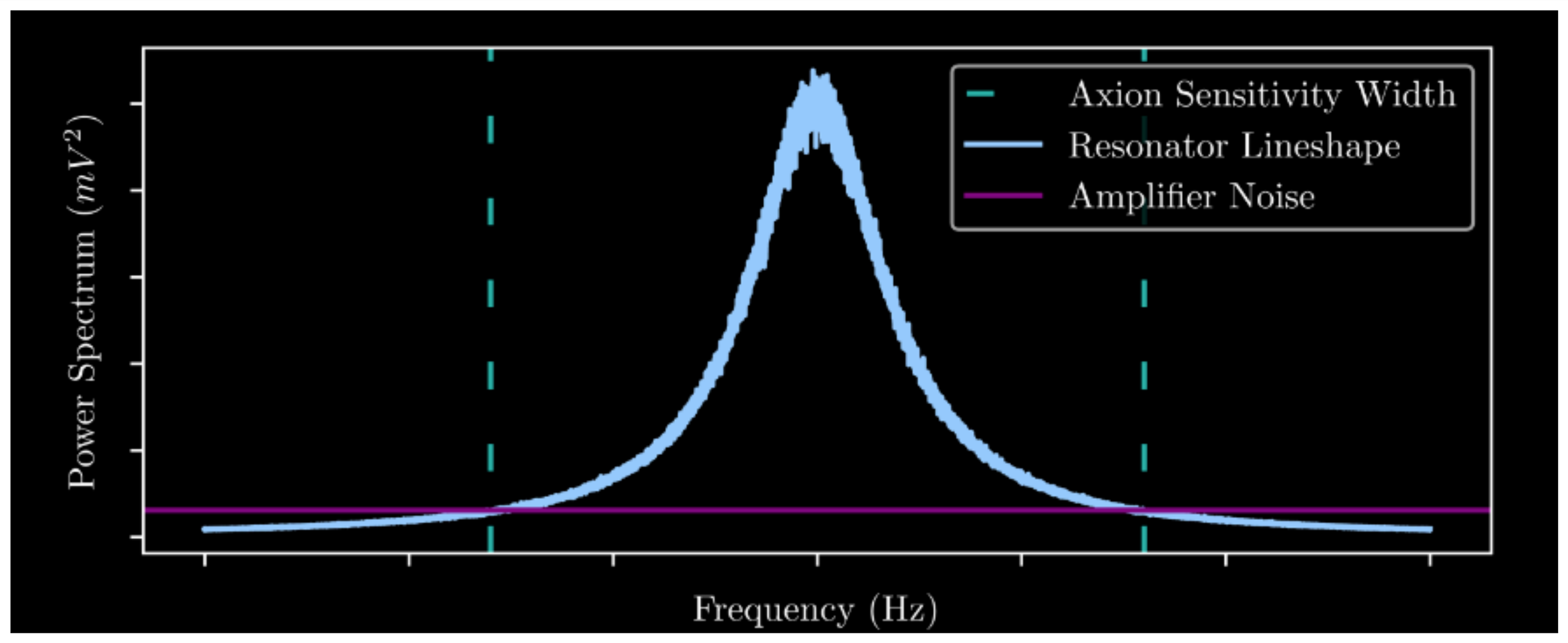

…happy to field more questions later!

ADMX high frequency prototype

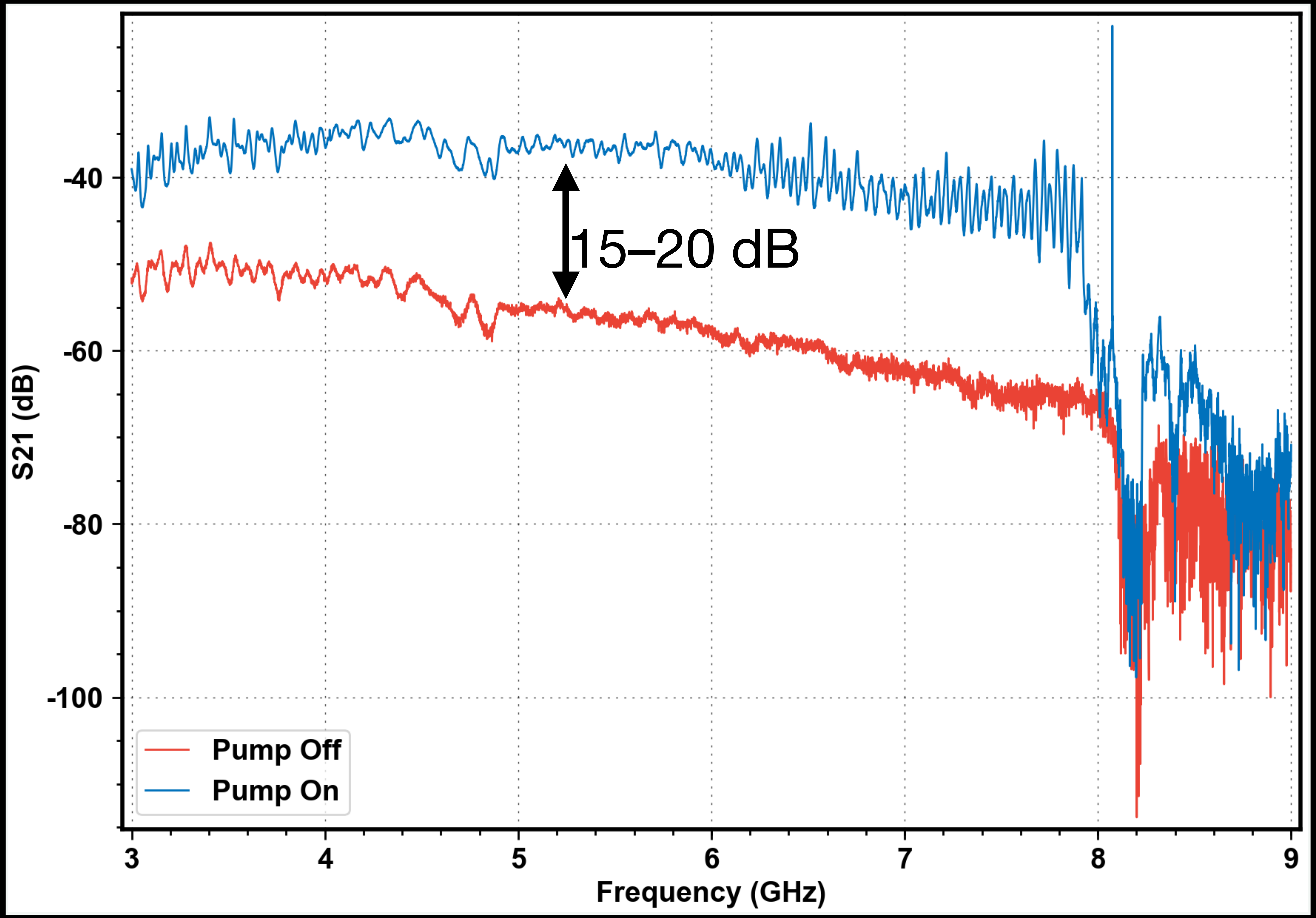

5 GHz

O(100) Josephson Junctions in series

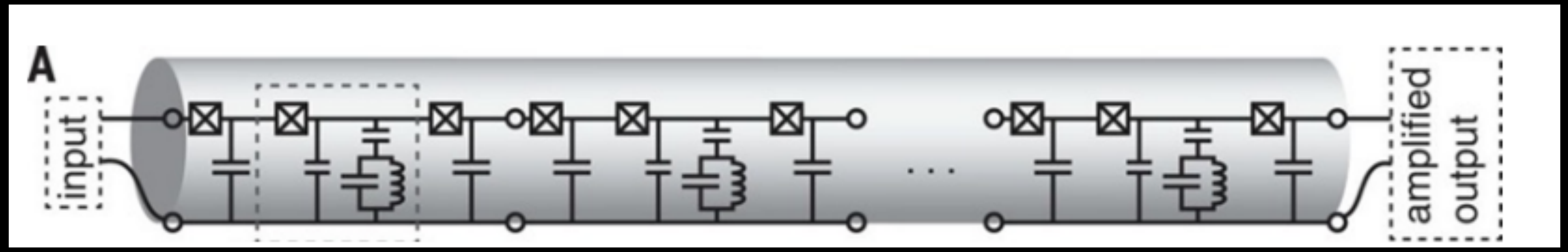

- Broadband gain
- Compact: requires one less circulator
- Optimize adjusting pump frequency and power

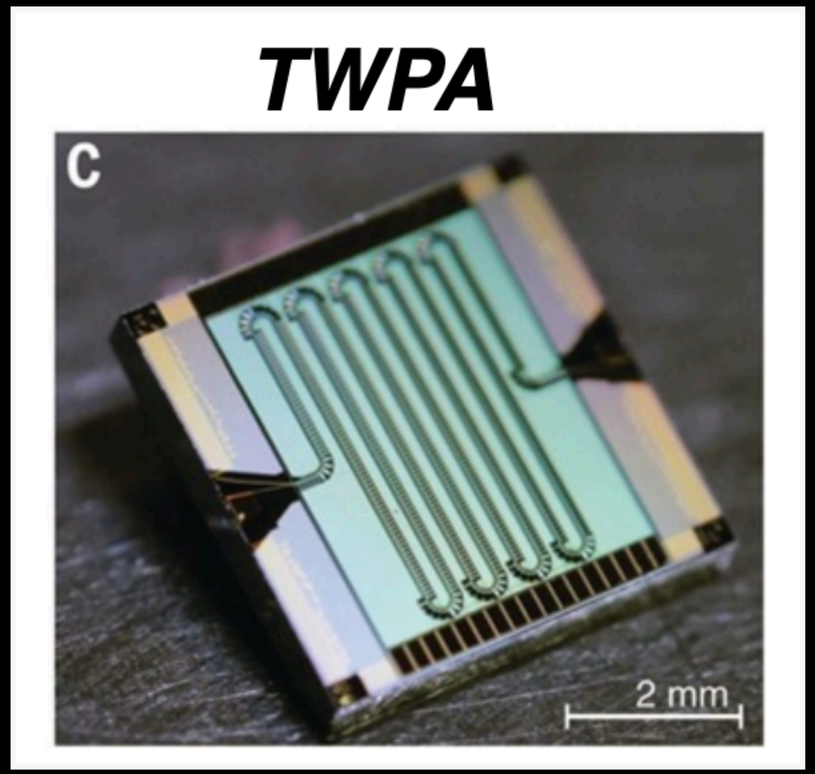

Measurement noise composition

- Imprecision noise:
  - Voltage fluctuations at the output of the amplifier. Can be referred to current noise on the input.
  - Adds uncertainty independent of input circuit
- Backaction noise:
  - Injects noise back into the input circuit, which filters the noise according to the circuit impedance. The back action is then amplified, appearing on the amplifier output

Standard Quantum Limit

Fundamental noise source that is added by measurement

1/2 photon from zero-point fluctuations + 1/2 photon (min) from amplifier

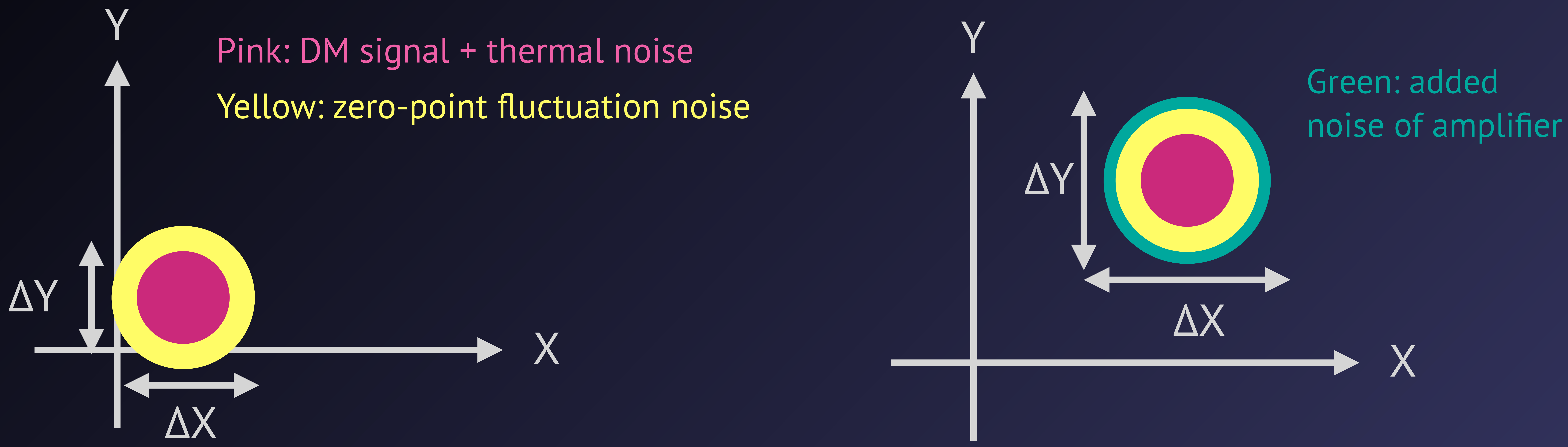

Strategies to increase bandwidth

Adjust relative contributions from

1. Backaction
2. Imprecision noise

to improve sensitivity bandwidth

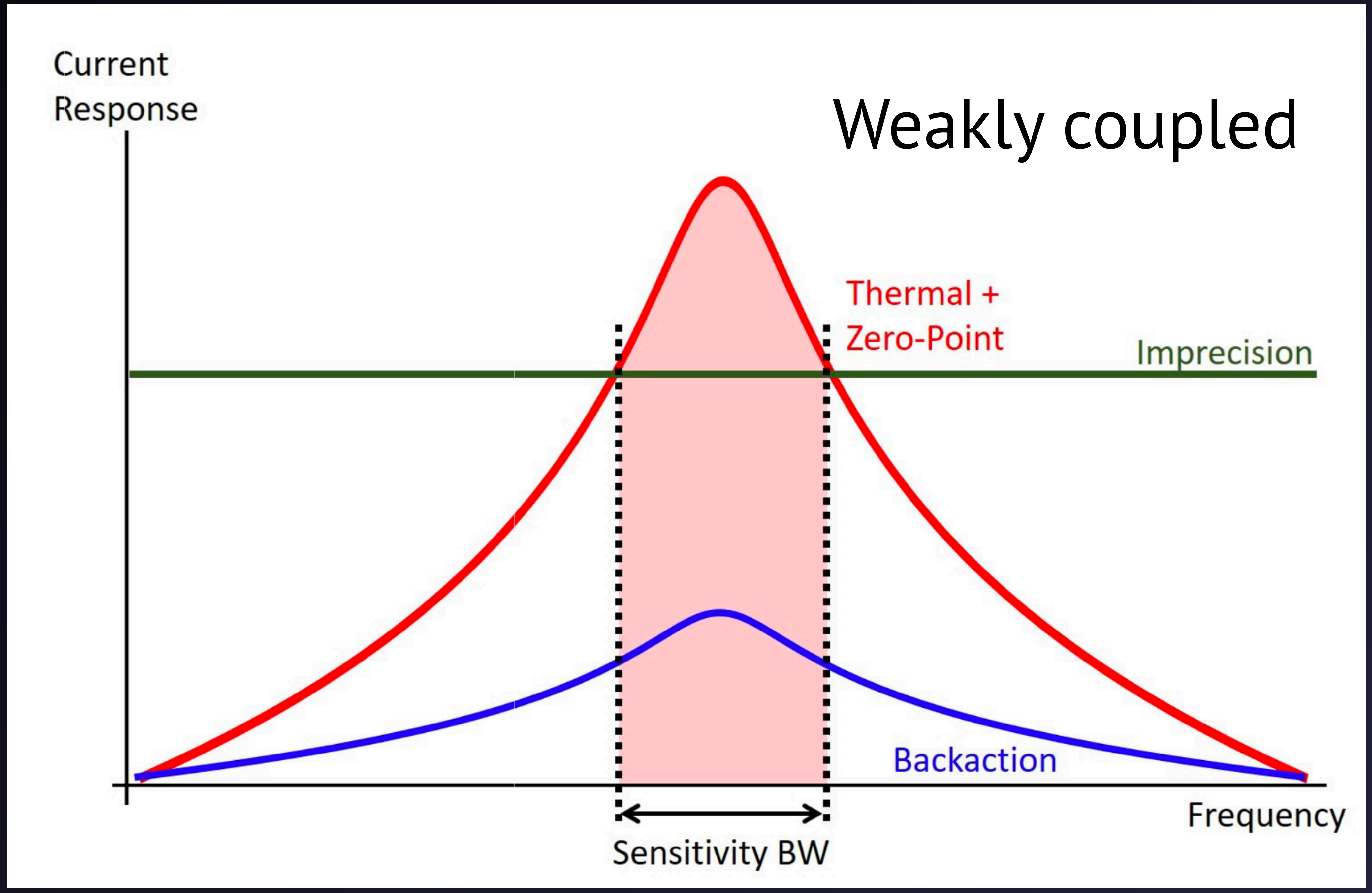

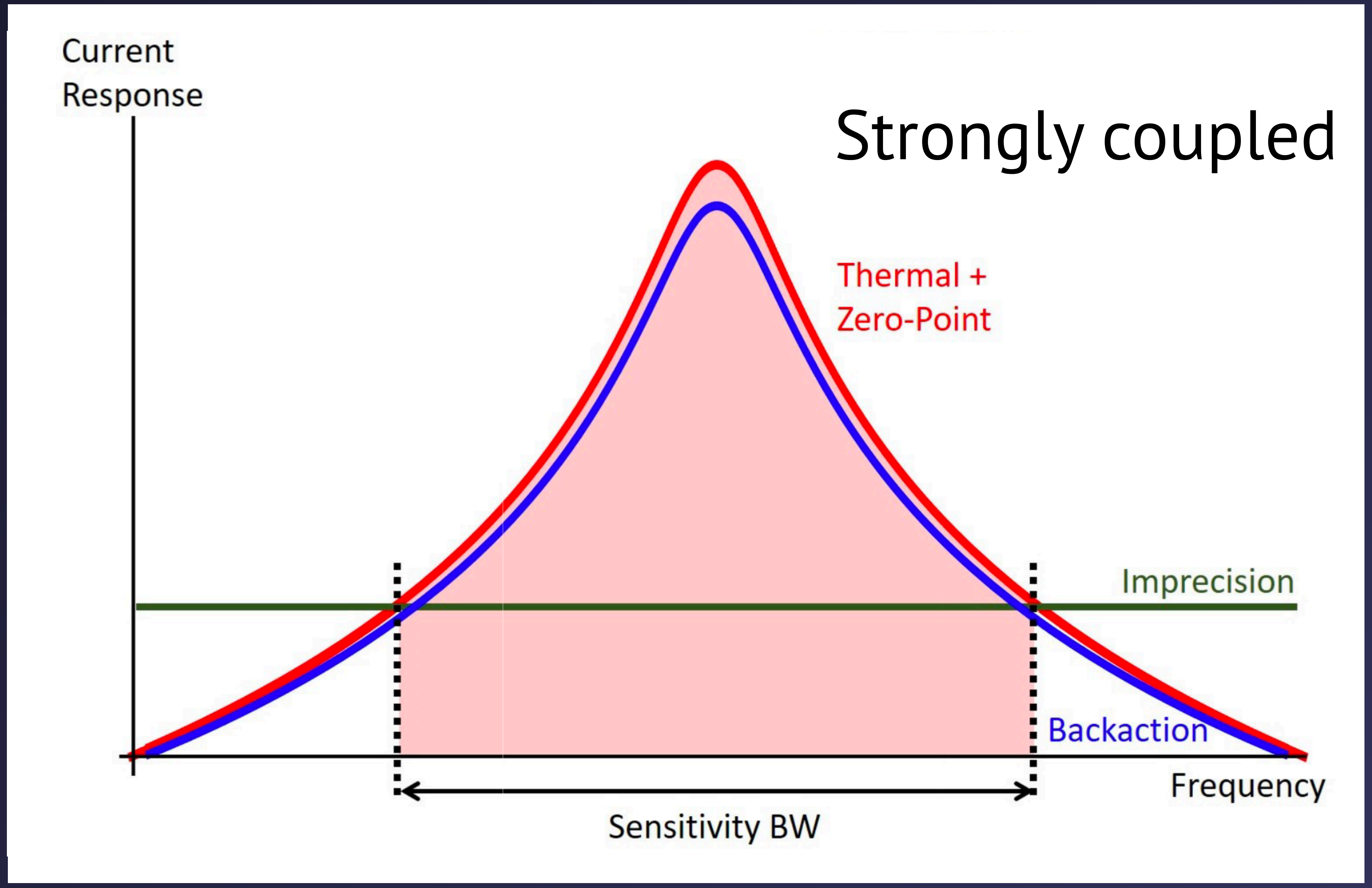

Radiofrequency Quantum Upconverter (RQU)

Device borrows concept from cavity optomechanics

- Two modes at different frequencies ($\omega_a >> \omega_b$)
  - High frequency EM mode (a)
  - Low frequency mechanical mode (b)
  - Quantized with ladder operators

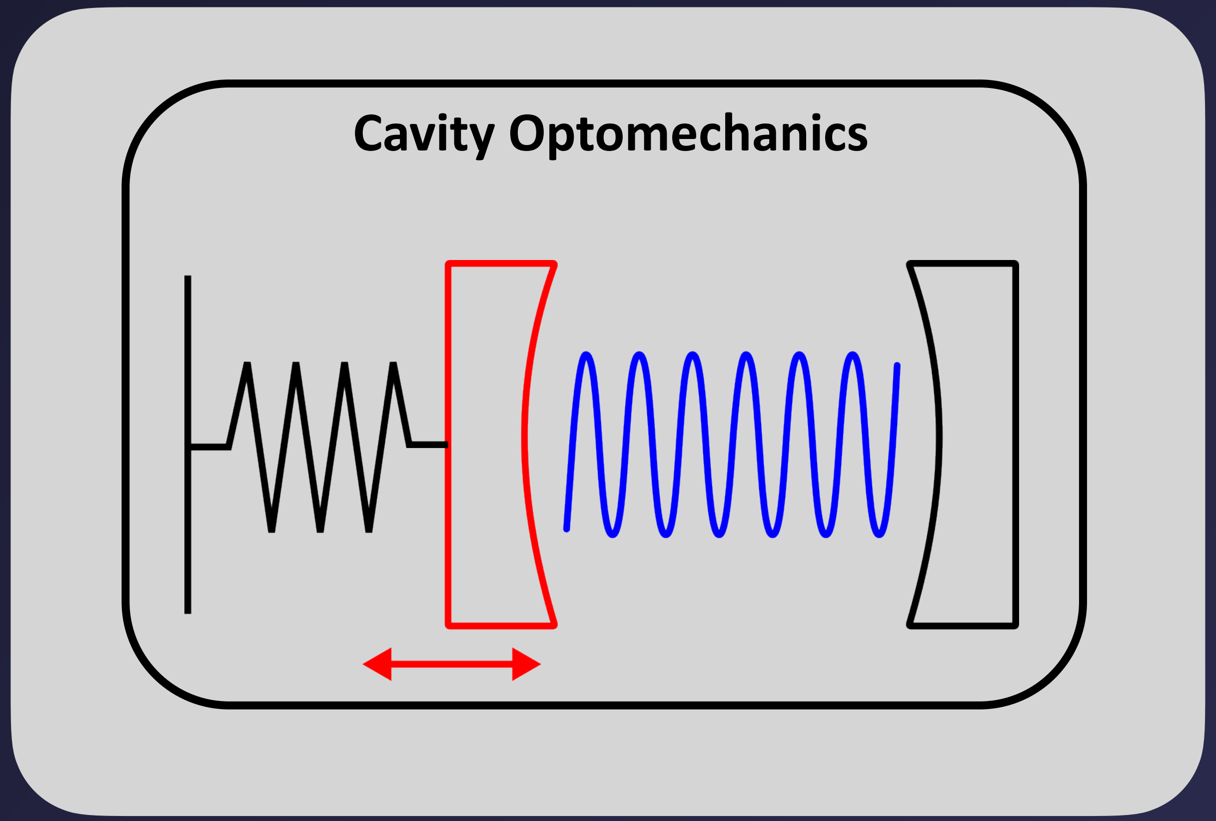

$$\hat{H} = \hbar\omega_a \left(\hat{a}^\dagger a + \frac{1}{2}\right) + \hbar\omega_b \left(\hat{b}^\dagger b + \frac{1}{2}\right) + \hbar g_0 \hat{a}^\dagger \hat{a} \left(\hat{b}^\dagger + \hat{b}\right)$$

Kuenstner, Stephen E., et al. "Quantum metrology of low frequency electromagnetic modes with frequency upconverters." *arXiv preprint arXiv:2210.05576* (2022).

Radiofrequency Quantum Upconverter (RQU)

Phase-preserving readout: Inject single tone into microwave source

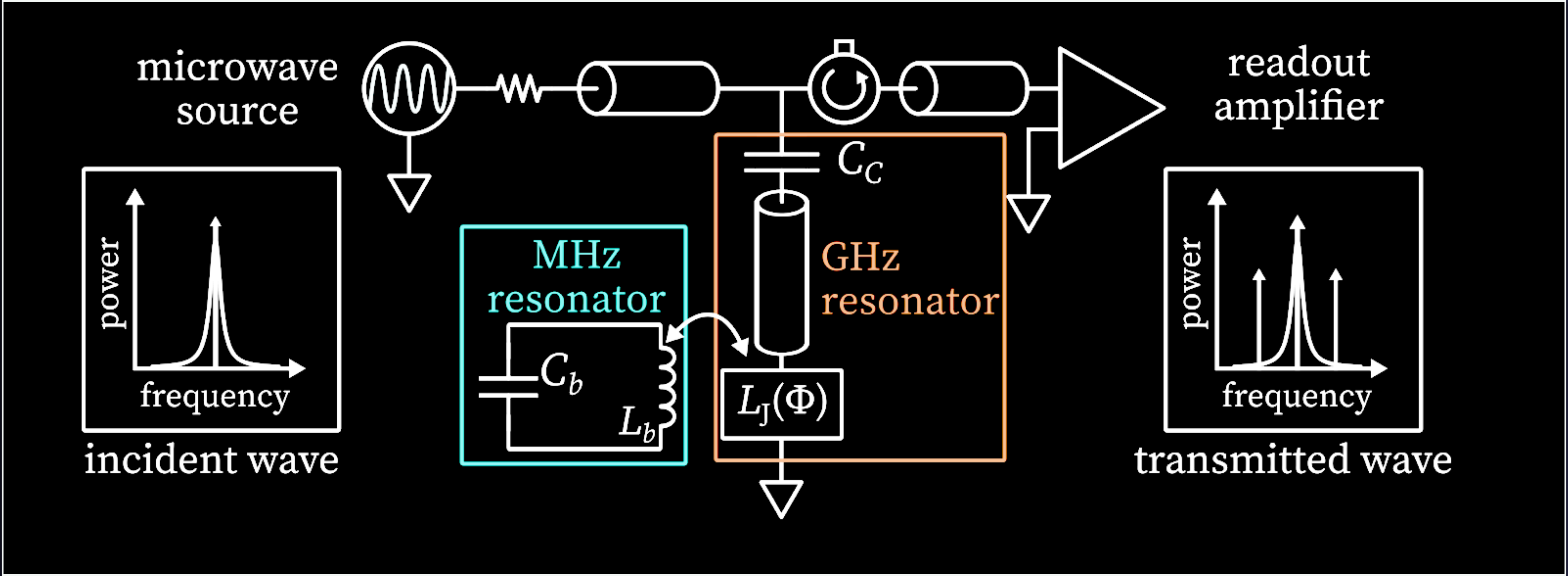

Phase-preserving readout mode

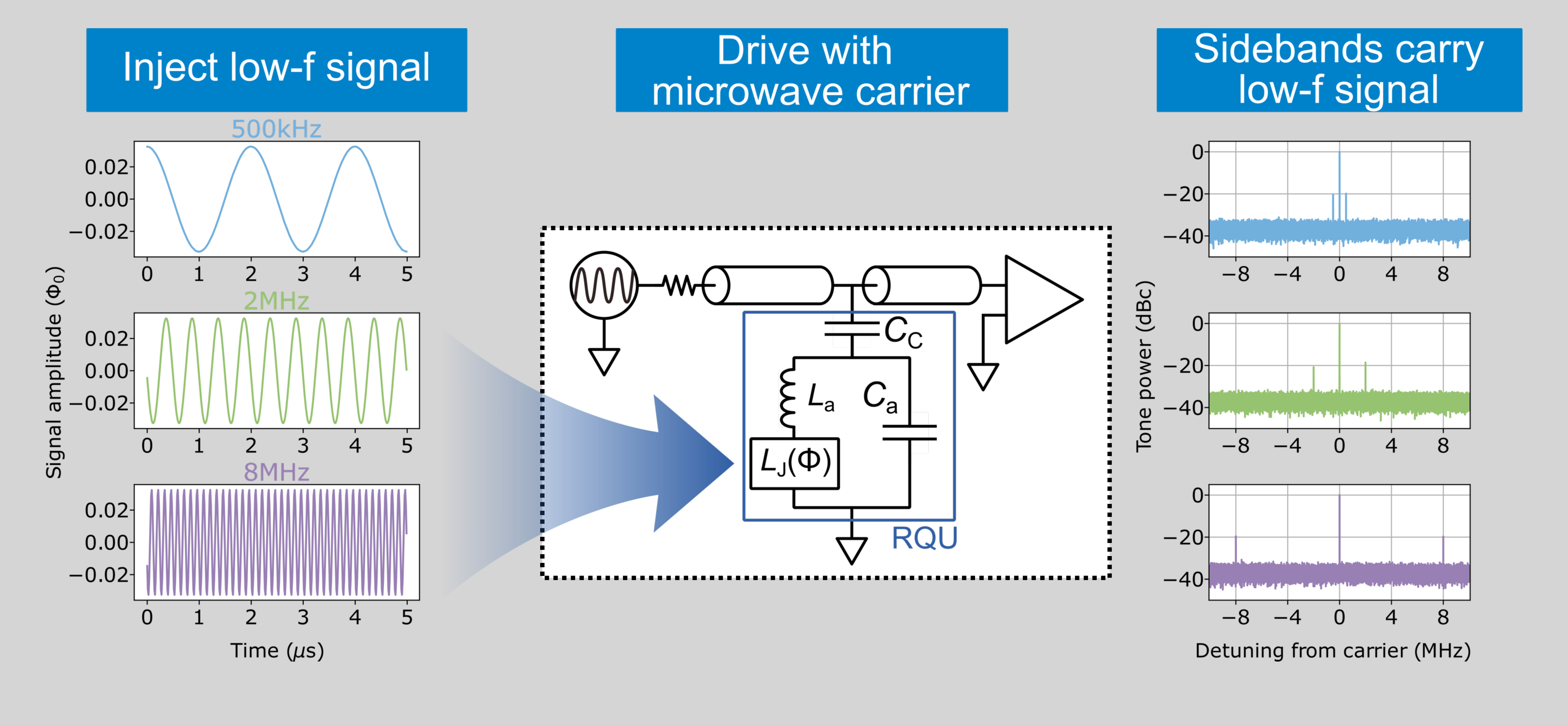

Phase-preserving readout mode

- Functions as op-amp mode EM amplifier
  - Maps the flux variable of the LF signal onto the microwave
- Flux is changing the electrical length of the transmission line and therefore the phase of the input microwave signal
- Cannot extend sensitivity beyond SQL

Radiofrequency Quantum Upconverter (RQU)

Phase-sensitive readout: Inject two tones into microwave source

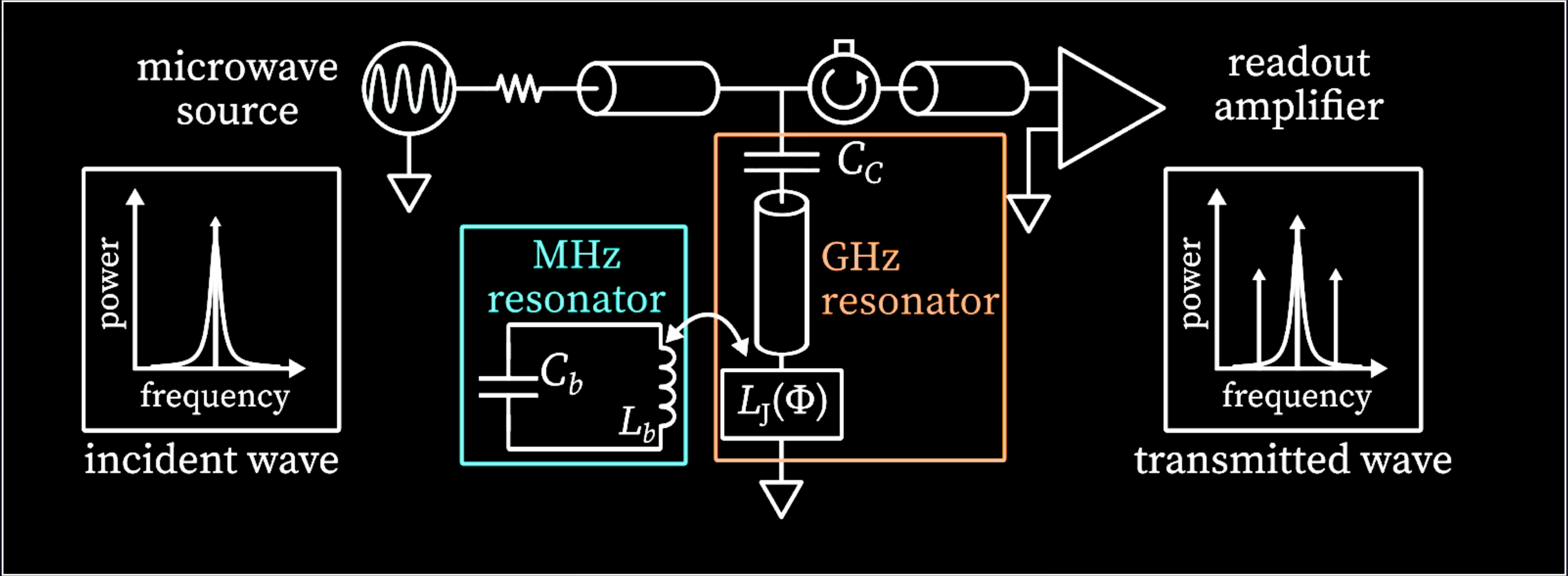

Phase-sensitive readout mode

- Microwave drive determines measurement strength.
- We can use two drive tones to amplify and therefore measure the signal in only one quadrature.
- Beyond SQL readout.

$$A_{in}(t) = X\cos(\omega_0 t) + Y\sin(\omega_0 t)$$

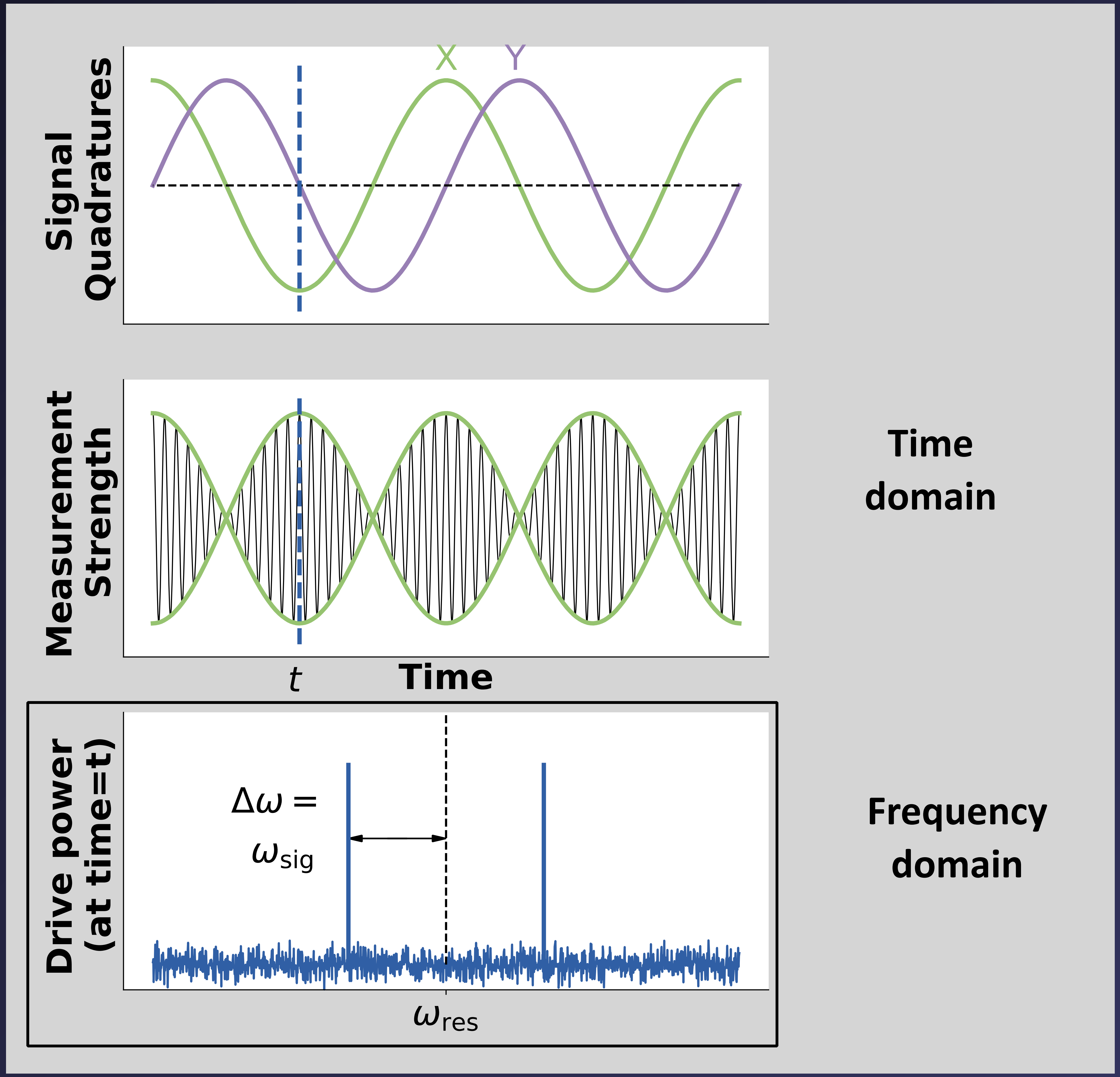

Beyond Bode-Fano

Bode-Fano criteria:

Any receiver that is

1. Linear
2. Time-invariant
3. Passive

demonstrates sensitivity over limited bandwidth

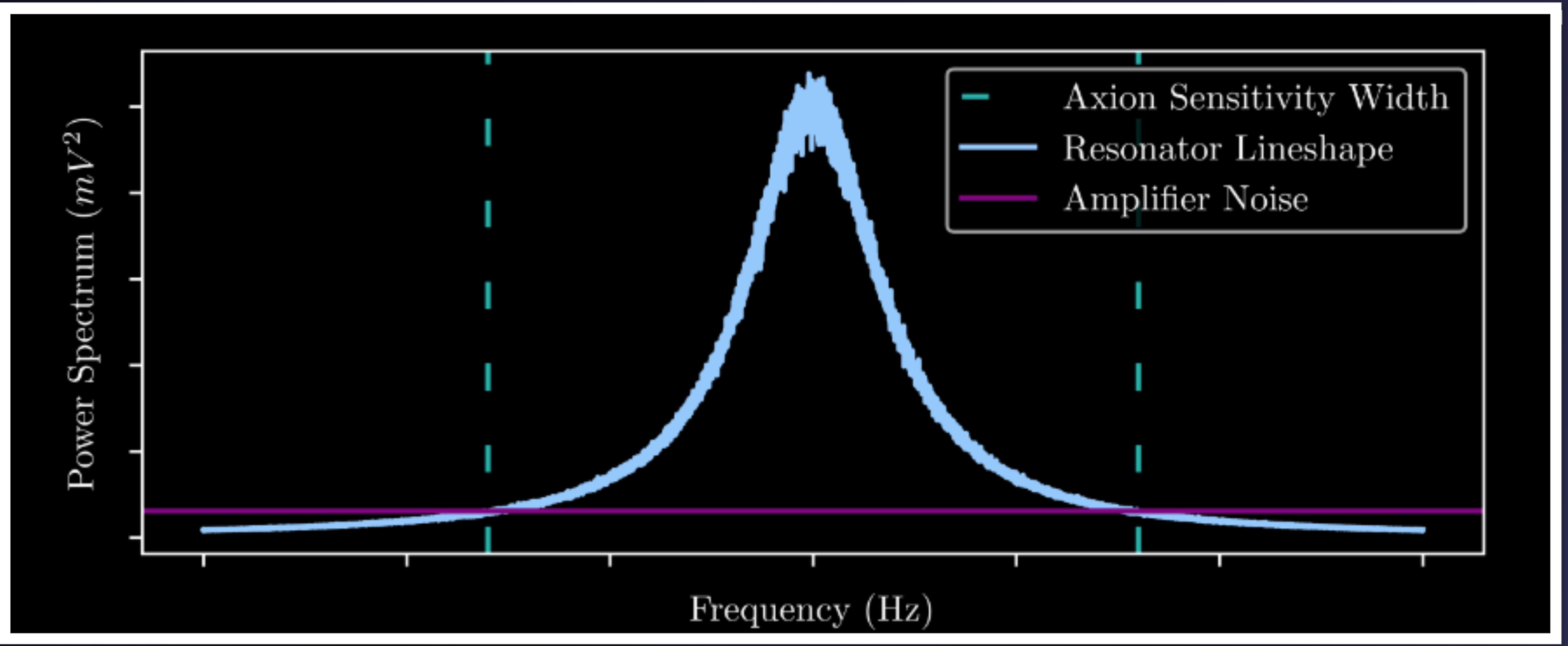

Image courtesy of Jessica Fry

Haloscope equivalent circuit

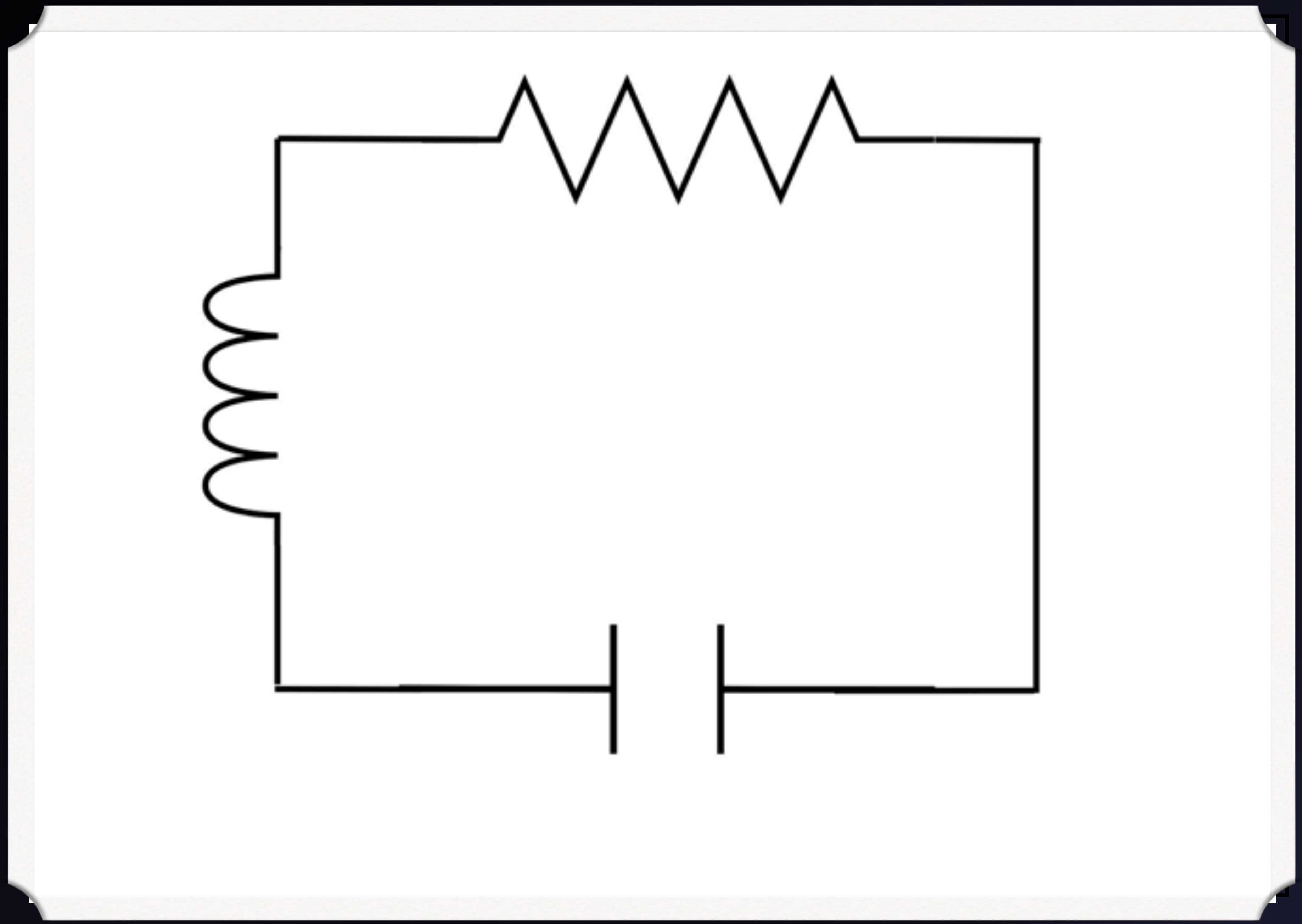

$$P_{\mathrm{rms}} \propto V_{\mathrm{rms}}^2 / Z$$

$$Z \propto \sqrt{\left(\omega L - \frac{1}{\omega C}\right)^2 + R^2}$$

- Axion signal is an AC source
- On resonance, signal enhanced by cancellation of reactances

Haloscope equivalent circuit

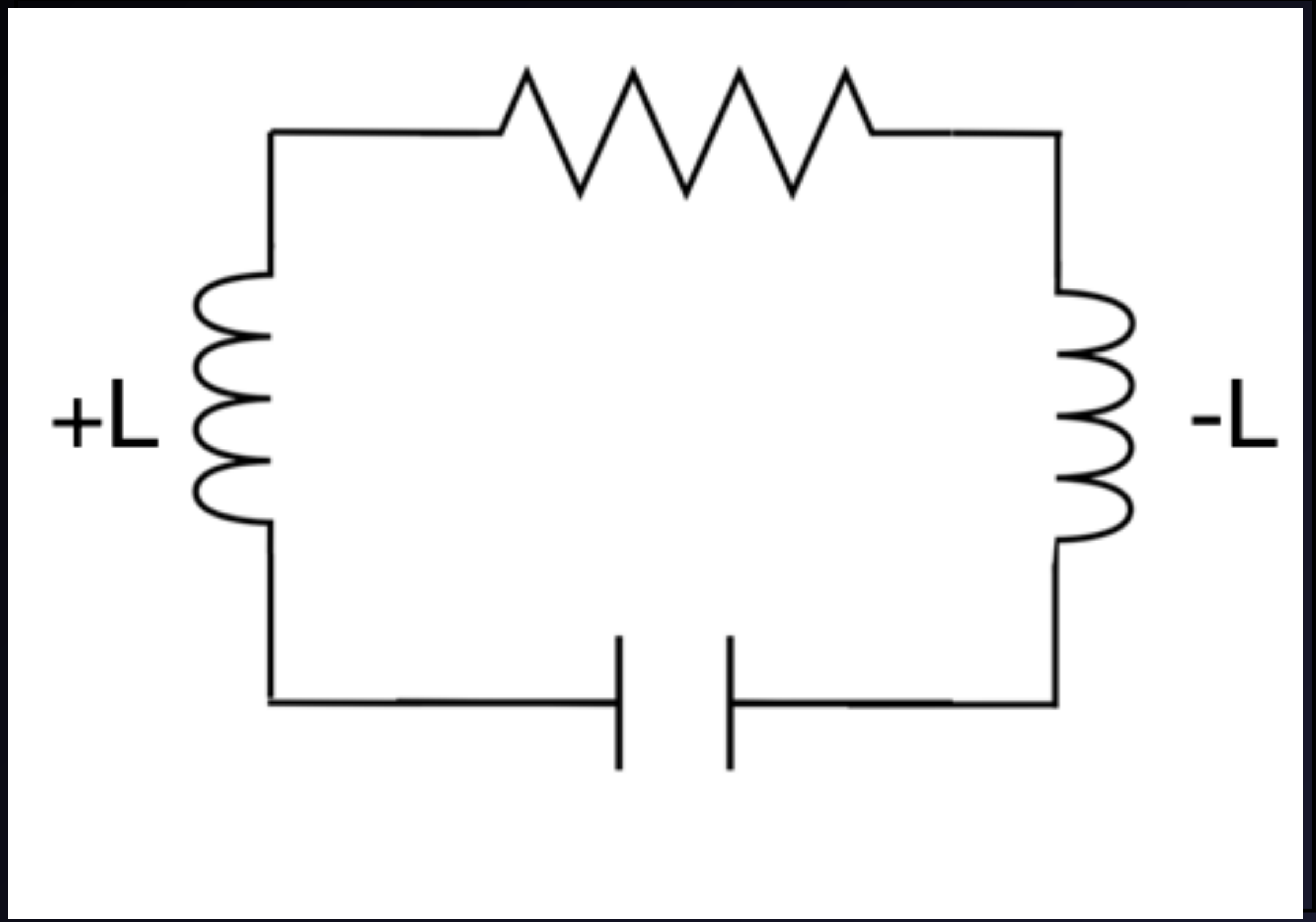

$$P_{\mathrm{rms}} \propto V_{\mathrm{rms}}^2 / Z$$

$$Z \propto \sqrt{\left(\omega L - \frac{1}{\omega C} - \omega L\right)^2 + R^2}$$

Cancellation now between these terms

- Lower impedance -> more power extracted from axion field -> greater sensitivity
- Cancellation over all frequencies -> broadband

Negative impedance devices

- Negative impedance converters or “NICs” (1950s)*
  - Transistor based circuits
  - Noisy
  - Room Temperature

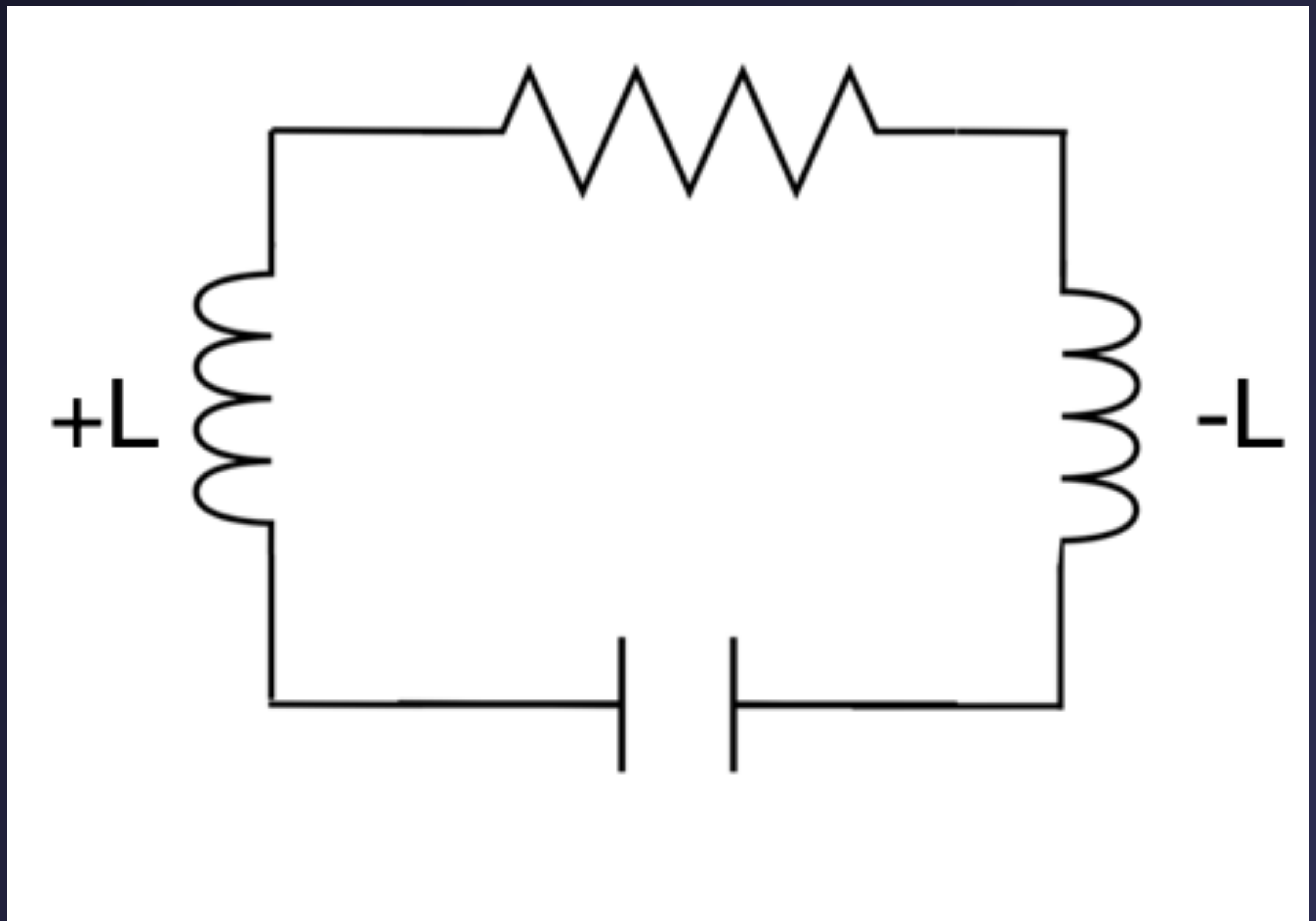

*Linvill, John G. "Transistor negative-impedance converters." *Proceedings of the IRE* 41.6 (1953): 725-729.

Can we devise low-noise negative impedance component that works at cryogenic temperatures?

Josephson Junctions

Josephson Relations

$$I = I_0 \sin\phi \quad V = d\phi/dt$$

Josephson Inductance

$$L \propto \frac{\Phi_0}{2\pi I_c \cos\phi}$$

Other ideas?

PHYSICAL REVIEW B VOLUME 13, NUMBER 9 1 MAY 1976

Current-phase relation and phase-dependent conductance of superconducting point contacts from rf impedance measurements*

Robert Rifkin and Bascom S. Deaver, Jr.
Department of Physics, University of Virginia, Charlottesville, Virginia 22901
(Received 24 November 1975)

The rf impedance of superconducting point contacts has been measured as a function of the quantum-mechanical phase difference ϕ across the point contact. By representing the point contact as a parallel combination of an inductor $\mathfrak{L}(\phi) = (\hbar/2e)(\partial I_p/\partial\phi)^{-1}$ and a resistor $R \equiv 1/G(\phi)$ the current-phase relation $I_p(\phi)$ and the phase-dependent conductance $G(\phi)$ have been determined from measurements at 30 MHz on phase-biased niobium point contacts. For point contacts with sufficiently small critical current I_c, the inductance was $\mathfrak{L}(\phi) = \hbar/2eI_c\cos\phi$ yielding the expected negative inductance branch for $\pi/2 \le \phi \le \pi$ and a sinusoidal current-phase relation. For larger critical currents there were departures from the sinusoidal form for the measured $I_p(\phi)$. There was a phase-dependent conductance that is an increasing function of ϕ corresponding to a negative coefficient for the $\cos\phi$ term in the Josephson current.

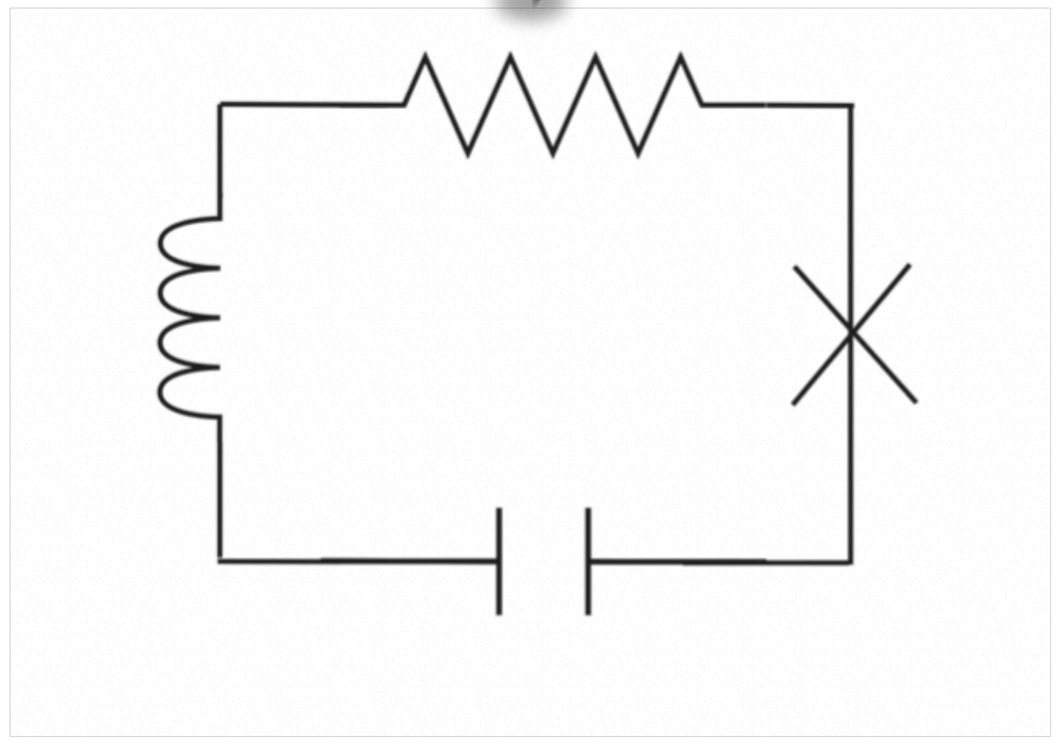

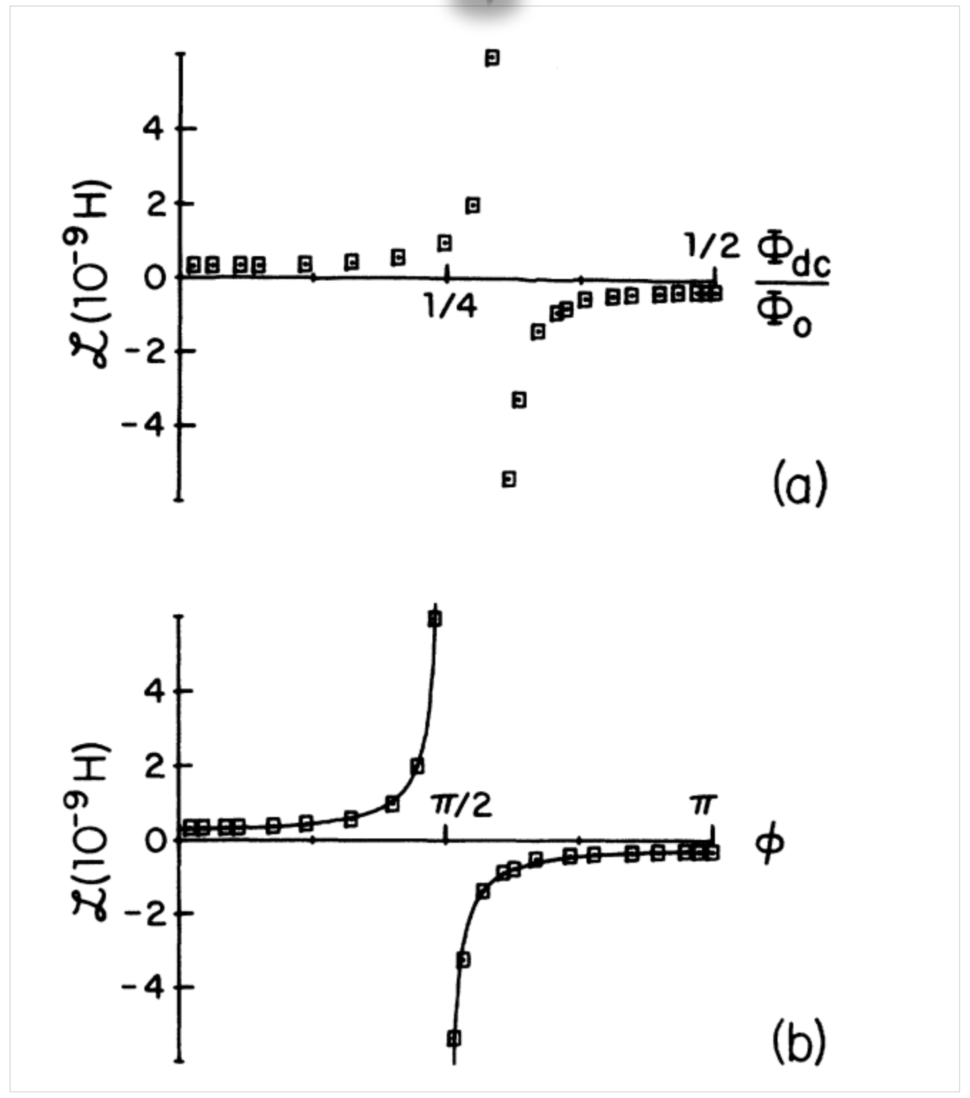

More scan rate considerations

As the resonant frequency of the cavity goes up

Volume decreases like $V \sim \frac{1}{f^3}$

Quality factor decreases like $Q \sim \frac{1}{f^{2/3}}$

Noise power increases like $T_{\mathrm{amp}} \sim f$